Doctoral Thesis

The Role of APC/C-Cdh1 in Alzheimer's Disease

by Tanja Fuchsberger

Directed by

Dr. José Viña Ribes

Dr. Ana Lloret Alcañiz

VNIVERSITAT DE VALÈNCIA

Facultad de Medicina y Odontología

Departamento de Fisiología

Programa de Doctorado en Fisiologia

Valencia, September 2016

Prof. D. José Viña Ribes, Catedrático del Dpto. de Fisiología de la Facultad de Medicina y Odontología de la Universitat de Valencia.

Prof. Dña. Ana Lloret Alcañiz, Profesora Titular del Dpto. de Fisiología de la Facultad de Medicina y Odontología de la Universitat de Valencia.

CERTIFICA/N:

Que la presente memoria, titulada “The Role of APC/C-Cdh1 in Alzheimer’s Disease”, corresponde al trabajo realizado bajo su dirección por Dña. Tanja Fuchsberger, para su presentación como Tesis Doctoral en el Programa de Doctorado en Fisiología de la Universitat de Valencia.

Y para que conste firman el presente certificado en Valencia, a 21 de octubre de 2016.

Fdo. Don José Viña Ribes Fdo. Dña. Ana Lloret Alcañiz

I want to thank everybody that was involved in this work. Particularly I want to thank the thesis directors, José Viña and Ana Lloret, and also all my workmates. I also want to thank my family and all my friends.

INDEX

Abbreviations

Aβ	amyloid beta
AD	Alzheimer Disease
ADP	adenosine diphosphate
APP	amyloid beta precursor protein
APC/C	anaphase Promoting Complex/Cyclosome
BSA	bovin serum albumin
Ca^{2+}	calcium
cdk	cyclin dependent kinase
CNS	central nervous system
ddH2O	double-distilled water
GlDH	glutamate dehydrogenase
gls	glutaminase
NAD+	nicotinamide adenine dinucleotide
NMDA	n-methyl-D-aspartate
NTF	neurofibrillary tangle
PBS	phosphate-buffered saline
pfkfb3	6-phosphofructo-2-kinase/fructose-2, 6-bisphosphatase-3
PPP	pentose phosphate pathway
PS 1/2	persenilins 1/2
ROS	reactive oxygen species
RT	room temperature
SCF	skp1/CUL1/F-box protein
UPS	ubiquitin proteasome system

1. SUMMARY

Alzheimer's disease (AD) is the most common cause of dementia among elderly individuals above 65 years. Estimations suggest that there are currently about 47.5 million people worldwide suffering from dementia, of which 60-70% are AD cases (World Health Organization, 2015). It is an irreversible disease of progressive nature, which leads to deterioration in cognitive functions beyond what is normal in a healthy aging process. Among the affected cognitive functions are memory, thinking skills and orientation.

AD is one of the major causes of disability among older people and has a big impact on socio-economical capacities. There is currently no treatment to cure AD and it is a very active field in biomedical research. Numerous new treatments are being tested in various stages of the disease to alter its progressive course.

The pathological hallmarks of AD are deposition of plaques of amyloid peptides and the formation of neurofibrillary tangles (NFTs), which are mainly constituted by hyperphosphorylated aggregates of the microtubule-associated protein tau. These accumulations cause damage to cells and trigger progressive, diffuse and massive neuronal loss. The most affected areas are the neocortex, hippocampus, amygdala, and their associated cortices. Moreover, various molecules and signalling pathways are altered in AD, which might contribute substantially to the onset and/or progress of the disease. In this work we analyzed the implication of the E3 ubiquitin ligase, the anaphase promoting complex/cyclosome (APC/C) in AD.

APC/C is a large protein complex, forming an E3 RING finger ubiquitin ligase that is one of the main regulators of the cell cycle in proliferating cells. APC/C recognizes proteins by specific amino acid motifs, like KEN-BOX or D-BOX

sequences and targets them for degradation. Within the last decade, important neurobiological functions of APC/C and its activator subunits cdh1 and cdc20 have been discovered. It was shown that APC/C is involved in the control of neuronal G0 maintenance, axonal growth, coordinates neurogenesis and synaptic development. Up to date, 15 substrates have been identified, which are directly involved in processes in the nervous system. Accumulation of some of these proteins has been associated with neurodegeneration. In this work we tested the hypothesis that APC/C could have a relevant pathophysiological role in AD.

We showed in neurons in primary culture that amyloid beta (Aβ), a peptide related to AD, causes the degradation of cdh1 in a proteasome-dependent manner. This leads to a subsequent increase of the APC/C substrate glutaminase, which causes an elevation of glutamate levels. Increased glutamate levels cause intraneuronal Ca^{2+} dysregulation, resulting in excitotoxicity and neuronal apoptosis. Glutaminase inhibition prevents these Aβ-induced alterations. Ca^{2+} dysregulation induced by glutamate causes a similar effect on cdh1 and glutaminase as Aβ. We confirmed these findings *in vivo* using microinjection of either Aβ or glutamate in the CA1 region of the rat hippocampus. We showed here for the first time *in vivo* that both, Aβ and glutamate, cause nuclear exclusion of cdh1 and a subsequent increase of glutaminase. These results indicate that maintaining normal APC/C-Cdh1 activity may be a useful target in AD treatment.

2. INTRODUCTION

2.1. APC/C Ubiquitin Ligase: An Introduction

Ubiquitination is a post-translational modification in which ubiquitin, a small regulatory protein (8,5 kDa), is attached to a substrate protein. The ubiquitination system consists of three classes of enzymes termed, E1 ubiquitin-activating enzymes, E2 ubiquitin-conjugating enzymes and E3 ubiquitin ligases. The E3 ligases impart the specificity to the substrates (Ciechanover et al., 1978, Ciechanover et al.,1980, Hershko et al., 1982; Pickart et al., 2004). A sequential cascade of these enzymes results in the addition of ubiquitin to an amino group of the target protein. An isopeptide bond is formed between terminal glycine of ubiquitin and, in most cases, a lysine residue in the amino group (Bloom et al., 2003). Ubiquitination can affect the substrate activity, the cellular localization or promote their degradation (Pickart et al., 2004). In general, ubiquitin-dependent proteolysis is a major regulatory mechanism for the reorganization of the proteome.

APC/C was first discovered by King et al. (1995) when they observed that cyclin B was degraded at the onset of the anaphase by an ubiquitin-dependent proteolytic system. It is a multimeric protein complex that belongs to the cullin–RING ubiquitin ligases, which represent the largest known class of E3 ubiquitin ligases. Cullins are proteins that are part of ubiquitin ligases and they combine with RING proteins (Bosu and Kipreos, 2008). Nine cullins are encoded in the human genome (Cul1, 2, 3, 4A, 4B, 5, and 7, PARC, and APC2), and each uses a different set of adaptors and substrate specificity factors. They are collectively termed as the cullin-RING ligases (Emanuele et al., 2011). In the APC/C complex the catalytic module is formed by the APC2 (cullin) and APC11 (RING) proteins.

The activity of APC/C strictly depends on regulatory coactivator subunits, which promote the interactions and stimulate the catalytic reaction of APC/C and the substrate. They are termed cell-division cycle protein 20 (cdc20) and cdc20 homologue-1 (cdh1) (Visintin et al., 1997; Chang et al., 2014). The coactivators recognize conserved destruction motifs, the D box (RxxLxxxxN/D/E), KEN box (KENxxxN), A box and Cry box (CRYxPS) (Glotzer et al., 1991; Pfleger and Kirschner, 2000; Reis et al., 2006; Littlepage and Ruderman, 2002) and recruit the substrates to the APC/C. However, these consensus sequences can also be found in proteins that are not substrates of APC/C. Therefore, more information about recognition and ubiquitination mechanisms is necessary to identify putative APC/C substrates only by their sequence (Li and Zhang, 2009).

The timed activation of APC/C-Cdc20 and APC/C-Cdh1 has a critical role for cell cycle regulation. APC/C is also implicated in other essential processes including genomic integrity and metabolism, and has major functions in development and in the nervous system (Qiao et al., 2010; Almeida et al., 2010; Almeida 2012; Delgado-Esteban et al., 2013). The structure and functions of APC/C will be discussed in more detail in the following sections.

2.1.1. Components and structure of APC/C

Chang et al. (2014) identified the definite molecular structure of all subunits of the APC/C complex. Moreover, Chang et al. (2015) described the atomic structure of APC/C and its mechanism of protein ubiquitination. They determined the structural architecture by reconstruction of cryo-electron microscopy of a human APC/C-coactivator-substrate complex. APC/C is a large multimeric protein complex of 1,2 mDa that consist of 15 different proteins assembled to 20 subunits (see Table 2.1).

Subunit	Mass (kDa)	N	Function	Location	Structural domains
Apc1	216.5	1	Scaffolding	Platform	WD40/mid-helical/PC
Apc4	92.1	1	Scaffolding	Platform	WD40/four helix bundle
Apc5	85.1	1	Scaffolding	Platform	N-terminal helical domain/13 TPR
Apc3	91.9	2	Scaffolding	TPR lobe	14 TPR
Apc6	71.7	2	Scaffolding	TPR lobe	14 TPR
Apc7	66.9	2	Scaffolding	TPR lobe	14 TPR
Apc8	68.8	2	Scaffolding	TPR lobe	14 TPR
Apc12	9.8	2	TPR-accessory	TPR lobe	Extended/α-helix
Apc13	8.5	1	TPR-accessory	TPR lobe	Extended/α-helix
Apc16	11.7	1	TPR-accessory	TPR lobe	α-helix
Apc2	93.8	1	Catalytic	Catalytic module	Cullin repeats/CTD
Apc11	9.8	1	Catalytic	Catalytic module	RING
Apc10	21.2	1	D box recognition	Sub recognition module	Doc homology/IR tail
Apc15	14.3	1	MCC interaction	Platform	Extended/α-helix
Coactivator Cdc20/Cdh1	54.7/55.2	1	D box and KEN box recognition	Sub recognition module	C box/helical/WD40/IR tail
Total APC/C^{Cdh1}	1222.6		-		-

Table 2.1 | **APC/C subunits: their functions, location and structural domains.** MCC: mitotic checkpoint complex, PC: Proteasome/cyclosome, TPR: Tetratricopeptide repeat, N: stoichiometry, total mass includes subunit stoichiometry (Table from: Chang et al., 2014).

APC/C forms a triangular shape. Seven subunits function as scaffolds for the coordination of the juxtaposition of the catalytic and recognition modules. All of them contain multiple repeat motifs. However, the authors do not exclude that some of the scaffold subunits might also have a direct role in interactions with substrates or with E2 ubiquitin conjugating enzymes (e.g. UbcH10). The tetratricopeptide repeat (TPR) proteins and their accessory subunits form at the back and the top of the complex a bowl shaped lobe, consisting of V-shaped homodimers. The platform subunits, APC4 and APC5 combine with two domains of APC1, which contacts the TPR lobe. For substrate recognition two subunits, APC10 and coactivator cdc20 or cdh1, are responsible. The recognition module is located at the top of the cavity where APC10 interacts with the APC1

Proteasome/cyclosome (PC) domain. The catalytic subunits APC2 and APC11 are positioned at the front of the cavity below APC10 and coactivator (see Figure 2.1).

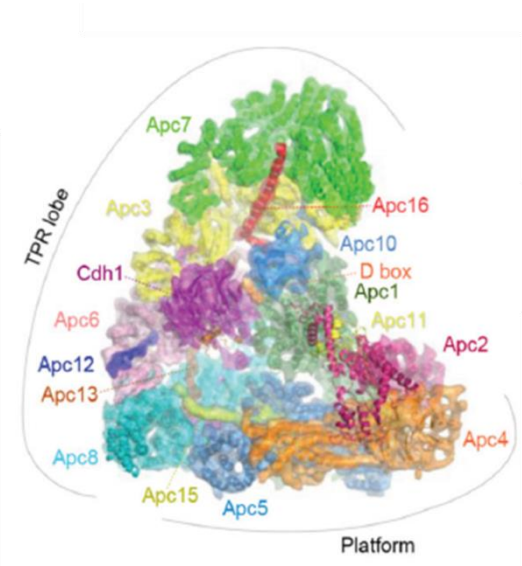

Figure 2.1 | **APC/C-Cdh1 ternary structure**. EM reconstruction of APC/C-Cdh1 of H. sapiens at 7.4 Å resolution. The EM map is coloured according to subunit assignments (Figure from: Chang et al., 2014).

The coactivator proteins cdc20 and cdh1 are WD40 proteins. WD-repeat proteins are made up of highly conserved units forming structural repeated motifs. They usually contain a tryptophan-aspartic acid dipeptide end. The C-terminal end of cdh1 and APC10 share structurally related Ile-Arg motifs that interact with the TPR motif (with the C-terminal end of APC3 homo-dimer). Substrates bind between the WD40 β-propeller domain of cdh1. Independent of substrate recognition, the N-terminus of the coactivator induces conformational changes of the APC/C complex that stimulate the activity of the APC/C ubiquitin ligase (Chang et al., 2014).

2.1.2. APC/C-Cdh1 coactivator substrate recognition

The recognition site of the KEN box is centred on the upper surface of Cdh1 WD40. The D-box recognition site was observed as a channel on the edge of Cdh1 WD40 domain, where the residues P1-P7 RxxLxx(V/I/L) are engaged. The residues P8 to P10 interact with a surface of APC10. Mutation of P8-P10 attenuates APC/C-Cdh1 ubiquitination activity. The authors confirm that the D-box motif is a bipartite degron, which had been previously suggested (Fonseca et al., 2010), with a N-terminal RxxLxx(V/I/L/M) site and a hydrophilic C-terminal APC10 binding site (P8-P10) (Chang et al., 2014). Furthermore it was shown that the catalytic site of UbcH10 has a distance of about 40 A° from the D box or KEN box binding site to the coactivator cdh1. Therefore an extended linker of ten amino acid residues in C-terminal direction of the D-box places the lysine (ubiquitin binding site) at the UbcH10-ubiqutin catalytic site. Consistent with this finding, peptides with lysines at positions K1, K4 or K7 relative to the D box were not ubiquitinated, while lysines at positions K10, K13 and K18 were ubiquitinated (Chang et al., 2015). This additional information for D-box and KEN box recognition and ubiquitination sites could be helpful for the identification of putative APC/C substrates.

The following recognition motifs are common among APC/C substrates (including the recently found features by Chang et al., 2014; Chang et al 2015):

Destruction box consensus: RxxLxx[LIVM]. Example: Securin

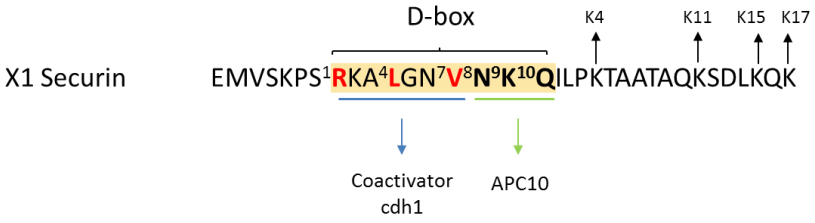

Figure 2.2 | **The D-box degron of X1 Securin.** The bipartite degron of the D-box consist of residues P1-P7 with the sequence motif RxxLxx[LIVM], which is recognized by cdh1, and a hydrophilic C-terminal end (P8-P10), which is recognized by APC10. The lysine residues are indicated. According to Chang et al. (2015) lysine residues with a distance of K > 10 amino acids can be ubiquitinated by UbcH10. Here, possible ubiquitination sites are K11, K15 and K17 (Figure adapted from: Chang et al., 2015).

KEN box consensus: KENxx(P). Example: Cdc20

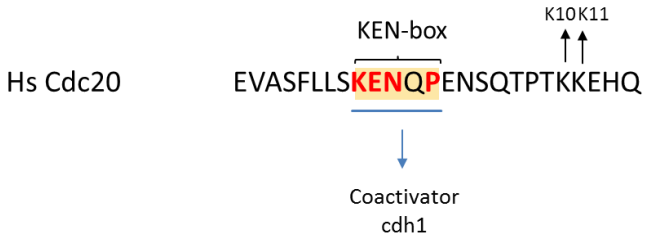

Figure 2.3 | **The KEN-box degron of Hs Cdc20.** The degron of the KEN-box has the sequence motif KENxx(P) which is recognized by cdh1. The lysine residues are marked, starting in the position after the "N". According to Chang et al. (2015) lysine residues with a distance of K > 10 amino acids can be ubiquitinated by UbcH10. In this example possible ubiquitination sites are K10, K11. (Figure adapted from: Chang et al., 2015)

These two, the D-box and KEN-box motifs, are the most commonly recognized APC/C sequence degrons. Other sequence motifs that have been related to APC/C are: ORC destruction box (O-box) LxxxN, GxEN box and LxExxxN. Furthermore, "pseudo-substrates" of APC/C have been identified. These are proteins that contain the recognition sequence D-box or KEN-box, but are not targeted for degradation

by APC/C. This can have an inhibitory effect on APC/C activity. For example Emi1, Mad3 and Acm1 have been identified as pseudo-substrates (Pines, 2011).

2.1.3. Functions of APC/C: The cell cycle

A key mechanism in the cell cycle is the rapid destruction of specific cell cycle proteins to provide a directional switch to ensure that mitosis follows DNA replication and that each cell receives an identical set of chromosomes. These timed transitions are regulated mainly by two ubiquitin ligases: APC/C and Skp1/CUL1/F-box protein (SCF) (Li et al., 2009; Sajman et al., 2015).

The cell cycle can be divided in four major phases: **G1**, a gap phase, in which cells are prepared to enter the **S-phase**, when the DNA replication takes place; this is followed by **G2**, the second gap phase, for the preparation to the following **M-phase** in which the cell division occurs.

Within the regulation of the APC/C activity in these phases, the temporal coordination of the two coactivators Cdc20 and Cdh1 promotes cell cycle progression. They mediate proteolysis of regulatory proteins that control maintenance of G1, the initiation of DNA replication, chromosome segregation, events of cytokinesis, and mitotic exit (Pines, 2011). Specifically, APC/C-Cdc20 is primarily active in early mitosis in the metaphase to anaphase transition and in mitotic exit, while APC/C-Cdh1 becomes active at the end of the mitotic exit and in the early G1 phase (Figure 2.4). There, it also regulates DNA damage response and repair, acting as an important checkpoint regulator. Dysregulation of Cdh1 causes impaired cytokinesis, DNA re-replication and aberrant centrosome formation. Therefore a crucial role for Cdh1 in maintaining genomic integrity has been appointed (Wasch et al., 2010).

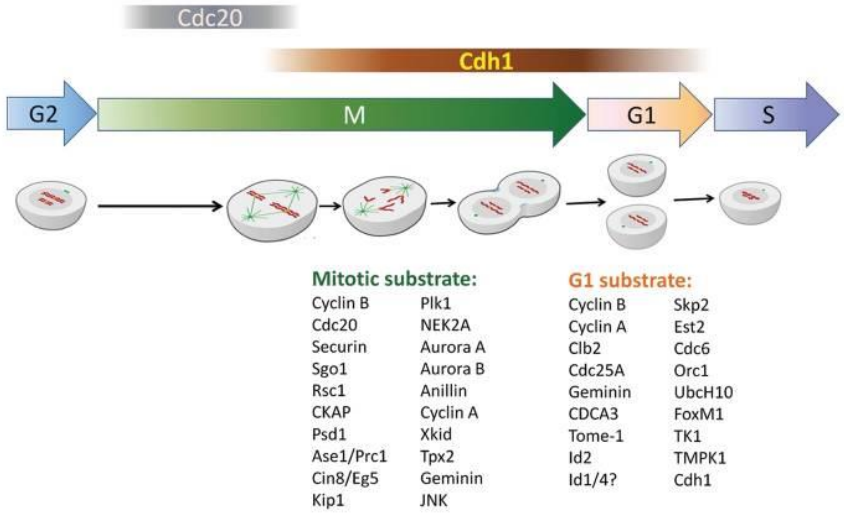

Figure 2.4 | **Activation of Cdc20 and Cdh1 during mitosis and G1 progression.** The initiation of DNA replication, the onset of the anaphase, cytokinesis and mitotic exit are coordinated by Cdc20 and Cdh1 through the sequential destruction of cell cycle proteins (Figure from: Qiao et al., 2010).

Another emerging role for APC/C-Cdh1 has been described. It regulates the decision to divide or to differentiate through degradation of inhibitors of cyclin-dependent kinases and transcription factors, which are involved in cell cycle withdrawal and onset of differentiation. The stabilization of p21 and p27 via the downregulation of Skp2 is a key event in cell cycle withdrawal. To induce terminal differentiation, the destruction of the transcriptional inhibitors Id1, 2 and 4 is crucial. This occurs typically in in the G1 phase where the transition into G0 phase is made when they commit to differentiate. Examples include lens differentiation, the generation of cardiomyocytes, bud formation and neuronal morphogenesis, which will be discussed in detail in the following sections (Qiao et al., 2010).

2.2. Functions of APC/C and Its Targets in the Nervous System

First indications of an implication of APC/C in the central nervous system were shown by mRNA expression data in neurons of the APC/C subunits APC1 and APC8 (Starborg et al., 1994; Zhao et al., 1998).

Gieffers et al. (1999) reported for the first time presence of APC/C subunits and cdh1 in several human tissues which contain differentiated cells, including the adult brain. They observed that APC/C and cdh1 were ubiquitously expressed in fully differentiated cultured rat hippocampal neurons. In brain sections of mouse and human samples they detected APC/C subunits including cdh1, but not cdc20, in neurons of the cortex, hippocampus and cerebellum. They proposed that APC/C-Cdh1 functions were not restricted to cell cycle regulation in proliferating cells but may regulate unidentified substrates for ubiquitination in differentiated cells (Gieffers et al., 1999). These findings initiated the search for functions of APC/C-Cdh1 in neurons. Since then, several fundamental processes in the central nervous system have been described to be regulated by APC/C-Cdh1: Axonal growth and patterning (Konishi et al., 2004; Stegmüller et al., 2006), neuronal cell cycle exit (Lasorella et al., 2006), neuronal differentiation (Harmey et al., 2009) and neurogenesis (Delgado-Esteban et al., 2013), degradation of AMPA regulating homeostatic plasticity (Fu et al., 2011), long term potentiation (Li et al., 2008) and long-term depression (Huang et al., 2015). Furthermore, Kim et al. (2009) discovered that also APC/C-Cdc20 is involved in the central nervous system as it controls dendrite morphogenesis in postmitotic neurons (Kim et al., 2009).

Here a summary of experimentally identified APC/C substrates is presented, which are directly related to the processes in the nervous system (Table 2.2).

UniProt	Substrates	Function	Motif	Coactivator	Reference
Q15784	Neurogenic differentiation factor 2 (Neuro D2)	Regulates presynaptic differentiation	D-box	cdc20	Yang et al., 2009
Q9VM93	Liprin-alpha	Regulation of synaptic size and activity	D-box	cdh1	van Roessel et al., 2004
P42261	Glutamate receptor 1 (GluR1)	Regulation of AMPA receptors in homeostatic plasticity	D-box	cdh1	Fu et al., 2011
P41134	DNA-binding protein inhibitor (Id1)	Invovled in dendrite morphogenesis in neurons	D-box	cdh1, cdc20	Kim et al., 2011; Wang et al., 2008
P12757	SnoN	Cell-intrinsic regulation of axonal morphogenesis	D-box	cdh1	Stroschein et al., 2001; Stegmüller et al., 2006
Q9HCE7	Smurf1	E3 Ubiquitin ligase that targets RhoA, regulates axon growth	D-box	cdh1	Kannan et al., 2012
Q02363	DNA-binding protein inhibitor (Id2)	Axonal growth and cell cycle exit	D-box	cdh1	Lasorella et al., 2006
P48730	Casein Kinase 1 δ	Regulation of cerebellar granule cell neurogenesis	D-box	cdh1	Penas et al., 2015
O00716	Transcription factor E2F3	Cell cycle exit and neuronal differentiation	D-box	cdh1	Ping et al., 2012
P07818	Cyclin B1	Maintains cell cycle exit and promotes neuronal survival	D-box	cdh1	King et al., 1996; Maestre et al., 2008
Q16875	6-phosphofructo-2-kinase/fructose-2,6-bisphosphatase 3 (Pfkfb3)	Downregulates glycolytic pathway in in neurons, prevents neurodegeneration	KEN box	cdh1	Rodriguez-Rodriguez et al., 2012
O94925	Glutaminase kidney isoform, mitochondrial	Regulates the levels of the neurotransmitter glutamate in neurons	KEN box	cdh1	Colombo et al., 2010
Q06787	FMRP	Drives mGluR-dependent synaptic plasticity	D-box	cdh1	Huang et al., 2015
Q8IWQ3	Brain-specific kinase 2 (BRSK2)	Serine/threonine kinase, regulates polarization of neurons and axonogenesis, cell cycle progress and insulin secretion	KEN box, D-box	cdh1	Li et al., 2012
Q7JUM5	Drosophila MCPH1 (isoform B)	Cell cycle; Homolog of a causative gene for autosomal recessive primary microcephaly in human	D-box	cdh1	Hainline et al., 2014

Table 2.2 | **This APC/C substrates are directly involved in the regulation of various processes in the central nervous system**. APC/C-Cdh1 and APC/C-Cdc20 regulate neurogenesis, axonal and dendrite growth, synaptic differentiation, synaptic regulation, cell cycle exit, neuronal survival and metabolic processes in neurons.

2.2.1. APC/C-Cdh1 and axonal growth in the cerebellar cortex

Axon growth is essential in the developing brain but it is very limited in the adult brain due to intrinsic and extrinsic inhibition. The activity of APC/C-Cdh1 is required for the inhibition of axon growth in mammalian neurons (Konishi et al., 2004). This was shown by using RNA interference to acutely knockdown cdh1 in primary cerebellar granule neurons, which had no effect on the survival of the neurons, but induced a change in the morphology of neuronal processes. They measured growth of dendrites and axons (marked by the somato-dendritic marker MAP2 and the axonal marker Tau) and observed that the cdh1 knockdown caused a substantial increase in growth rate and significant elongation of the axonal length, but not of dendrites. Moreover, they generated a dominant interfering form of the subunit APC11 in granule neurons which caused an induction of axonal growth. The inhibition of APC/C by Emi1 had the same effect. This was also tested *in vivo* by using shcdh1 plasmid in the cerebellar cortex of P6 rat pups. The shcdh1 and an expression plasmid encoding GFP were injected and then the animals were subjected to electroporation. Five days later they isolated the cerebellum and it was analysed using immunohistochemistry. The injection of a control plasmid was used to confirm cdh1 specificity. Shcdh1expressing granule neurons were drastically altered and several axons grew abnormally off a regular track in parallel fibres. Furthermore, cdh1 knockdown was shown to override the effect of adult rat myelin on axonal growth inhibition. The authors suggested that APC/C-Cdh1 has a cell-autonomous function in axonal growth and patterning of granule neurons in the developing cerebellum *in vivo* and that it may also contribute to the inhibition of axon growth in injured neurons in the adult brain (Konishi et al., 2004).

Stegmüller et al. (2006) reported a mechanism by which the ubiquitin ligase APC/C-Cdh1 controls axonal morphogenesis. They showed that APC/C-Cdh1 operates in the nucleus for inhibition of axonal growth by targeting the transcriptional corepressor SnoN for ubiquitin-dependent proteasomal degradation.

The knockdown of SnoN in primary cerebellar granule neurons reduced the growth of axons and inhibited the previously observed growth of axons when simultaneously using cdh1 RNA interference. High protein levels of SnoN stimulated the growth of axons. This was also confirmed *in vivo* by knockdown of SnoN in the developing rat cerebellum, which caused inhibition of elongation of granule neuron parallel fibres. Thereby, the authors described a mechanism of axonal growth regulation through APC/C-Cdh1 and the SnoN substrate. Additionally, it was shown that the APC/C-Cdh1/SnoN pathway is co-regulated by TGFβ/Smad2. Smad2 signalling influences axonal growth, as it associates with SnoN in neurons and recruits APC/C-Cdh1 to its substrate. Inhibition of TGFβ inactivates Smad2 signalling, which caused an increase in SnoN and thereby axonal growth was stimulated (Stegmüller et al., 2008).

Furthermore, the inhibitor of DNA binding 2 (Id2) protein is involved in axon growth regulation as APC/C-Cdh1 substrate. In the developing nervous system Id2 is an inhibitor of neurogenic basic helix-loop-helix transcription factors, enhances cell proliferation and promotes tumor progression. It is a very unstable protein, which is degraded by APC/C-Cdh1 as the cells enter a quiescent state. Depletion of cdh1 causes the stabilisation of Id2. High levels of Id2 enhance axonal growth in cerebellar granule neurons. Activation of helix-loop-helix transcription factors induces the expression of genes with inhibitory effect on axonal growth, e.g. the Nogo receptor. Therefore, degradation of Id2 by APC/C-Cdh1 allows the accumulation of axon growth inhibitors (Lasorella et al., 2006).

Another novel APC/C-Cdh1 target is Smurf1, an E3 ubiquitin ligase, which is also involved for axon growth regulation. Smurf1 had previously been related to axon initiation and growth of neurons (Cheng et al., 2011; Sato and Heuckeroth, 2008). Knockdown of Smurf1 in cerebellar granule neurons causes a decrease in axonal length. *In vivo* knockdown of Smurf1 causes a disruption of neuronal migration in

the developing cerebellar cortex. When Smurf1 is stabilized it overcomes myelin-induced inhibition of axon growth. Furthermore, it was shown that a protein targeted by Smurf1, the small GTPase RhoA, has a crucial role in axon growth inhibition. APC/C-Cdh1 acts upstream of the Smurf1/RhoA pathway in the control of axon growth, and it was shown that this pathway acts in parallel to the previously identified substrates SnoN and Id2 (Kannan et al., 2012).

2.2.2. APC/C-Cdh1 and neurogenesis

APC/C-Cdh1 coordinates the cell cycle exit and initiates the differentiation of neural progenitors.

In Sox2-Cre cdh1-conditional knockout mice (embryo-restricted cdh1 knock-out), the cell cycle exit is delayed in neural progenitor cells and that causes replicative stress and p53-mediated apoptotic death. This results in increased length of the ventricular and the subventricular zone, while cortical neurons are decreased in number and a reduction of cortical size occurs. It was shown that these aberrations occur due to a dysregulation of Skp2, a F-box protein that had previously been described as a substrate of APC/C-Cdh1 (Bashir et al., 2004). The degradation of Skp2 promotes the stabilization of p27, which is an inhibitor of Cdk's, and that results in cell cycle exit. In this cdh1 knock-out model, Skp2 accumulates and that results in delayed cell-cycle exit (Delgado-Esteban et al., 2013). It was also shown that E2F3A, an APC/C-Cdh1 substrate, decreases steadily in differentiating neuroblastoma cells in an APC/C-Cdh1 dependent manner. This was accompanied by an increase in p27 and a decrease in cyclin A (Ping et al., 2012).
The phenotype of cdh1 knockout mice resembles the one of microcephaly. Interestingly, the *Drosophila* homolog of MCPH1 B, a protein encoded by a causative gene of autosomal recessive primary microcephaly, was identified as a

substrate of APC/C-Cdh1 (Hainline et al., 2014). Further research would be needed to deepen the understanding of the involvement of APC/C-Cdh1 in microcephaly.

Eguren et al., (2013) analysed mice in which cdh1 was eliminated in the developing nervous system by a Cre recombinase which was expressed under a nestin regulatory sequence. They suffered defects in neural progenitor cells, accumulation of cerebrospinal fluid in the brain cavities, and death. Cdh1 is required during neurogenesis as it prevents replicative stress. In cdh1-depleted neuronal progenitors, replicative stress induces p53-dependent apoptosis. The ablation of p53 prevents apoptosis, but not replicative stress, which results in the presence of damaged neurons in the adult brain (Eguren et al., 2013).

Penas et al. (2015) showed that casein kinase 1 (ck 1) δ is an APC/C-Cdh1 substrate, which regulates neurogenesis in cerebellar granule cells. The ck 1 family is highly conserved in eukaryotes and controls a broad spectrum of biological processes, e.g. circadian rhythms, signal transduction, apoptosis, neurite outgrowth. It was shown that ck 1 δ is an APC/C-Cdh1 substrate in a D-box dependent manner. Knockout of cdh1 in cerebellar granule cell progenitors (GCP's) stabilizes ck 1 δ. APC/C-Cdh1 normally downregulates the kinase during cell cycle exit and thereby controls the balance of proliferation and cell cycle stop in the developing brain. Overexpression of the kinase results in increased proliferation, while loss of ck 1 δ inhibits the expansion of GCP's (Penas et al., 2015).

2.2.3. APC/C-Cdh1 in the regulation of synaptic plasticity

The adaptive response of the nervous system to experience is thought to be represented by synaptic plasticity. The physiological correlation of learning and memory has been characterized by two forms of synaptic plasticity: Long-term potentiation (LTP) and long-term depression (LTD). Synaptic plasticity is often

affected in neurological diseases. Several studies showed that ubiquitin-dependent regulations are involved in synaptic plasticity. In the recent years the role of APC/C-Cdh1 has been studied in this context. In the following section the main findings of the involvement of APC/C-Cdh1 in synaptic plasticity will be summarized.

In the nematode *C. elegans* APC/C regulates the abundance of GLR1, a non-NMDA glutamate receptor (GluR). Mutations in APC/C subunits increased GLR1 in the ventral nerve cord, while the overexpression of ubiquitin decreased GLR1 in synapses. APC/C mutants have increased synaptic strength and that caused defects in locomotion. However, based on amino-acid sequence analysis GLR1 seems to be unlikely a direct target of degradation of APC/C and the authors hypothesized that it is possible that GLR1 might be associated to a scaffolding protein that is targeted for ubiquitination (Juo and Kaplan, 2004).

Moreover, in the mammalian brain in rodents, a role of APC/C-Cdh1 in synaptic plasticity was shown. It is involved in the regulation of homeostatic plasticity, which is the counteraction on synaptic strength to unrestrained changes and thereby the neuronal output is maintained. This occurs when chronic elevation of synaptic activity reduces the amplitude of miniature excitatory postsynaptic currents (mEPSC). EphA4 belong to the Eph receptor family that bind ephrins, and that are involved in synaptic plasticity and memory by regulating excitatory neurotransmission and play a role in cytoskeleton remodelling. They are activated by elevated synaptic activity. This leads to phosphorylation of EphA4, which causes its association to APC/C-Cdh1 and thereby targets GluR1 for degradation, resulting in an attenuation of the mEPSC amplitude. In neurons *in vitro* the depletion of cdh1 prevented the EphA4-dependent degradation of GluR1 (Fu et al., 2011).

In *Drosophila*, APC/C subunits and cdh1 are located at neuromuscular synapses. Loss of function of APC/C subunits leads to overgrowth of synaptic boutons. That was accompanied by altered synaptic transmission and lead to an increase in the amount of postsynaptic glutamate receptors. This was correlated to an increase in Liprin-alpha, a possible substrate of APC/C (van Roessel et al., 2004).

APC/C-Cdh1 and LTP

Li et al. (2008) showed that APC/C-Cdh1 has a role in learning and memory. In this study cdh1 deficient mice were analysed. The lack of cdh1 (a gene-trap construct was inserted in intron 5 of cdh1) causes early lethality in homozygous mice. In heterozygous mice, where a reduction of cdh1 of 50% had occurred, late-phase long-term potentiation (LTP) in the hippocampus was impaired. Furthermore, they showed defects in contextual fear-conditioning (Li et al., 2008).

In a conditional knockout model, in which cdh1 was specifically eliminated in neurons from the onset of differentiation by using a neuron-specific enolase promotor, a role for cdh1 in long-term potentiation was confirmed. Hippocampal slices from cdh1 knock-out mice displayed reduced late-phase LTP. These animals exhibited impaired flexibility in behavioural tasks and reduced extinction of associative fear memory. However, in this model, spatial memory tasks were not affected (Pick et al., 2013).

In an alternative conditional knockout model for cdh1, based on a cre-lox system, cdh1 was eliminated in adult mice from excitatory neurons in the forebrain, to test the effects of post-developmental removal of cdh1. In coronal slices from the amygdala from these cdh1 knock-out mice, late-phase LTP was impaired compared to wildtypes when thalamic afferents were stimulated and recorded in the amygdala. After the LTP-inducing stimulation the proteins Shank1, a scaffolding

protein and the NMDAR subunit, NR2A, accumulated in the amygdala in the cdh1 knockout. Coherently, contextual and cued fear memory was impaired. However, in this cdh1 mouse model, no change in hippocampal LTP was detected (Pick et al., 2013).

APC/C-Cdh1 and LTD

Huang et al. (2015) reported for the first time a role of APC/C-Cdh1 in the regulation of LTD. They created a forebrain-specific conditional knockout of cdh1 (mice carrying Cre recombinase, which is expressed in neocortical and hippocampal excitatory neurons, under the control of the forebrain-specific driver Emx) and showed that metabotropic glutamate receptor (mGluR)-dependent LTD is impaired in the hippocampus in this mouse model. It was shown in the CA1 layer in the hippocampus that the induction of mGluR-dependent LTD is dysregulated, but not NMDAR-dependent LTD.

In this study it was also reported that the fragile X syndrome protein (FMRP) is a substrate of APC/C-Cdh1. FRMP governs the mGluR-dependent LTD. A major feature of the fragile X syndrome is exaggerated mGluR-dependent LTD. Surprisingly, mGluR-LTD is regulated by cdh1 in the cytoplasm rather than in the nucleus (Huang et al., 2015).

In the following Table 2.3, cdh1 knock-out models, which were discussed in the previous sections, are summarized. Most of them show phenotype defects related to the nervous system.

Cdh1 knock-out *(Fzr1* gene)	Description	Phenotype defetcs	Reference
Gene-trap (gt) construct, inserted into intron 5 of *Fzr1* , generating a dysfunctional allele of *Fzr1*	homozygous mice $Cdh1^{gt/gt}$ (intercrossed heterozygous mice $Cdh1^{gt}$)	early embryonic lethality (died at ~ E9.5), replicative senescence prematurely of fibroblasts	Li et al., 2008
	heterozygous $Cdh1^{gt}$ (50% cdh1 reduction)	defects in hippocampal late phase LTP, deficient in contextual fear-conditioning	Li et al., 2008
Two loxP sites eliminate exons 2 and 3 from the F*rz1* gene, cre recombinase expressed under the Sox2 promoter	conditional cdh1 knockout mice, embry-restricted Cdh1 knock-out	loss of genomic stability, increased susceptibility to spontaneous tumours	García-Higuera et al., 2008
		replicative stress, p53-mediated apoptotic death, alterations in neurogenesis resembling microcephaly	Delgado Esteban et al., 2013
Two loxP sites eliminate exons 2 and 3 from the F*rz1* gene, cre recombinase expressed under nestin regulatory sequences	conditional cdh1 knockout mice, knock out restricted to the developing nervous system	hypoplastic brain and hydrocephalus	Eguren et al., 2013
Two loxP sites eliminate exons 2 and 3 from the *Frz1* gene, cre recombinase expressed under a CaMKII promoter	conditional cdh1 knockout mice, deletion of cdh1 in excitatory neurons in the adult hippocampus and forebrain late in brain development	impaired memory, impaired long-term potentiation in amygdala slices	Pick et al., 2013
Two loxP sites eliminate exons 2 and 3 from the Frz1 gene, cre recombinase exressed under a neuron-specific enolase promoter	conditional cdh1 knockout mice, restricting neuronal cdh1 expression from the beginning of development in neurons	impaired behavioral flexibility and extinction of previously consolidated memories, impaired long-term potentiation in hippocampal slices	Pick et al., 2013
Two loxP sites eliminate exons 2 and 3 from the Frz1 gene, Cre recombinase expressed under the control of the forebrain-specific driver Emx	conditional cdh1 knockout mice, deletion in neocortical and hippocampal excitatory neurons but not GABAergic interneurons	profoundly impaired induction of mGluR-dependent long-term depression in the hippocampus	Huang et al., 2015

Table 2.3 | **Summary of cdh1 knock-out mouse models and their phenotype defects in the nervous system.**

2.2.4. Functions of APC/C-Cdc20 in the nervous system

The regulation of synapse development depends on ubiquitin-proteasome pathways, however it was not clear which E3 ubiquitin ligases are involved in the regulation of presynaptic differentiation (DiAntonio and Hicke, 2004).

It was shown in the rat cerebellar cortex and in primary post-mitotic neurons that APC/C-Cdc20 controls presynaptic differentiation by targeting the transcription

factor NeuroD2 for degradation. The target gene of NeuroD2, Complexin II, acts at presynaptic sites to suppress presynaptic differentiation. This finding identifies the ubiquitin signalling pathway APC/C-Cdc20 as a major regulator of neuronal plasticity and connectivity in the brain (Yang et al., 2009).

Kim et al. (2009) discovered that APC/C-Cdc20 is required for dendrite morphogenesis in post-mitotic neurons in the mammalian brain. It was shown that Cdc20 promotes growth and maintenance of dendritic arbores. It is enriched at the centrosome in neurons, where it is regulated by the class II b histone deacetylase HDAC6. In this study they also identified Id1 as a target of APC/C-Cdc20, which inhibits dendrite growth and is localized at the centromere (Kim et al., 2009; Puram et al., 2010).

2.3. Alzheimer's Disease: A Short Introduction

The majority of AD cases arise sporadically. Only in 1-5% of all cases is the disease inherited in an autosomal dominant pattern. Specific gene defects, like those of amyloid beta precursor protein (APP) or presenilins 1 and 2 (PS1 and PS2), were identified. Mutations in any of these genes are sufficient to cause a heritable form of AD. The majority of mutations in these genes influence β-site APP-cleaving enzyme (BACE1) and γ-secretase cleavages, which produce the neurotoxic peptide amyloid $beta_{1-42}$ (Aβ) (Price et al., 1998; Purves et al., 2004; Golde et al., 2011). In sporadic AD cases, mutations in certain alleles of the Apo E gene are known to increase the risk for AD (Bertram et al., 2008; Perrin et al., 2009).

However, there is a common pathogenic cascade of anomalies in AD, which results from both inherent and sporadic forms of AD. The pathological hallmarks of AD are the deposition of plaques of amyloid peptides and the formation of

neurofibrillary tangles (NFTs). The first of the two main hypothesis about AD describes the “amyloid cascade” as a common denominator of AD. It proposes that the accumulation of the toxic peptide Aβ is critical to the onset of the pathogenesis of AD. In neurons, APP is cleaved by β- and γ-secretases in endocytic compartments and in the plasma membrane, producing Aβ. These peptides are liberated to the extracellular space and where they form a major component of amyloid plaques (Buxbaum et al., 1998). Although these observations suggest that the accumulation of Aβ is the major initiator of the disease, the density of NFTs correlates more with the severity of the dementia. NTFs are intracytoplasmic inclusions in cell bodies, proximal dendrites and axons of affected neurons. They are mainly constituted by hyper-phosphorylated aggregates of the microtubule-associated protein tau. In normal conditions tau stabilizes tubulin and is therefore critical for microtubule assembly and stability. It was suggested that there might be a various molecular signalling connection between Aβ and tau pathology, whereby Aβ might initiate or enhance the phosphorylation of tau (Lloret et al., 2015).

Additional to these pathological hallmarks of AD, several other alterations have been described in the disorder, such as oxidative stress, ectopic cell cycle re-entry, impaired LTP, excitotoxicity and dysregulations of various signalling pathways. Some of these events can be related to altered APC/C activity, and we suggest that this might play a crucial role in the onset and in the pathophysiology of the disease.

2.3.1. The ectopic cell cycle in AD and its relation to APC/C-Cdh1

Once cells are committed to differentiate, they enter in the G0 phase in the cell cycle in a quiescent state. Neurons in adult brain are terminally differentiated cells are generally incapable of re-entering the cell cycle. This quiescent state underlies an active degradation of cell cycle related proteins. The re-entrance in an erroneous

departure of G0 into the G1 phase and S phase was related to neurodegeneration (Almeida et al., 2005).

It has been reported that the reactivation of an ectopic cell cycle in neurons occurs in AD. These neurons exhibit elevated levels of cell cycle markers compared to age matched controls (Smith et al., 1995; McShea et al., 1997; Nagy et al., 1997; Vicent et al., 1997). Moreover, progression through the S-phase of these neurons has been demonstrated, as they have elevated markers of DNA replication (Bonda et al., 2009).

In neuron cell culture, Aβ induces cell cycle re-activation resulting from increased levels of cdk's and cyclins. Neurons progress through the S-phase and replicate their DNA, but enter into apoptosis before mitosis (Copani et al., 2007). APC/C-Cdh1 targets the degradation of cyclin B1, a cell cycle protein that accumulates in neurons in AD brains (Vicent et al., 1997).

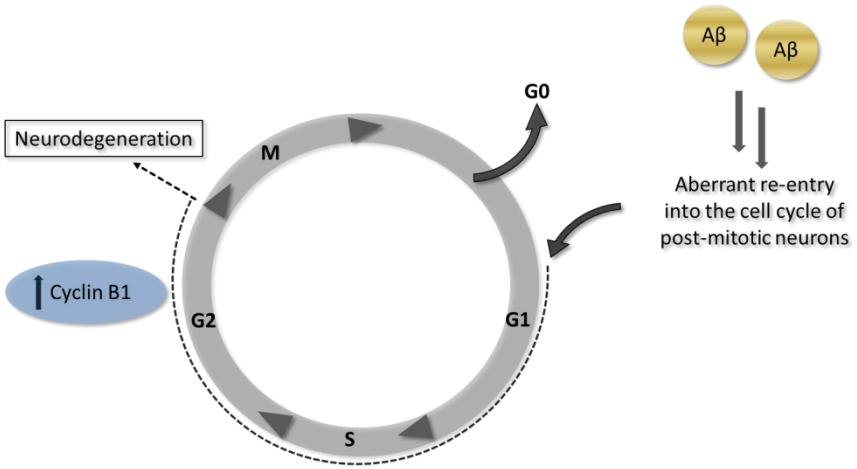

Figure 2.5 | **Schematic representation of the ectopic cell cycle re-entry in post-mitotic neurons**. Under normal conditions terminally differentiated neurons exit the cell cycle and remain in G0. Toxic

stimuli like Aβ, can induce cell cycle re-entry. In G2, cyclin B1 accumulates, before neurons undergo mitosis they enter into apoptosis.

A protein that has an important role in keeping up a post-mitotic status of neurons is cdk5, a non-traditional cdk. It is highly expressed in differentiated neurons and it is involved in the regulation of cell differentiation and migration, synapse formation and synaptic plasticity (Lopes et al., 2011). It was shown that neurons re-enter the cell cycle after Aβ treatment, and that this was accompanied by a translocation of cdk5 from the nucleus to the cytoplasm. When the nuclear export of cdk5 is blocked pharmacologically, neurons do not re-enter the cell cycle after the treatment. In $cdk5^{-/-}$ mutant brains of mice, cell cycle re-entry occurred in post-mitotic neurons, giving further evidence that cdk5 acts as a cell cycle suppressor (Zhang et al., 2008). Furthermore, cdk5 was shown to be activated in neurons in culture by an excitotoxic stimulus. Maestre et al. (2008) showed that cdk5 phosphorylates cdh1 which stabilizes cyclin B1 and induces neuronal apoptosis.

2.3.2. Impaired neurogenesis in AD and its relation to APC/C-Cdh1

A growing body of evidence suggests that neurogenesis is impaired in AD. Enhanced neurogenesis in the adult hippocampus represents an early critical event in the course of AD (Mu and Gage, 2011). An increased number in proliferating progenitors was detected in APP/PS1 using bromodeoxyuidine (BrdU) staining (Yu et al., 2009). However, although proliferation of neuronal progenitors is increased, it was shown that the newly generated neurons do not become mature neurons in the dentate gyrus of AD brains (Li et al., 2008).

Furthermore, Crews et al. (2011) showed that aberrant cdk5 signalling is involved in defects in neurogenesis in AD. In an *in vitro* model of neuronal progenitor cells,

which were exposed to Aβ and infected with a viral vector expressing p35, they observed neurite outgrowth and impaired maturation. This was reversed by inhibition of cdk5. Moreover, in a transgenic mouse model of AD *in vivo*, the inhibition of cdk5 rescued impaired neurogenesis (Crews et al., 2011).

It has been reported that cdk5 phosphorylates cdh1 (Maestre et al., 2008), suggesting that the ubiquitin ligase which has a major role as a regulator of neuronal progenitors, might be involved in impaired neurogenesis in AD. Furthermore, enhanced proliferation of neuronal progenitors together with decrease in mature neurons, which has been observed in AD, is in line with the phenotype of cdh1 knock-out models.

2.3.3. Oxidative stress in AD and its relation to APC/C-Cdh1

AD has long been related to the occurrence of oxidative stress. Aβ has been shown to cause oxidative stress through the interference with normal electron flow caused by the interaction of Aβ with heme groups in the mitochondrial membrane. This results in the production of reactive oxygen species and causes damage (Lloret et al., 2008; Viña et al., 2011). Besides the direct cause of ROS by Aβ, the toxic peptide induces alterations in various signalling ways in neurons, which were related to oxidative stress and neurodegeneration. Among these, it was shown that the downregulation of APC/C-Cdh1 induces impaired regulation of the oxidant and antioxidant homeostasis in neurons.

Neurons are the cells in the brain which have the highest energy consume with a comparatively low rate of glycolysis. They metabolize glucose through the pentose-phosphate pathway (PPP), which helps them to maintain their antioxidant status by regenerating reduced glutathione. They are unable to upregulate glycolysis due to low levels of 6-phosphofructo-2-kinase/fructose-2, 6-

bisphosphatase-3 (pfkfb3), the enzyme that generates fructose-2, 6-bisphosphate. This is the most potent activator of of the 6-phosphofructo-1-kinase (pfk1), one of the main regulators of glycolysis. Pfkfb3 levels are downregulated by APC/C-Cdh1. The inhibition of cdh1 in neuron culture leads to increased levels of pfkfb3 resulting in activation of glycolysis. Less glucose is used for the PPP, which results in oxidative stress and apoptosis (Herrero-Mendez et al., 2009). Furthermore, it was shown that an excitotoxic stimulus inhibits APC/C-Cdh1 activity, leading to an accumulation of pfkfb3, causing neurodegeneration (Rodriguez-Rodriguez et al., 2012).

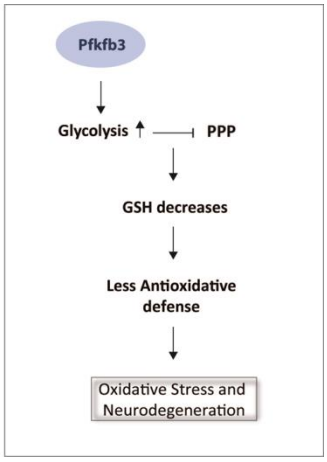

Figure 2.6 | **Schematic representation of pfkfb3-induced neurodegeneration**. High levels of pfkfb3 stimulate glycolysis, which reduces glucose metabolism through the pentose-phosphate pathway (PPP). Reduced glutathione (GSH) is a potent antioxidant enzyme. This causes oxidative stress and neurodegeneration in neurons.

2.3.4. Excitotoxicity in AD and its relation to APC/C-Cdh1

The amino acid L-glutamate is the major excitatory neurotransmitter in the brain and spinal cord. It is mostly synthesized in neurons through the following ways:

- The most prevalent precursor of glutamate in synaptic terminals is glutamine. The conversion from glutamine to glutamate is driven by the phosphate activated glutaminase in mitochondria. Glutamate directed to act as neurotransmitter is compartmentalized in synaptic vesicles. Glutamate is

released at neuronal terminals and the majority of glutamate is taken up by surrounding glia cells (transport by e.g. GLT). There, glutamate is converted to glutamine through glutamine synthetase, a cytosolic enzyme of astrocytes and oligodendrocytes which is not expressed in neurons. Glutamine, which does not have a neurotransmitter function, is then transported (SN1/SN2 transporters) to neurons where it is again converted to glutamate. This cycle is called the 'glutamate-glutamine cycle'.

- Reuptake of neurons at glutamatergic nerve terminals has been shown for a GLT isoform.
- Glutamate can also be synthesized by transamination. Glucose is converted to α-ketoglutarate in the tricarboxylic (TCA) cycle, which can be converted to glutamate.

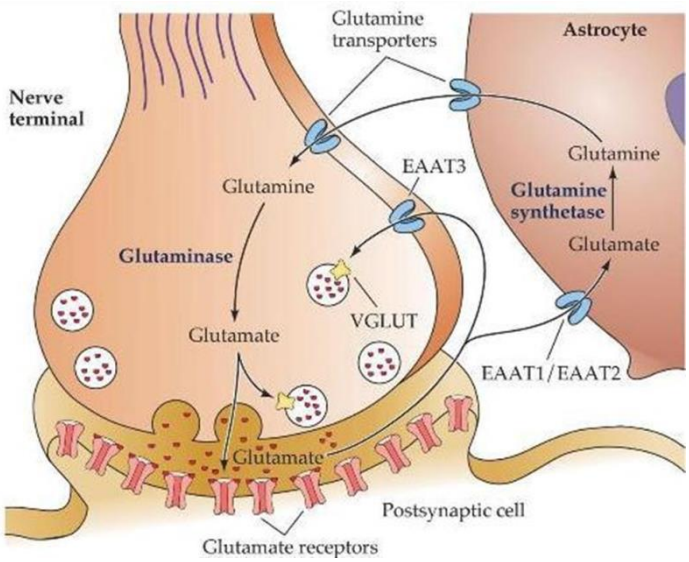

Figure 2.7 | **Glutamate-Glutamine metabolism in neurons and astrocytes**. Figure from: Synaptic Plasticity: Gliotransmission and the tripartite synapse (Santello et al., 2012).

Glutamate binds to receptors that can be divided into two broad categories: ionotropic (iGluR) and metabotropic (mGluR) receptors. iGluR are ligand gated channels, where the channel opens directly by ligand binding, while mGluR are G-protein coupled receptors that gate channels indirectly through second messengers. There are three major subtypes of iGluRs: N-methyl-D-aspartate (NMDA), α-amino-3-hydroxy-5-methyl-4-isoxazolepropionic acid (AMPA) and kainate receptors.

The NMDA receptor is widespread throughout the CNS. It mediates post-synaptic Ca^{2+} as well as Na^{+} and K^{+} influx when activated by glutamate and glycine. The intracellular rise of Ca^{2+} activates various calcium-dependent signalling cascades. These biochemical signals can lead to long lasting changes in synaptic strength. Long term synaptic plasticity is important during development and also for the regulation of neuronal circuits in the adult brain involved in memory storage. In particular, long term potentiation (LTP), mediated by e.g. the calcium-calmodulin-dependent protein kinase II (CaMKII) depends on glutamate receptor activation (Kandel et al., 2013; Brady et al., 2011).

Excitotoxicity, refers to the injuries caused by excessively high concentration or prolonged exposure of glutamate. It is a pathological phenomenon in various diseases, such as stroke, Huntington's disease and AD. Increased glutamate causes an overload of Ca^{2+} in neurons which is neurotoxic, leading to degradation of proteins, membranes and nucleic acids, induces oxidative stress, altered synaptic plasticity, apoptosis and necrosis (LaFerla el al., 2002; Dong et al., 2009) (see Figure 2.8).

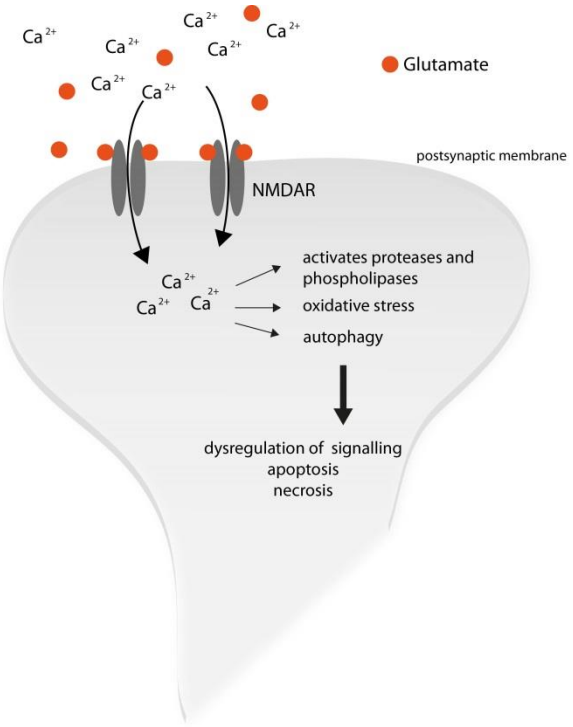

Figure 2.8 | **Schematic summary of excitotoxicity in neurons.** Excessive glutamate levels lead to prolonged opening of glutamate receptors (e.g. NMDA receptors) and increased entrance of Ca^{2+} ions. This induces various processes leading to neurotoxicity.

Furthermore, some signalling cascades have been described, which are altered by excitotoxicity. Among these, one can be linked to APC/C-Cdh1. High levels of intracellular Ca^{2+} activate calcium dependent proteases and phospholipases, which alter the cyclin dependent kinase 5 (cdk5) signalling. The Ca^{2+}-dependent protease calpain stimulates the cleavage of p35 to the more stable p25, an activator of cdk5. Excessive cdk5-p25 activation can, among other toxic effects, lead to hyper-phosphorylation of cytoskeletal proteins, like tau. It was also reported that a dysregulation of Ca^{2+} homeostasis enhances the production of Aβ (Bordji et al., 2011).

Therefore, cdk5 has been proposed to be an attractive candidate to link Aβ toxicity and tau phosphorylation (Lopes and Agostinho, 2011; Lloret et al., 2015). Additionally, increased cdk5 levels lead to an activation of further catabolic enzymes, which degrade neuronal structural proteins that can lead to a cytoskeletal breakdown (Hynd et al., 2004).

Experimental evidence has shown that Cdk5-p25 phosphorylates cdh1 in excitotoxicity, which demonstrates a direct link between the AD-related kinase cdk5 and the ubiquitin ligase APC/C-Cdh1 (Maestre et al., 2008).

2.3.5. LTP impairment in AD and its relation to APC/C-Cdh1

Defects in synaptic plasticity often appear in neurobiological disease, such as in AD (Chen et al., 2002; Koch et al., 2012). It was shown in APP/PS1 mice that they have defects in LTP (Gengler et al., 2010). Alterations of APC/C-Cdh1 have been widely related to impaired synaptic plasticity, LTP and LTD (see section 2.2.3).

EphA4 receptors, which are involved in excitatory neurotransmission, interact with APC/C-Cdh1 to stimulate the degradation of GluR1. Simón et al. (2009) reported in mouse models of AD changes in hippocampal Eph receptors appear before the onset of memory decline. They found reduced EphA4 and EphB2 levels in the hippocampus (Simón et al., 2009). These data suggest that the interaction of EphA4 and APC/C-Cdh1 signalling might be involved in LTP deficiency in AD models. However, more research will be needed to clearly demonstrate their role in LTP impairment in AD.

2.4. Summary of APC/C Substrates in the Nervous System

In the previous sections major functions of APC/C and their substrates in the nervous system were discussed, and how some of them are related to AD. Based on these data we built up a hypothesis that paved the way for the investigation of APC/C in AD in this project. At the end of this introductory chapter, a graphical summary of APC/C and its substrates in the nervous system is presented (Figure 2.9).

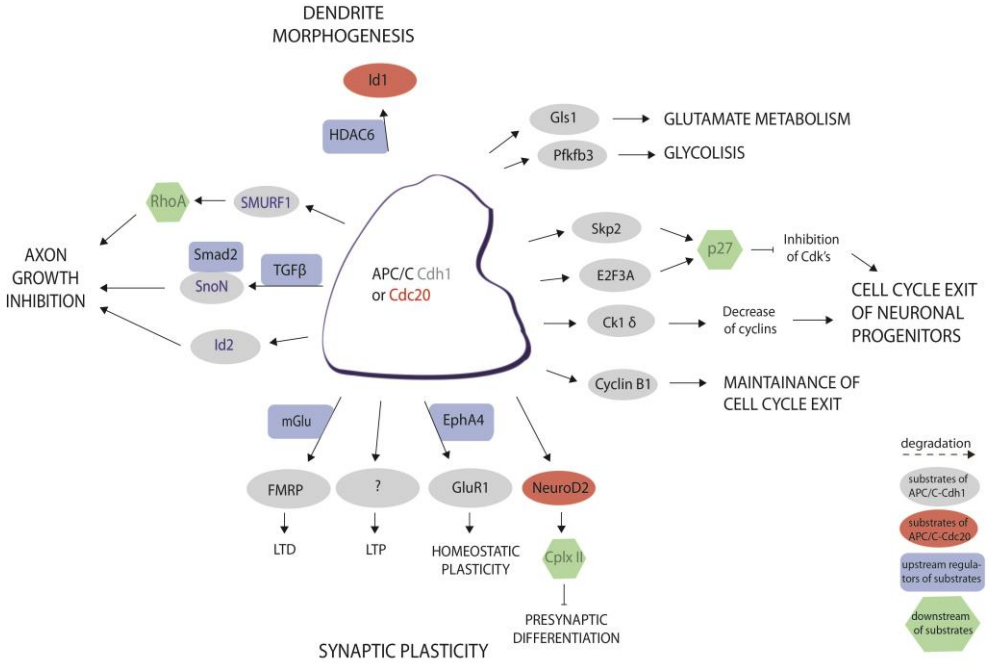

Figure 2.9 | **Summary of APC/C-Cdh1 and APC/C-Cdc20 substrates in the nervous system.** They are implicated in regulation of axon growth, dendrite morphogenesis, glutamate metabolism and glycolysis, neurogenesis, maintenance of cell cycle exit, presynaptic differentiation and synaptic plasticity.

3. HYPOTHESIS & OBJECTIVES

Many experimental evidences have shown a major role of APC/C in the nervous system, underlying a complex regulation. We spotted a link between the ubiquitin ligase and AD, when it was described that cdk5 phosphorylates cdh1 in excitotoxicity, a kinase which has been shown to be dysregulated in AD. Furthermore, accumulation of various targets of APC/C has been related to neurodegeneration. Based on these facts, we hypothesized that APC/C-Cdh1 might be involved in the pathophysiology of AD.

First, we were interested in evaluating whether Aβ affects cdh1 protein steady state levels and the activity of the ubiquitin ligase *in vitro*. Then, it should be determined whether this is mediated by cdk5 and if other kinases or phosphatases regulate cdh1 in neurons.

The second main goal was to describe if there was a relevant regulation of APC/C-Cdh1 of glutaminase in neurons, which was previously described as a target of the ubiquitin ligase in lymphocytes (Colombo et al., 2010). The regulation of glutaminase by APC/C might be of potential great importance, as this would link APC/C activity with glutamate metabolism in neurons. Alterations in glutamate metabolism and excitotoxicity play a major role in AD. Then we addressed if the impaired APC/C signalling caused neurodegeneration.

This can be carried out by in in vitro assays, but finally this should be tested in the mouse model APP/PS1, which is commonly used in AD research. Based on this hypothesis, we defined the objectives listed below.

1. Determination of the effect and mechanism of Aβ on the cdh1 steady state protein level in neurons *in vitro*.

2. Analysis of upstream regulators of cdh1 in neurons *in vitro*.

3. Measurement of protein levels of AD-related substrates of APC/C-Cdh1 in neurons *in vitro* upon Aβ treatment.

4. Determine the regulation of the ubiquitin ligase of its substrate glutaminase in neurons and measure further downstream effects of this regulation on glutamate, ammonia and Ca^{2+} levels.

5. Test whether APC/C-Cdh1 and glutaminase dysregulation is involved in neurodegeneration.

6. Investigate the effect of Aβ and glutamate on APC/C-Cdh1 and its substrates *in vivo*.

4. MATERIAL & METHODS

4.1. Material and Equipment

4.1.1. Buffers, solutions and mediums

- **APS 10%** *[10% (w/v) ammonium peroxo disulphate p.a.]*

  Dilute 1 g ammonium peroxo disulphate p.a. in 10 ml dH_2O, stored in 1 ml aliquots at 4°C.

- **Blocking solution** *[5% (w/v) non-fat dry milk or BSA]*

  Dilute 5 g non-fat dry milk or BSA in 100 ml *1x TBST*. Prepared fresh, stored at 4°C.

- **Immunoblot transfer Buffer** *[25 mM Tris, 190 mM glycine, 20% (v/v) methanol p.a.]*

  Add 3 g Tris, 14,4 g glycine and 200 ml methanol p.a. to 1000 ml dH_2O, stored at RT.

- **Lysis Buffer** *[50 mM Tris, 2% (w/v) SDS, 10% (v/v) glycerol]*

  Dilute 0,927 g Tris in 100 ml ddH_2O and bring it to pH 6.8. Take 83 ml and add 2 g SDS and 10 ml glycerol.

- **SDS 10%** *[10% (w/v) sodium dodecyl sulfate p.a.]*

  Dilute 1 g *sodium dodecyl sulfate* p.a. in 10 ml dH_2O, stored in 1 ml aliquots at RT.

- **SDS gel-loading buffer 1x** *[60 mM Tris HCl pH 6.8, 3% (w/v) SDS, 10% (v/v) glycerol, 0,005% (w/v) bromophenol blue, 5% (v/v) 2-mercaptoethanol]*

  Add 0,6 ml 1 M Tris HCl pH 6.8, 1,5 ml 20% (w/v) SDS, 1 ml glycerol, 50 µl 1% (w/v) bromophenol blue and fill up to 9,5 ml dH_2O, stored at RT. Prior to use 500 µl 2-mercaptoethanol is added.

- **Separating gel acrylamide mix 12,5%** *[1,5 M Tris pH 8.8, 40% (w/v) acrylamide/ bisacrylamide 29:1, SDS 10%, APS 10%, TEMED]*

  Add 1686 µl dH_2O, 1000 µl Tris 1,5 M, 1250 µl acrylamid/bisacrylamid, 40 µl SDS, 20 µl APS, 4 µl TEMED, stored at 4°C.

- **Stacking gel acrylamide mix 4%** *[0,5 M Tris pH 6.8, 40% (w/v) acrylamide/ bisacrylamide 29:1, SDS 10%, APS 10%, TEMED]*

  Add 1880 µl dH_2O, 750 µl Tris 0,5 M, 300 µl acrylamid/bisacrylamid, 30 µl SDS, 30 µl APS, 3,8 µl TEMED, stored at 4°C.

- **Transfer Buffer** *[Tris 25 mM, 192 mM glycine, 20% (v/v) methanol]*

  Add 6,06 g Tris, 28,8 g glycine, 400 ml methanol and fill up to 2000 ml dH_2O.

- **TBS** *[10 x TBS]* pH 7.6

  Add 24,2 Tris and 80 g NaCl, fill up to 1000 ml dH_2O.

- **TBS-T 1x** *[0,1% TweenÒ]*

  Dilute 100 ml 1x TBS in 900 ml dH_2O, add 1 ml Tween, prepared fresh.

- **Tris-glycine electrophoresis buffer** *[25 mM Tris, 190 mM glycine, 0,1% (w/v) SDS]*

  Add 15 g Tris, 71,88 g glycine, 5 g SDS and fill up to 5000 ml dH_2O, stored at RT.

- **Tris HCl** *[1 M]*, pH 6.8

  Add 60,55 g Tris to 400 ml dH_2O and adjust to pH 6.8 with HCl conc., fill up to 500 ml with dH_2O, stored at RT.

- **Tris HCl** *[1.5 M]*, pH 8.8

  Add 90,83 g Tris base to 400 ml dH_2O and adjust to pH 8.8 with HCl conc., then fill up to 500 ml with dH_2O, stored at RT.

- **Ponceau S staining Solution** *[0,2% (w/v) Ponceau S, 3% (w/v) TCA]*

  Add 2 g Ponceau S (3-hydroxy- 4-(2-sulfo-4-[sulfophenylazo]-phenylazo)-2,7-aphthalene disulphuric acid, 30 g trichloro acetic acid (TCA) and fill up to 1000 ml.

- **Phosphate-Buffered Saline** (PBS), pH 7.4, 10010-056, *Gibco.*
- **Dulbecco's Modified Eagle Medium 1x** (DMEM), 41965-062, *Gibco.*
- **Dulbecco's Modified Eagle Medium** 1x (DMEM), 11960-044, *Gibco.*
- **Fetal Bovine Serum** (FBS), Qualified E.U. Approved 10270-106, *Gibco.*
- **Penicillin-Streptomycin Antibiotics**, 15140-122, *Gibco.*

4.1.2. Reagents and kits

- Fluorescence mounting medium, S3023**,** *DAKO.*
- Folin & Ciocalteu's phenol reagent, F9252-500ML (18 ml added to 80 ml ddH_2O), *Sigma.*
- High Capacity cDNA Reverse Transcription Kit, 4368814, *Thermo Fisher*.
- High Pure PCR Template Preparation Kit, 11796828001, *Roche*.

- Luminata Classico Western HRP Substrate, WBLUC0500, *Millipore.*
- Lowry Reagent, L3540-1VL (2 g added to 40 ml ddH_2O), *Sigma.*
- Maxima SYBR Green/ROX qPCR Master Mix (2X) K0223, *Thermo Scientific.*
- Poly-l-lysine solution *[0,01%]*, P4707, *Sigma-Aldrich.*
- Restore Western Blot Stripping Buffer, 21059, *Thermo Scientific.*
- TRIzol Reagent, 15596-026, *Life technologies*.
- VECTASHIELD Mounting Medium with DAPI, H1200, *Vector Laboratories*.
- Ammonia Assay Kit, AA0100, *Sigma.*
- Apoptosis Detection Kit FITC, ANXVKF-100T, *Immunostep.*
- NE-PER® Nuclear and Cytoplasmic Extraction Reagents, 78835, *Thermo scientific.*

4.1.3. Fluorochromes

- Annexin V: Alexa Fluor® 555 (555/565), A35108, *Invitrogen Molecular Probes*.
- SYTOX® Green Nucleic Acid Stain, S7020, *Invitrogen Molecular Probes.*
- Fluo-4, AM, cell permeant, F-14201, *Life Technologies*.
- Hoechst, H3570, *Invitrogen Molecular Probes.*

4.1.4. Proteins

Primary Antibodies

CDC20, 4823, *Werfen*, molecular wt.: 51 kDa, source: rabbit. In this work this antibody was used for detection of cdh1 in immunoblots of samples of rat primary culture neurons (dilution: 1:1000).

Cdh1, NBP1-54465, *Novus Biologicals*, molecular wt.: 55 kDa, source: mouse. In this work this antibody was used for detection of cdh1 in immunoblots of samples of rat primary culture neurons (dilution: 1:500).

Cdh1, NBP2-15840, *Novus Biologicals*, molecular wt.: 55 kDa, source: rabbit. In this work this antibody was used for detection of cdh1 in immunohistochemical preparations (dilution 1:100) and for immunocytochemistry of rat primary neurons (1:100).

Cdh1, ab3242, *Abcam*, molecular wt.: 55 kDa, source: mouse. In this work this antibody was used in to detect cdh1 in immunoblots (dilution 2 µg/ml) of samples of mouse brain homogenates.

Cdh1, 34-2000, *Invitrogen*, molecular wt.: 55 kDa, source: rabbit. In this work this antibody was used for detection of cdh1 in immunohistochemical preparations (dilution: 1:100).

Cyclin B1, 4138, *Cell Signaling Technology*, molecular wt.: 60 kDa, source: rabbit. In this work this antibody was used for detection of cyclin B1 in immunoblots (dilution: 1:1000) of samples of rat primary culture neurons.

Cdk5, 2506, *Cell Signaling Technology*, molecular wt.: 30 kDa, source: rabbit. In this work this antibody was used for detection of cdk5 in immunoblots (dilution: 1:1000) of samples of rat primary culture neurons.

p25/p35, 2680, *Cell Signaling Technology*, molecular wt.: 25, 35 kDa, source: rabbit. In this work this antibody was used for detection of p25/p35 in immunoblots (dilution: 1:1000) of samples of rat primary culture neurons.

Glutaminase 1, 12855-1-AP, *Proteintech*, molecular wt.: 65 kDa, 58 kDa, source: rabbit. In this work this antibody was used for detection of glutaminase 1 in immunoblots (dilution: 1:1000) of samples of rat primary culture neurons and of mouse brain homogenates.

Histon H3, ab1791, *Abcam*, dilution: 1:50000, molecular wt.: 17 kDa, source: rabbit. In this work this antibody was used for detection of histone H3 in immunoblots (dilution: 1:1000) of samples of the nuclear fractions of rat primary culture neurons.

MAP2, M9942, *Sigma*, dilution: 280 kDa, 70 kDa, source: mouse. In this work this antibody was used for detection of Map2 in immunocytochemical preparations (dilution 1:100) of rat primary neurons.

Pfkfb3, 13763-1-AP, *Proteintech*, molecular wt.: 75 kDa, source: rabbit. In this work this antibody was used for detection of pfkfb3 in immunoblots (dilution: 1:300) of samples of rat primary culture neurons.

α-Tubulin, sc-8035, *Santa Cruz Biotechnology*, molcular wt.: 55 kDa, source: mouse. In this work this antibody was used for detection of tubulin in immunoblots (dilution: 1:1000) of samples of rat primary culture neurons and samples mouse brain homogenates.

β-actin, A1978, *Sigma Aldrich*, dilution: 1:1000, molecular wt.: 42 kDa, source: mouse. In this work this antibody was used for detection of actin in immunoblots (dilution: 1:1000) of samples of the nuclear and cytosolic of fractions of rat primary culture neurons.

Secondary Antibodies

Anti-Mouse IgG, H&L Chain Specific Peroxidase Conjugate 401215, *Calbiochem*, dilution: 1:3000.

Anti-Rabbit IgG, HRP-linked Antibody 7074, *Cell Signaling*, dilution: 1:3000.

Anti-Rabbit IgG (H+L), $F(ab')_{2,}$ Fragment (Alexa Fluor 488 Conjugate), 4412, dilution: 1:1000, *Cell Signaling.*

Anti-Mouse IgG (H+L), $F(ab')_{2,}$ Fragment (Alexa Fluor 647 Conjugate), 4410, dilution: 1:1000, *Cell Signaling*.

Anti-Rabbit IgG Alex Fluor 700, A21038, *Molecular Probes*, dilution: 2-5 fluorophore molecules per IgG molecule.

Peptides

Amyloid-beta (1-42), Human RP10017-1, *Gene Script.*

Amyloid-beta (1-42), 20276, *AnaSpec*.

Enzymes

L-Glutamic Dehydrogenase from bovine liver, G2626, *Sigma Aldrich*.

4.1.5. Inhibitors

Compound 968 (glutaminase inhibitor), 352010, *Merk Millipore Calbiochem*.

MG-132 (proteasome inhibitor), M7449, *Sigma*.

proTAME (APC/C inhibitor), I-440, *Boston Biochem*.

Roscovitin (cdk inhibitor), R7772, *Sigma*.

4.1.6. Equipment

- Analogue Block Heater, Stuart SBH130, S*tuart.*
- Balance AHZ-600, *Gram.*
- Biomolecular imager, ImageQuant™ LAS 4000, *GE Healthcare Bio-Sciences.*
- Confocal laser-scanning microscope, TCS SP2 scanning multiphoton and confocal unit with an inverted DM1RB microscope, Ar-He-Ne, *LEICA Microsystems.*
- FACSVerse™ flow cytometer, *BD Biosciences.*
- Homogenizer Rw20 DZM, *Janke & Kunkel.*
- Fast Real-Time PCR System, 7900HT, *Applied Biosystems.*
- Incubator Sanyo CO_2, MCO-19AIC, *Sanyo.*
- Lab-Tek II Chambered 1.5 German Coverglass System 155382, 155409, *Lab-Tek.*
- Microcentrifuge, Sigma 1-14, 90616, *Sigma.*
- Microscope cell culture, Eclipse Ts 100, *Nikon.*
- Mid bench centrifuge, Hettich Rotina 35R, *Labcare.*
- Nanodrop, 2000c, *Thermo Scientific.*
- PH Meter, GLP 21, *Crison.*
- Pipettes: Finnpipette F1 (0,2 µl – 2 µl), Finnpipette F1 (2 µl– 20 µl), Finnpipette F1 (20 µl – 200 µl), Finnpipette F1 (100 µl– 1000 µl), GH 65970 (1 µl– 10 µl), GH 78060 (10 µl – 100 µl), *Thermo scientific.*

- Platform shaker Duomax, 1030, *Heidolf.*
- Roller-mixer, 51788, *Labolan.*
- Spectrophotometer, cecil 3021, *Cecil.*
- TPP cell scraper, 99003, *TPP.*
- TPP centrifuge tubes, 91015 (15 ml), 91050 (50 ml), *TPP.*
- TPP seriological pipettes, 94005 (5 ml), 94010 (10 ml), 94024 (25 ml), *TPP.*
- TPP tissue culture flask, 90026 (growth area 25 cm^2), *TPP.*

4.2. Primary Culture of Cortical Neurons

Primary culture of cortical neurons was prepared from brains of Wistar rat fetus (14 days of gestation). Cortices were dissected mechanically, dispersed in Dulbecco's Modified Eagle Medium (DMEM) and filtered through a nylon net (90 μm pores). Per brain we added 5 ml standard culture medium (DMEM supplemented with 10% (v/v) fetal bovine serum (FBS) and 1% antibiotics Penicillin and Streptomycin mix (P/S)). Three ml of the medium containing cells were carefully poured on poly-L-lysine-covered T-25 flask (25 cm^2) and gently rocked, resulting in an average amount of cells of $1\text{-}2*10^4$ cells/cm^2. The culture flasks were incubated at 37°C in a 5% CO_2-containing atmosphere. Within 2 hours, the cells attached to the poly-L-lysine-covered culture flasks, and the supernatant was discarded, fresh standard culture medium was added and they were further incubated. Three days after plating the cells, cytosine-arabinosid (10 mM) was added to the culture medium, and one day later it was replaced by culture medium containing the half amount of cytosine-arabinosid, in order to inhibit proliferation of mitotic cells (e.g. glia cells, fibroblasts). The following day, the medium was removed and replaced by standard culture medium. After 6-7 days, we obtained a 95% pure neuron culture, which was used for treatments (see Figure 4.1). For

fluorescent microscopy, neurons were seeded on poly-L-lysine covered chambered coverglass plates. Culture and treatment conditions were accomplished as described above.

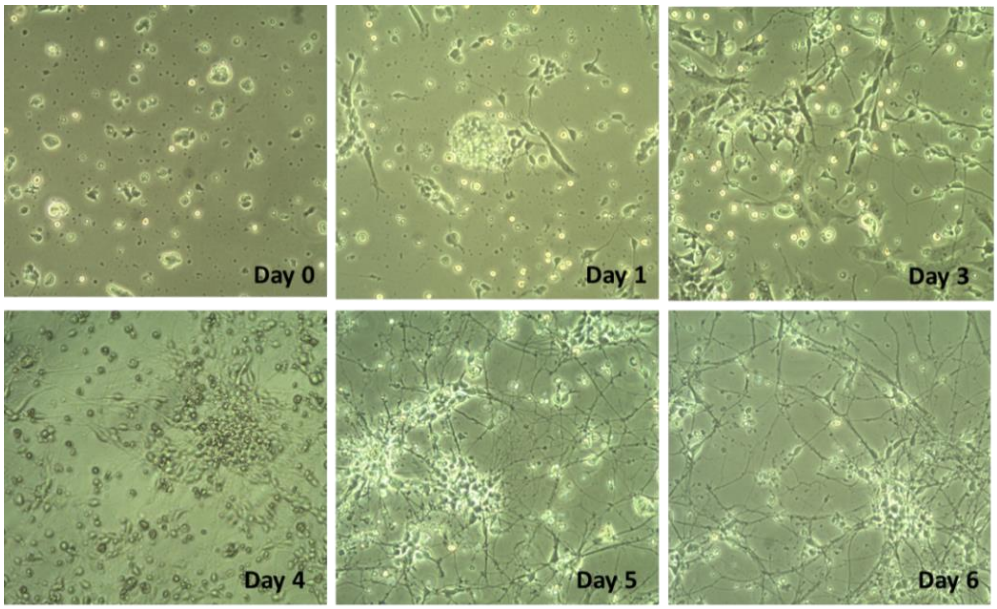

Figure 4.1 | **Light microscope images show the development of neurons from the first day of isolation to differentiated neurons**. On day 0 (photo was taken two hours after plating the cells) the cells were round and did not yet resemble neurons. After one day of culture, neurons started growing prolongations. After three days of culture we could observe further development of neuron cells and glia cells and cytosine-arabinosid was added to the culture medium. On the following day 4, the cells were incubated with medium containing the half concentration of cytosine. On day 5 the number of glia cells was clearly reduced and a further progression of growth of axonal and dendritic arbors of neurons was observed. On day 6 developed neurons were used for treatments.

4.2.1. Treatments of neurons in primary culture

Previously, oligomeric Aβ was prepared: an alkaline solution, 100 µl of NH_4 (1% in 1x PBS) or 20 µl DMSO, was added to 1 mg of $A\beta_{(1-42)}$, which dissolves immediately. Subsequently, 1x PBS was added to dilute the dissolved Aβ in total volume of 2216 µl and incubated the solution at 4°C for 24 h to allow the formation of oligomers. It was then used immediately or stored at -20°C and used within 2 months after preparation (Protocol for Aβ oligomer preparation was adapted from Teplow 2006, Dahlgren et al., 2002, Lambert et al., 1998).

The culture medium was replaced by fresh culture medium by the time of the treatments. The components were previously mixed with the culture medium and after addition, the plates were gently rocked. The neurons were treated at the following concentrations if not indicated otherwise: Aβ (5 µM) (amyloid-beta 1-42, 20276, AnaSpec, Fremont, USA), glutamate (500 µM) (G-1251, Sigma, St. Louis, USA), proTAME (12 µM) (I-440, BostonBiochem, Cambridge MA, USA), glutaminase inhibitor 'compound 968' (100 µM) (352010, Calbiochem, Nottingham, UK), cdk inhibitor 'roscovitine' (15 µM) (R 7772, Sigma, Missouri, USA); the incubation times are indicated in the figure legends.

4.2.2. Cdh1 silencing by siRNA interference in neurons in primary culture

For silencing of cdh1, ON-TARGETplus SMART pool silencing RNA (siRNA) was used with the target sequence 5' - UGAGAAGUCUCCCAGUCAG - 3' (Thermo Scientific, Rockford IL, USA). We used GenMuteTM siRNA Transfection Reagent, which is preoptimized for transfection of neurons in primary culture, (SL100568-PNN, SignaGen Laboratories, Ijamsville, USA) according to manufacturer's instructions. For a T-25 flask a total volume of 3 ml (medium plus containing reagents) was used. Sixty minutes before the transfection, the culture

medium was removed and fresh culture medium was added. The siRNA (90 pmol) was incubated with 1x transfection buffer (300 µl) and transfection reagent (9 µl) for 15 min at RT to let the transfection complex form. Then the transfection mix was added to the cells and incubated. The transfection medium was replaced by growth medium 5-8 h afterwards. The neurons were collected for analysis 48 h after the transfection.

Alternatively, we used Accell SMARTpool Fzr1 siRNA (E-100432-00-0050, Dharmacon), and Accell non-targeting siRNA as control (D-001910-01-20, Dharmacon): 1 µM siRNA per ml culture medium with reduced serum to 1% for 96 h, then the cells were collected for analysis.

4.2.3. Lysate preparation of neurons in primary culture

Sixteen to 24 h after the initiation of the treatments (if not indicated otherwise) the supernatant was collected and used for further analysis and the neurons were washed two times with 2 ml of 1x PBS. When the samples were collected for western blot analysis 100 µl of 1x lysis buffer were added to the cells in each flask and put on ice for 2 min. They were scraped from the flask surface and collected in tubes. The cell extracts were heated to 95°C for 10 min and stored at this stage at -80°C or directly used for protein determination.

One hundred µl 1x PBS were added to samples which were used for nucleus/cytosol separation or for glutamate determination. The cells were carefully scraped down and transferred into reaction tubes. Cell extracts in 1x PBS were directly preceded to nucleus and cytosol separation or stored at this stage at -80°C till use.

4.2.4. Separation of nucleus and cytosol

NE-PER Nuclear and cytoplasmic extraction reagents kit was used for separation of nucleus and cytosol according to manufacturer's instructions (REF Thermo Scientific). Histon and actin specific antibodies were used to demonstrate a successful separation of proteins from nucleus and cytosol.

4.3. Experimental Animals

Double transgenic mice APPswe, PSEN1dE9-85Dbo/J (APP/PS1) were used as an animal model for AD. Animals were maintained in the animal facility in the Central Investigation Unit in the Faculty of Medicine, University of Valencia. Mice were maintained individually under a 12:12-h dark-light cycle at 23±1˚C and 60% relative humidity, and were provided with a standard chow diet (PANLAB S.L.) and water *ad libitum*.

Transgenic mice and wild type mice from the same colony aged nine months were used in this study. DNA was extracted from tale samples using the High Pure PCR Template Preparation Kit (Roche) and the genotype determination was carried out by the "Unidad de genotipado y diagnostic genetico", Facultat de Medicina, Valencia. In the image the amplified fragments of APP and PS are visible (Figure 4.2).

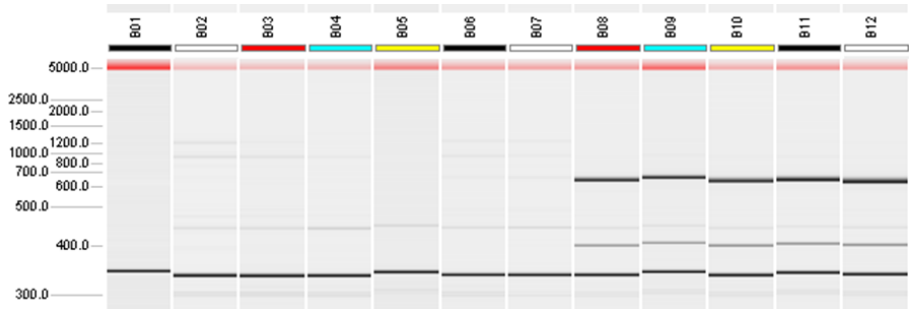

Figure 4.2 | **Genotype determination of wildtyp and heterozygous APP/PS1 mice.** In this example samples in wells B01-B07 are wildtypes, while B08-B12 were determined as transgenic animals.

4.3.1. Preparation of mouse brain homogenates

The animals were anesthetized with inhalatory anesthesia (SEVOrane®) and then sacrificed. Hippocampi and cortices were isolated, freeze-clamped and stored at -80ºC. The tissues were weighted out and the according amount of 1x lysis buffer (Tris: 76,5 mM, pH: 6.8, SDS: 2%, Glycerol 10%; supplemented with sodium ortovanadate (2 mM) and protease inhibitor (Sigma-Aldrich)) was added (1 ml 1x lysis buffer/100 mg brain tissue) and the tissues were homogenized for Western blot determinations. For immunohistological analysis, animals were transcardially perfused as described below.

4.3.2. Intrahippocampal infusion

For microinjections in the hippocampus of Wistar rats, they were treated with atropine methyl nitrate (0,4 mg/kg, i.p.), anesthetized with a mixture of Ketamine (60 mg/kg i.p.) (Imalgen, 0.05 g/ml; Rhone Mérieux, Lyon, France) and Xylazine (10 mg/kg i.p.) (Xilagesic, 20 mg/ml; Lab. Calier, Barcelona, Spain), and mounted in a Kopf stereotaxic apparatus (Kopf Instruments, Tujunga, USA). In order to minimize animals' suffering, subcutaneous lidocaine was injected in the surgery area. The scalp was incised and retracted, and the head position was adjusted to place bregma and lambda references in the same horizontal plane. Small trephine holes (1 mm in diameter) were drilled in the skull unilaterally.

Intrahippocampal infusions were made using a stainless steel cannula system (Plastics One, Roanoke, VA) consisting of an outer guide tube (24 gauge) and an inner infusion tube (31 gauge). The cannulas were stereotaxically placed 4,36 mm

posterior to bregma, 1,4 mm lateral from the mid-sagittal line, and implanted 3,4 mm below the outer surface of the skull into the left-side CA1 hippocampal region, according to the atlas of Paxinos and Watson (1998) (see Figure 4.3). The infusion cannula was connected to a 10 µl Hamilton microsyringe by a polyethylene tube. A total volume of 10 µl of infusion solutions (1 mM glutamate in 1 x PBS; 5 µM Aβ dissolved in 0,5% DMSO in 1x PBS) were injected into hippocampus at 0,5 µl/min controlled by a syringe pump. Control rats received vehicle solution (same volume and same rate).

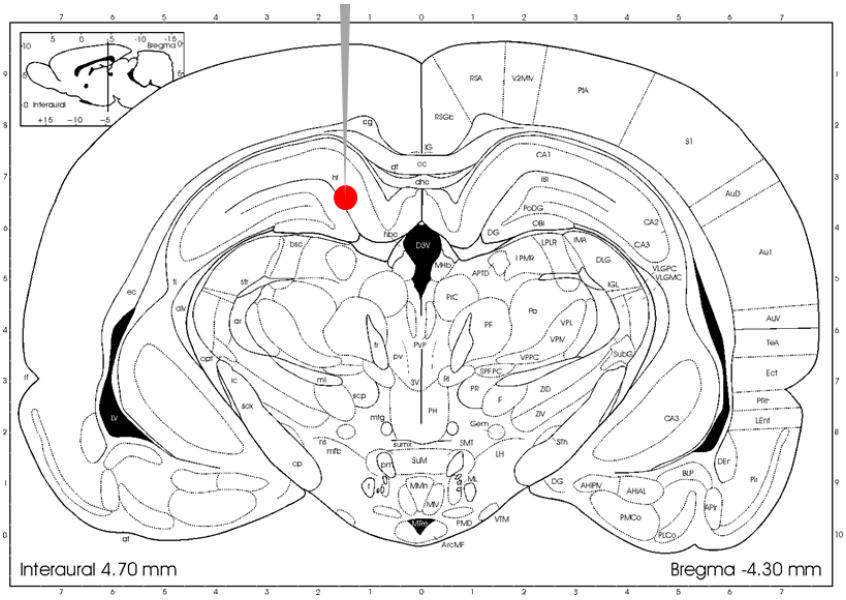

Figure 4.3 | **Stereotaxic placement of injection site in rat hippocampus**. The red dot indicates the approximate injection site. Atlas Source: Paxinos, George, and Charles Watson. The rat brain in stereotaxic coordinates: hard cover edition. Access Online via Elsevier, 2006.

4.3.3. Fixation and tissue preparation

After 48 h of the treatments, animals were anaesthetised with a lethal dose of sodium pentobarbital (100 mg/kg, 20%) (Dolethal Vetoquinol Madrid, Spain) and transcardially perfused with heparinized saline (0,1%, pH 7) followed by paraformaldehyde (4%) in phosphate buffer (0,1 M, pH 7.4). Brains were post-fixed for 24 h at 4ºC and maintained for 2 days in sucrose (30%) at 4ºC for cryoprotection. Coronal sections of 40 μm were obtained by freezing microtomy (Leica) and stored in phosphate buffer (0,1 M, pH 7.4) at 4ºC.

4.3.4. Tissue preparation for immunoblotting

Brain tissue (10 mg - 100 mg) was weighted out and the corresponding amount of 1x lysis buffer was added (1 ml lysis buffer/100 mg brain tissue). The tissue was homogenized using a tissue homogenizer and the samples were stored at -80°C or directly used for protein determination.

4.4. Analytical Methods

4.4.1. Protein determination

Protein concentrations in cell suspensions were determined using the Lowry protein assay. Bovine serum albumin was used in different concentrations as a standard (0,39; 0,78; 1,56; 3,125; 6,25; 12,5; 25; 50 mg/ml). Ten µl of sample (or standard solution) were added to 990 µl ddH2O; for the blanc 10 µl of ddH2O was used. One ml lowry reagent was added, shortly vortexed and kept for 20 min in the dark. Then, 500 µl of folin reagent were added and kept for 30 min in the dark. The

protein concentration in the samples was then measured by absorbance at 660 nm in disposable cuvettes in a standard photometer (Cecil 3021).

4.4.2. SDS PAGE and immunoblotting

After determination of the protein concentrations using Lowry protein assay, to the same amounts of total protein in the samples (20 µg - 30 µg), 8 µl of 1x loading buffer was added and the samples were heated to 95°C for 10 min. Afterwards they were subjected to sodium dodecyl sulphate (SDS) polyacrylamide gel electrophoresis (PAGE) to separate the proteins according to their molecular weight. They were blotted on a nitrocellulose membrane using a wet protein transfer system. The membranes were blocked in 5% (w/v) low-fat milk or 5% BSA in 1x TBST for 1 h at room temperature (RT). They were incubated with a specific primary antibody, at an appropriate concentration, for 1-2 h at RT or overnight at 4°C: cdh1 (DCS-266, 1:500, Novus Biologicals), glutaminase 1 (12855-1-AP, Proteintech, 1:1000), cdk5 (2506, Cell Signaling Technology, 1:1000), p35/25 (2680, 1:1000, Cell Singaling Technology), α-Tubulin (sc-8035, Santa Cruz Biotechnology, 1:8000), histone H3 (07-690, Merk Millipore, 1:25000), β-actin (A1978, Sigma, 1:1000). We used two distinct ladder proteins as indicators for molecular weight correspondence of specific proteins: The 'PageRuler Plus Prestained Protein Ladder' (26620, Thermo Scientific, Rockford, USA) and 'Precision Plus Protein Standards Dual Color' (161-0374, BioRAD, CA, USA) (Figure 4.4). Membranes were incubated with corresponding secondary antibodies and signal detection was performed using "Luminata Classico Western HRP Substrate" (WBLUC0500, Millipore Corporation). Western blot images were developed with a biomolecular imager (ImageQuant™ LAS 4000, GE Healthcare Bio-Sciences). After identification of a specific band at the corresponding molecular weight, the bands were quantified by densitometry using

ImageGauge4.0. Loading control proteins (α-tubulin, histones or β-actin) were also quantified and the specific antibody band was normalized to the band of the loading control.

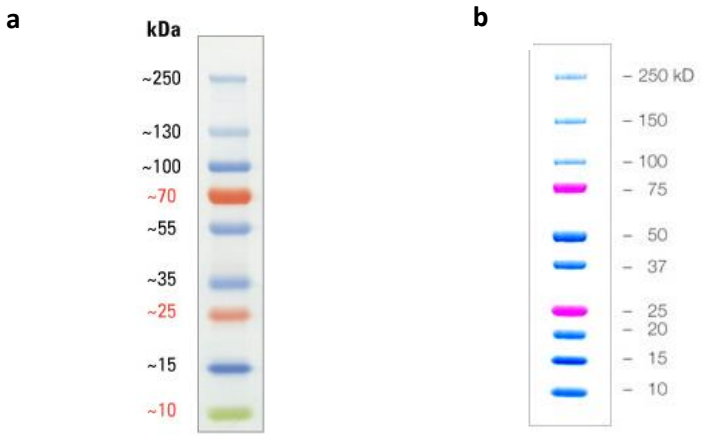

Figure 4.4 | **Representative images for ladder proteins used for western blotting within this work.** (a) PageRuler Plus Prestained Protein Ladder and (b) Precision Plus Protein Standards Dual Color.

4.4.3. Immunohistochemistry using DAB staining

Hippocampi were isolated and fixed in 4% formaldehyde in 1x PBS and embed in paraffin. Sections (5 µm) were analysed using glutaminase (12855-1-AP, Proteintech, 1:100) and cdh1 (NBP2-15840, Novus Biologicals, 1:500) antibodies. A 3,3′-Diaminobenzidine (DAB) Peroxidase Substrate Solution for staining. Nuclei were stained using haematoxylin.

4.4.4. Immunohistochemical labelling with fluorescent antibodies

Free floating sections were washed 3 times in 0,1% TBST at RT. Sections were incubated for 3 h at RT in a blocking solution of 2% BSA in TBST. The tissue was incubated 2 days at 4ºC in 2% BSA in TBST with the primary antibodies: rabbit anti-Glutaminase (Proteintech, 1:200), mouse anti-Cdh1 (Abcam, 1:100) or rabbit anti-Cdh1 (Novusbio, 1:250). Afterwards, sections were rinsed 2 times in TBST and 2 times in HEPES (10 mM) in PBS and were then incubated for 3 h at RT in a solution of 2% BSA in HEPES (10 mM) with the secondary antibody: Alexa Fluor 488 anti-rabbit (CellSignaling Tech, 1:1000) and Alexa Fluor 647 anti-mouse (CellSignaling Tech, 1:1000). Finally, sections were rinsed in HEPES (10 mM), mounted onto pig skin gelatin-coated slides (0,5%) and covered with a drop of VECTASHIELD Mounting Medium with DAPI (H1200, Vector) for nuclear staining and a drop of fluorescence mounting medium (S3023, DAKO).

4.4.5. Immunocytochemical labelling

Neuron cells were fixed in 4% formaldehyd in 1x PBS for 5 min at RT, to preserve the morphology of the cell. Afterwards the cells were incubated with methanol (-20°C) for 1 min, for further fixation. Then, they were washed in 1x PBS and at this step they were eventually stored at 4°C for several days or weeks, or they were directly proceeded to be used for staining. To reduce unspecific bindings, the cells were incubated in blocking solution (5% BSA) for 1 h at RT. The neurons were incubated with a specific primary antibody at an appropriate concentration overnight at 4°C. The next day, the cells were washed with 1x PBS and incubated with a fluorescent secondary antibody for 1 h at RT. The cells were washed in 1x PBS and were ready for analysis. For nucleus staining sytox green was added 5 min before analysis (S7020 SYTOX Green Nucleic Acid Stain, Molecular Probes). Sytox green stains nucleic acids that easily penetrates cells with compromised

plasma membranes. The emission maximum of the fluorochromes is at 523 nm. Sytox green (5 mM) was diluted 1:5000 in a phosphate free buffer, to reach a final concentration of 10 nM – 1 µM.

For analysis in living cells the following fluorochromes were used:

Annexin V – 555 is a marker of apoptotic cells and has an emission maximum at 560 nm (green). It binds to phosphatidylserine (PS) which is translocated from the inner to the outer leaflet of the plasma membrane in apoptotic cells. Five µl of the fluorochrome were added to 100 µl medium and incubated for 15 min at room temperature. Then the cells were washed with 1x PBS and analysed. Nuclei were stained with Hoechst for 5 min (H3570, Invitrogen).

Fluo-4 is a cell permeant Ca^{2+} indicator and has an emission maximum at 526 nm. Labeled calcium indicators are molecules that exhibit an increase in fluorescence upon binding of Ca^{2+}. Fifty µg of Fluo-4 (F-14201, Invitrogen) were dissolved in 50 µl filtered DMSO. Then 5 µl/ml medium were added directly to the culture medium and incubated for 45 min at 37°C. Then the medium was changed and the cells were further incubated for 30 min at 37°C and analysed. Nuclei were stained with Hoechst for 5 min (H3570, Invitrogen).

4.4.6. Image acquisition and image analysis

Immunocytochemical and immunohistochemical preparations were observed with a confocal laser-scanning microscope (Leica TCS SP2 scanning multiphoton and confocal unit with an inverted DM1RB microscope; Ar-He-Ne). Images containing hippocampal CA1 were analysed with *ImageJ*. To determine the nuclear and

cytoplasm localization of cdh1, the “intensity ratio nuclear cytoplasm” plugin for *ImageJ* with threshold setting “Huang” was used.

To compare protein levels, we used area proportions of the specific antibody signal normalized to nuclear staining (dapi). Ca^{2+} measurement in cells were analysed comparing changes in the intensity level of Fluo4 normalized to nuclear staining (hoechst); all images were taken with the same exposure settings.

4.4.7. Flow Cytometry analysis of neurons

For apoptosis assays, neurons were analysed with a BD FACSVerse™ flow cytometer using the annexin V-FITC Apoptosis Detection Kit (ANEXVKF-100T, Immunostep).

Neurons cells were detached from culture plates with trypsin (2 min, 37°C) and centrifuged (400 g, 5 min). Supernatants were also centrifuged to collect floating cells. Medium containing serum (10%) was added to inactivate trypsin and centrifuged. Neurons were washed twice in 1x PBS and re-suspended in 100 µl Annexin Buffer. Five µl of both, Annexin and Propidium Iodide (PI) were added to the cells for 15 min at RT. Neurons were further diluted in Annexin Buffer and analysed by flow cytometry. The measurements were previously calibrated using neurons with either Annexin or PI staining alone and unstained cells. Flow cytometry results were analysed with BD FACSuite software. Results are shown as 2D dot plots, with Annexin V-FITC on the x-axis and PI on the y-axis. The bivariate staining allows discrimination of the following groups (Figure 4.5): intact cells (Annexin negative, PI negative) in the square left/down-sided Q3, early apoptosis (Annexin positive PI, negative) in the square right/down-sided Q4, late apoptotic (Annexin positive, PI positive) in the square right/up-sided Q2, and necrotic cells (Annexin negative, PI positive) in the square left/up-sided Q1.

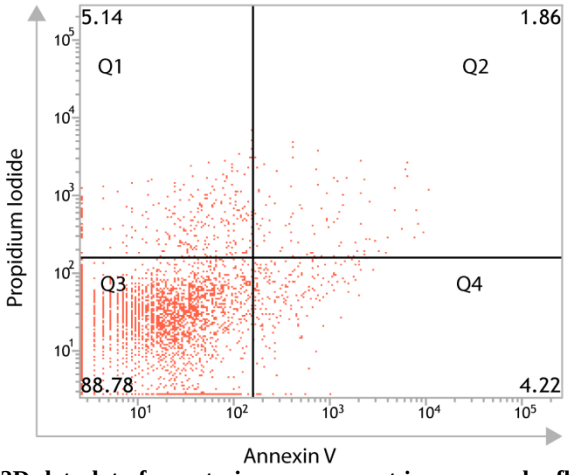

Figure 4.5 | **2D dot plot of apoptosis measurement in neurons by flow cytometry**. Q3: live cells, Q4: apoptotic cells, Q2: late-apoptosic cells, Q1: dead cells.

4.4.8. Glutamate measurement

To measure L-glutamate we followed the protocol of Bernt E. and Bergmeyer H.U. (1994), a photometric assay, based on the enzymatic reaction of glutamate dehydrogenase (GlDH, G2626, Sigma, St. Louis, USA).

$$\text{L-Glutamate} + NAD^+ + H_2O \xrightleftharpoons{\text{GlDH}} \text{2-Oxoglutarate} + NADH + NH_4^+$$

The amount of L-glutamate that is oxidized to 2-oxoglutarate is proportional to the increase of NADH, which is measured by the extinction change at 340 nm. ADP is added to activate and stabilize the reaction.

Solutions and reagents used in the assay:

Glycine-hydrazine buffer *[0,5 M glycine; 0,4 M hydrazine; pH 9.0]*

3,75 g glycine and 5,50 g of 24% hydrazine hydrate were dissolved in ddH_2O and adjusted to pH 9.0 with 1 N H_2SO_4 and filled up to 100 ml with ddH_2O.

Adenosine-5'-diphosphate *[33,5 mM ADP]*

45 mg ADP-Na_2 were dissolved in 2,5 ml ddH_2O.

Nicotinamide-adenine dinucleotide *[27 mM β-NAD]*

100 mg NAD were dissolved in 5 ml ddH_2O.

Glutamate dehydrogenase, GlDH *[ca. 10 mg protein/ml]*

Perchloric acid *[1 M]*

8,6 ml perchloric acid (70%) were diluted to 100 ml with ddH_2O.

Phosphate solution *[1,93 M K_3PO_4]*

51 g of K_3PO_4 were diluted in 100 ml ddH_2O.

Samples of cell-free supernatants of cultured neurons were deproteinized using perchloric acid (6%). The pH was adjusted using tripotassium phosphate solution. The mix was centrifuged for 10 min at 3000 g. One ml of the supernatant was adjusted to pH 9.0 by adding 200 µl phosphate solution and then the samples were put on ice for 10 min. The supernatant was used for the assay adding the following amounts:

- 750 µl glycine – hydrazine buffer
- 375 µl sample
- 37,5 µl ADP
- 75 µl NAD

After the components were mixed together the extinction was measured for the first time t = 0 (E1). Ten µl GlDH were added and absorption was measured after t = 45 min (E2). That was when the values stabilized, the reaction was saturated. Then the absorption ΔA was calculated: ΔA= E2 – E1. Then we calculated the concentration of glutamate in the sample:

$$\text{Glutamate (mM)} = \frac{\Delta A_{340} * 2 * 1{,}2 * 1246{,}9}{6{,}220 * 1 * 375} = \Delta A_{340} \times 1{,}280$$

ΔA_{340} = Final maximum absorbance at 340 nm

2 = dilution with 6% PCA

1,2 = dilution with phosphate salt

1246,9 = total reaction volume (µL)

375 = volume of sample in cuvette (µL)

6,22 = mM/cm (extinction coefficient of NADH at 340 nm)

1 = Lightpath (cm)

As control, we used a glutamate standard solution with the following concentrations and verified that samples up to 2,5 mM glutamate show an accurate measurement:

Standard [mM]	A [T=0]	A [T=45]	ΔA
5	0,292	2,16	1,868
2,5	0,301	1,532	1,231
1,25	0,3	1,084	0,784
0,625	0,296	0,779	0,483
0,315	0,301	0,55	0,249
0,156	0,309	0,429	0,12
0,078	0,287	0,365	0,078
0,031	0,29	0,332	0,042
0	0,295	0,296	0,001

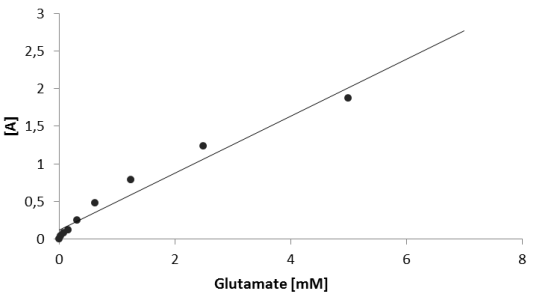

Figure 4.6 | **Glutamate standard measurement.** Glutamate standard concentrations (0-5 mM) measured in samples before (T=0) and after (T=45) the addition of glutaminase dehydrogenase. ΔT shows the increase of absorption (A).

After determination and calculation of the glutamate concentration in the sample, they were normalized to the protein concentration in the samples of neurons of the corresponding flask.

4.4.9. Ammonia measurement

For ammonia determination, cell-free supernatant samples were analyzed using the ammonia assay kit (Sigma-Aldrich, Saint Lois USA) according to manufacturer's instructions. 20 µl of supernatant was mixed with 200 µl assay buffer and 2 µl GlDH solution in 96-well plate for 5 min, and absorbance was measured at 340 nm. The background concentration of ammonia in the culture medium was substracted and the results are expressed as the increase of ammonia/100 µg protein.

4.4.10. Determination of mRNA expression by quantitative rtPCR

Total RNA was isolated from tissues or cells using the TRIzol Reagent (Life technologies, 15596-026) according to manufacturer's instructions. RNA concentration was determined using a NanoDrop spectrophotometer. One µg of purified RNA was reverse transcribed using High-Capacity cDNA Reverse Transcription Kit (Thermo Fisher, 4368814) according to the manufacturer's instructions. The quantitative PCR was performed using the detection system 7900HT Fast Real-Time PCR System (Applied Biosystems). Gene-specific primer pairs were designed using NCBI/Primer-BLAST:
cdh1 (Mus musculus) FW: 5'-GGACCAGGACTATGAGCGAA-3',
cdh1 (Mus musculus) RV: 5'-GGGTTCTCCGCATCTCTGAA -3';
APC/C 2 (Mus musculus) FW: 5'-ACCGTATCTATGCCACCCTAC-3',

APC/C 2 (Mus musculus) RV: 5'-GACACAAGAAGTTGCTGCCT-3';
gls (Mus musculus) FW: 5'GATGTGTTGGTCTCCTCCTCT-3',
gls (Mus musculus) RV: 5'-GGTTTATCACCGACTTCACCC-3';
GAPDH (Mus musculus) FW: 5'- TGCTGAGTATGTCGTGGAGT-3',
GAPDH (Mus musculus) RV: 5'-AGATGATGACCCGTTTGGCT-3';
cdh1 (Rattus norvegicus) FW: 5'- TCGTATCGTGTCCTCTACCTG-3',
cdh1 (Rattus norvegicus) RV: 5'- AACCGAAGGGTCTCATCTCC-3';
APC/C2 (Rattus norvegicus) FW: 5'- GAGAGAGTGGTTGGTTGGCT-3',
APC/C2 (Rattus norvegicus) RV: 5'-GGCTGGCATAGATTCGGTAGA-3';
gls (Rattus norvegicus) FW: 5' ATTACGACTCCAGAACAGCCC,
gls (Rattus norvegicus) RV: 5'-GCTTCCAGCAAAAACTTCACAAC-3';
GAPDH (Rattus norvegicus) FW: 5' TGATGGGTGTGAACCACGAG-3',
GAPDH (Rattus norvegicus) RV: 5'-TCATGAGCCCTTCCACGATG'-3.
The primers were obtained from *Life Technologies*. For the reaction, Maxima SYBR Green/ROX qPCR Master Mix (2X) (Thermo Scientific, K0223) was used and each sample was analysed in triplicates.

The relative standard curve method was used to evaluate the expression levels. Standard curves were prepared from dilutions of cDNA mix of the samples for each gene. The efficiency was estimated using a semi-log regression line plot of CT value vs. log of input nucleic acid (see example Figure 4.7).

standard	log (standard)	Ct
1	0	24,34
0,5	-0,301029996	25,21
0,1	-1	27,67
0,01	-2	30,96

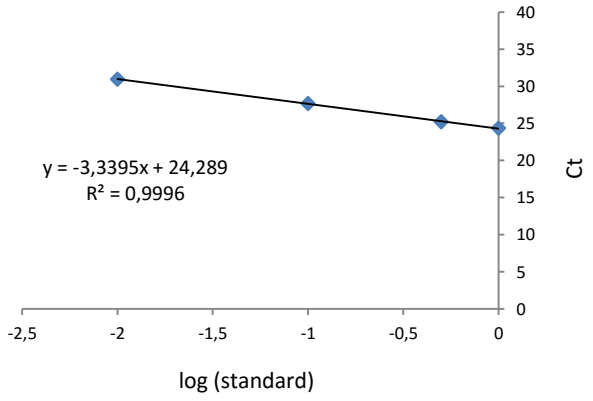

Figure 4.7 | **Relative standard curve method for qPCR quantification.** The diagram shows a semi-log regression line plot of CT value vs. log of input nucleic acid. The slope (here: -3,34) indicates the efficiency of the amplification of the gene.

For all experimental samples, the relative target quantity was determined by interpolating the threshold cycle (Ct) values from the standard curve. GAPDH was used in all samples to normalize gene expression for sample-to-sample differences in RNA input and quality. The fold change of samples of the control group compared to treated groups was represented.

4.5. Statistical analysis

To calculate protein half-life we used the following method: It was assumed that protein degradation follows first-order decay kinetics. The measured protein

intensity data was initially log-transformed, then a linear least-squares fit was used to determine the decay rate constant k, yielding a coefficient of determination (r-square). Moreover, we estimated the standard error of the slope. For assessing difference significance we used a Z-test. It is known that, under normality assumption of the fit errors, difference between slope estimates divided by the mean square root of their standard error follow a standard normal distribution. Finally, from the decay rate constant, the half-life was calculated ($T(1/2) = \ln(2)/k$).

The results are expressed as mean ± SD of data of at least three independent experiments. Statistical analyses were carried out, using a one-tail t-tests analysis or Mann Whitney U-test. P-values were graduated in the units of significance which were set as following: $p < 0,05$ significant (*), $p < 0,01$ very significant (**), $p < 0,001$ highly significant (***).

5. RESULTS

5.1. Cdh1 in Aβ Treated Neurons

5.1.1. Cdh1 protein level decreases upon Aβ treatment

In order to study the implication of APC/C-Cdh1 in AD, we first tested the effect of Aβ on cdh1 *in vitro* in neurons in primary culture. After six days of culture, the neurons were fully differentiated. For the Aβ treatment, culture medium was changed for all neurons and either standard culture medium (for controls) or medium containing soluble oligomeric $A\beta_{1\text{-}42}$ (5 µM) was added. The cells were collected after different time points between 0 and 24 h, and cdh1 protein levels were determined by western blotting. We detected cdh1 by a specific antibody at the corresponding molecular weight at 55 kDa (see Figure 5.1 a). Cdh1 protein levels were significantly decreased when treated with Aβ for 24 h compared to control conditions in three independent experiments (see Figure 5.1 a-c, 5.2). This result shows that Aβ affects cdh1 steady state levels directly or indirectly. Therefore we assumed that cdh1 and APC/C might have a potential role in AD.

a

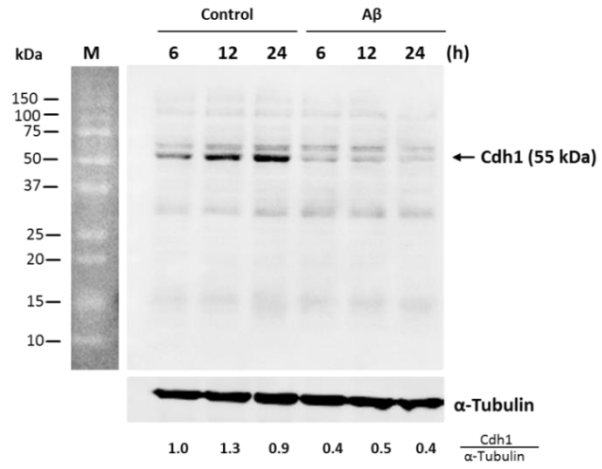

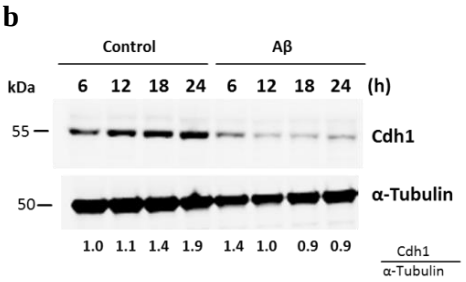

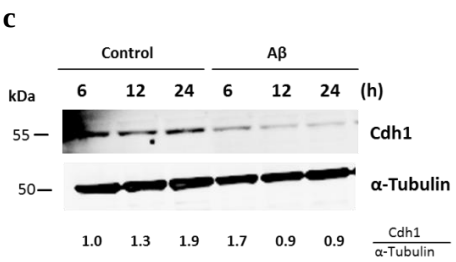

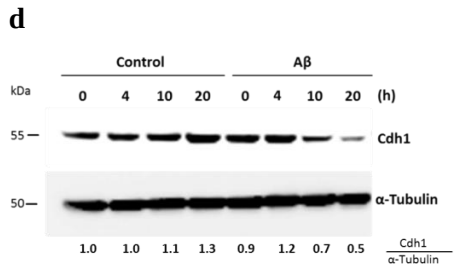

Figure 5.1 | **Cdh1 decreases after Aβ treatment.** (a-d) Neurons in primary culture were treated with Aβ and collected after different time points. Cdh1 and α-tubulin levels were determined in whole-cell lysates by immunoblotting using specific antibodies for cdh1 (dilution 1:1000) and α-tubulin (dilution 1:1000). Western blot images show a decrease of cdh1 with incubation of Aβ after approximately 10 h compared to control conditions. Blots were quantified by densitometry and normalized with α-tubulin; values are indicated below the blots.

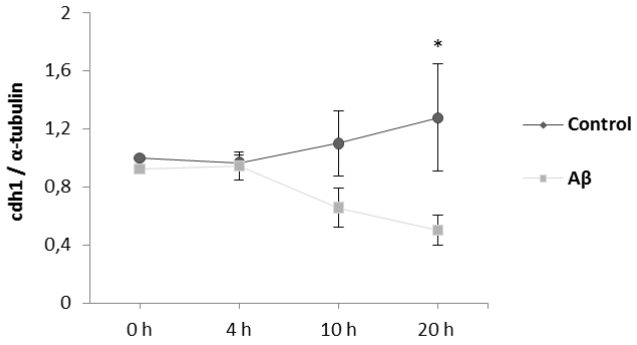

Figure 5.2 | **Quantification of cdh1 shows a significant decrease of cdh1 after Aβ treatment after 20 h.** Blots of three independent experiments were quantified. The mean values ± SD of cdh1 normalized to the loading control protein are shown and are statistically significant ($p < 0,05$).

5.1.2. Cdh1 protein level decreases in the nucleus upon Aβ treatment

The intracellular localization of cdh1 is determined by its phosphorylation status. Non-phosphorylated cdh1 is localized in the nucleus where it activates APC/C. Upon phosphorylation cdh1 is translocated to the cytoplasm where it is targeted for degradation by the SCF-complex (Zhou et al., 2003; Almeida, 2012). Therefore, in the following experiment we analysed whether cdh1 decreases after Aβ treatment in the nucleus and/or in the cytoplasm of neurons.

Cultured primary neurons in control conditions or treated with Aβ for 20 h were carefully collected in PBS and cytosol and nucleus were separated. A successful separation was demonstrated by quantification of cell compartment-specific proteins in the fraction of nucleus (Histone H3) and the cytosol (β-actin). These proteins were also used as a loading control in densitometry analysis of the blot.
We showed that cdh1 decreased significantly in the nucleus in three independent experiments after the Aβ treatment (Figure 5.3 a-c, 5.4). This indicates that Aβ induces nuclear export of cdh1, probably caused by phosphorylation of cdh1. There is no commercially available antibody for phopho-cdh1, therefore we could not directly test phosphorylation of cdh1.

While the decrease of nuclear cdh1 upon Aβ occurred in all repetitions, the cdh1 level in the cytosol did not decrease equally in all repetitions. This difference might have occurred due to a differential regulation of the degradation of cdh1 by the SCF complex.

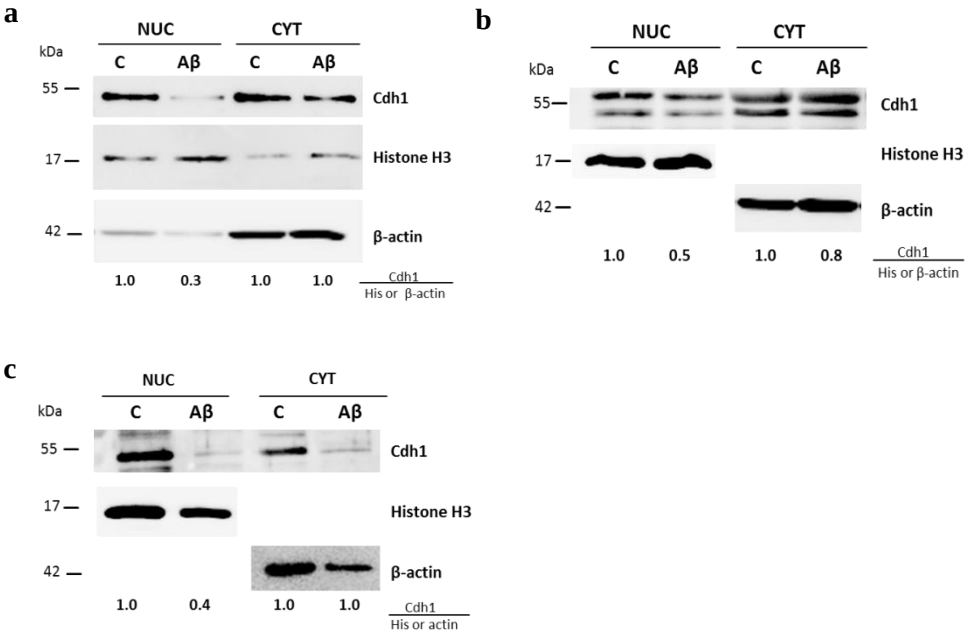

Figure 5.3 | **Cdh1 decreases after Aβ treatment in the nucleus.** (a-c) Neurons were treated with Aβ for 20 h. Cdh1 levels were determined by immunoblotting using specific antibodies for cdh1 (dilution 1:1000), histone (dilution 1:30000) or β-actin (dilution 1:1000) as loading controls. Western blot images show a decrease of cdh1 after treatment with Aβ for 20 h in the nucleus compared to control conditions. Blots were quantified by densitometry and normalized with H3 (for nuclear extracts) or β-actin (for cytosol extracts), values are indicated below the blots.

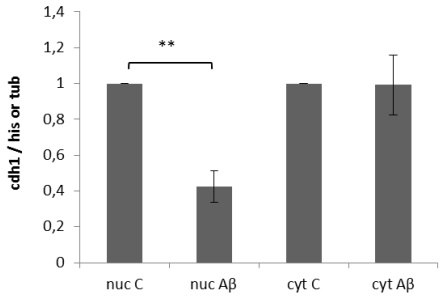

Figure 5.4 | **Quantification of cdh1 shows a significant decrease of cdh1 after Aβ treatment in the nucleus.** Blots of three independent experiments were quantified. The mean values ± SD of cdh1,

normalized to the loading control protein, are shown in the histogram. The result is statistically significant ($p < 0,01$).

To further confirm this result we analysed the cellular localization of cdh1 by confocal microscopy. Neurons were grown on chamber slides, and treatments were accomplished as stated above. Immunocytochemical analysis of cdh1 showed that the nucleus/cytosol ratio of cdh1 decreases significantly upon Aβ treatment (Figure 5.5).

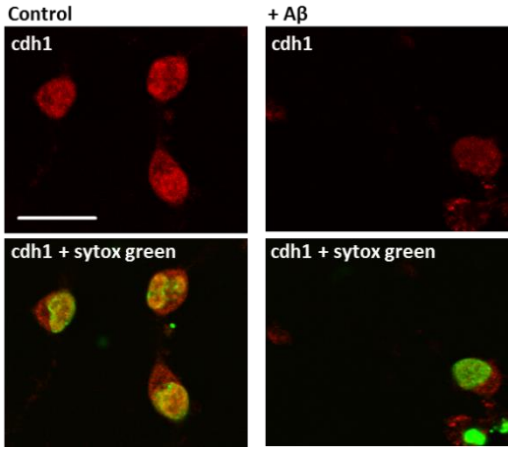

Figure 5.5 | **Cdh1 decreases after Aβ treatment in the nucleus.** Confocal microscope analysis of neurons shows cdh1 (red) and nuclei (sytox green). Representative images of three independent experiments are shown. Scale bar = 21.4 µm.

Additionally, we co-stained neurons with Map2, a neuronal marker, to confirm that nuclear-cytoplasm translocation of cdh1 upon Aβ treatment occurs specifically in neurons (Figure 5.6).

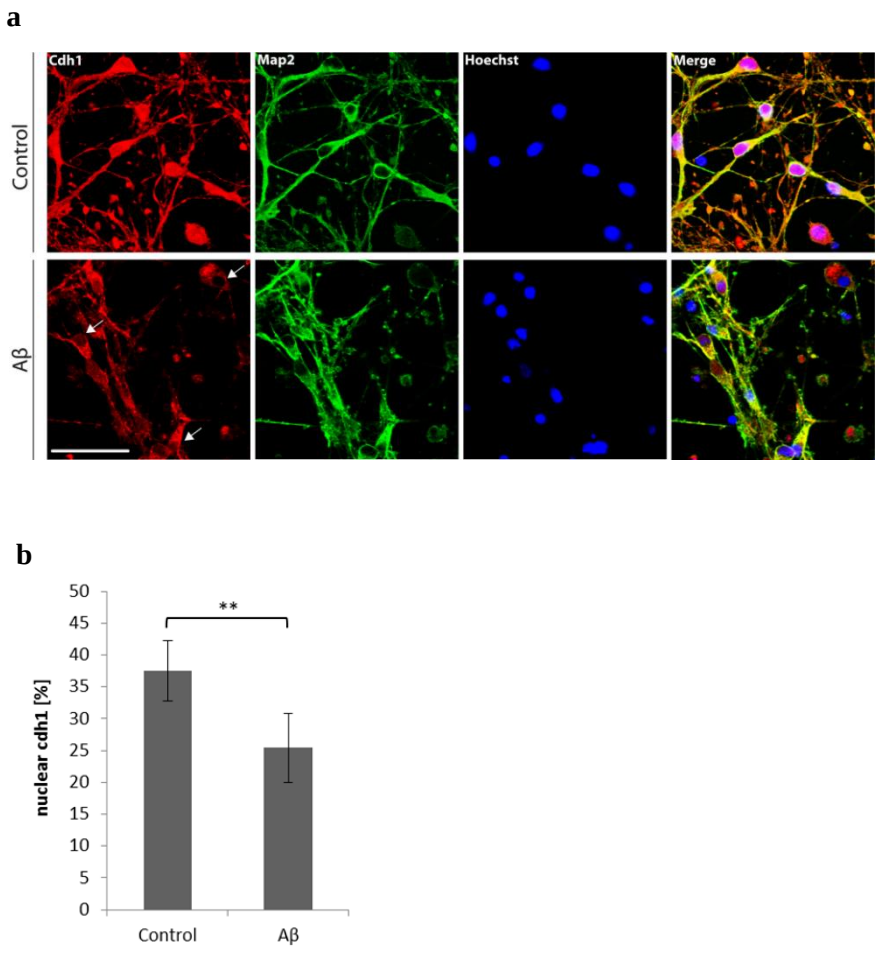

Figure 5.6 | **Cdh1 decreases after Aβ treatment in the nucleus of neurons.** (a) Confocal microscope analysis of neurons shows cdh1 (red) and nuclei stained by Hoechst (blue). Map2 staining (green) was used as a neuronal marker. Representative images of three independent experiments are shown. (b) Mean value ± SD of cdh1 in the nucleus is shown in the histogram. Scale bar = 47,62 µm.

5.1.3. Protein half-life of cdh1 is reduced upon Aβ treatment

We tested if the protein half-life of cdh1 changed with Aβ treatment. Therefore we measured cdh1 protein level when protein synthesis was inhibited using cycloheximide (CH) alone or in the presence of Aβ. We observed that the protein half-life of cdh1 was reduced from 5,9 h to 4,8 h when treated with Aβ, than in its absence (Figure 5.7).

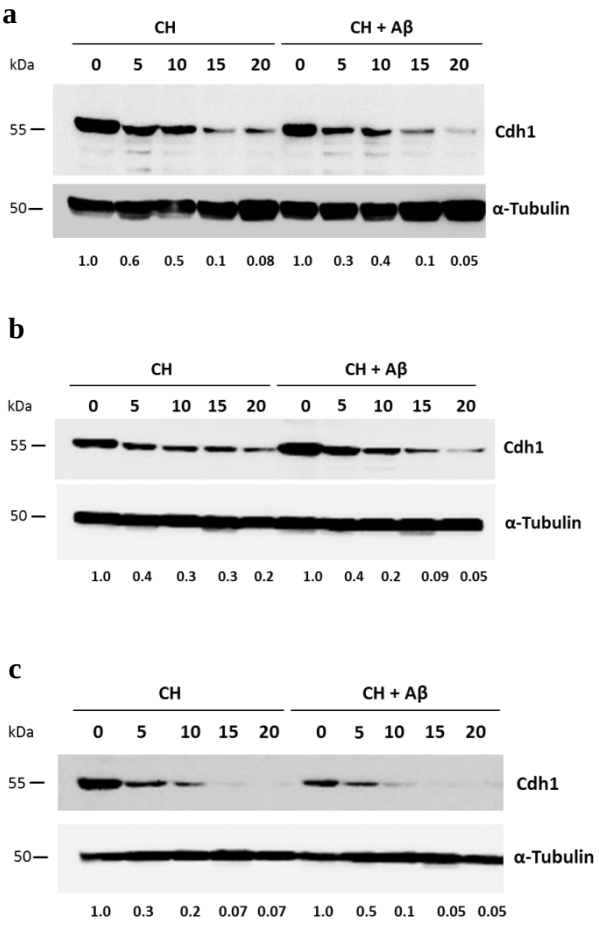

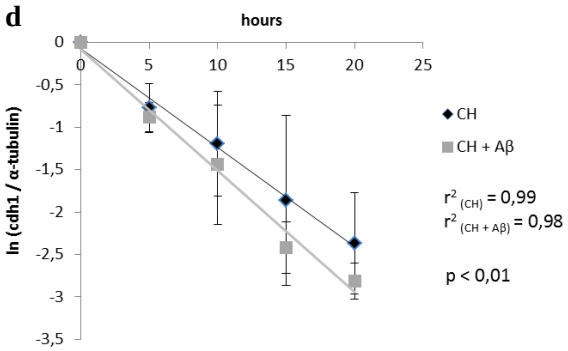

Figure 5.7 | **Cdh1 half-life decreases with Aβ**. (a-c) Western blot images of cdh1 at different time points after treatment with cycloheximide (CH) or CH + Aβ. (d) Blots of three independent experiments were quantified by densitometry and normalized against α-tubulin; the mean values ± SD are indicated.

5.1.4. Cdh1 is degraded by the proteasome when treated with Aβ

In the previous experiments, we observed a decrease of cdh1 when treated with Aβ. This decrease could have occurred due to transcriptional, translational or post-translational changes. Here we tested whether the inhibition of the proteasome using the specific inhibitor MG132 rescues cdh1 protein levels when treated with Aβ. We tested different concentrations and observed that the proteasome inhibition at a concentration of 10 µM MG132 was most effective to revert the effect of Aβ on cdh1 (Figure 5.8 a). We observed a statistical significant difference in cdh1 levels in three independent experiments (Figure 5.8 b-d, 5.9 e).

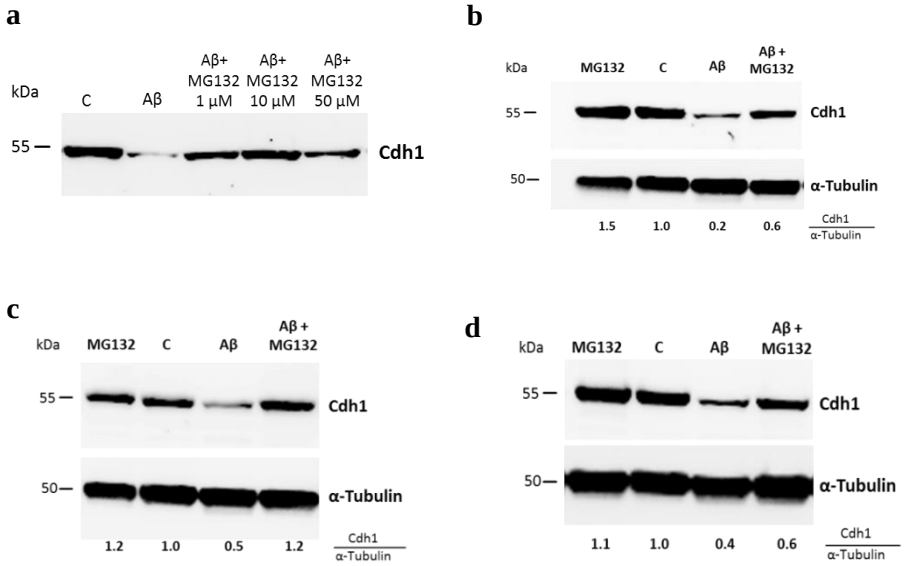

Figure 5.8 | **Cdh1 after Aβ treatment is degraded by the proteasome.** (a-d) Neurons in primary culture were treated with Aβ for 24 h and/or MG132. Cdh1 levels were determined by immunoblotting using specific antibodies for cdh1 (dilution 1:1000) and α-tubulin (1:1000) as loading controls. Western blot images show a decrease of cdh1 with incubation of Aβ after 24 h, but not when treated with MG132. Blot were quantified by densitometry and normalized to α-tubulin, values are indicated below the blots.

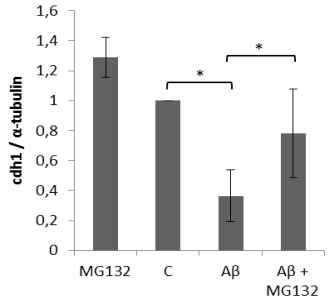

Figure 5.9 | **Quantification of cdh1 shows a significant decrease after Aβ treatment which does not occur when the proteasome is inhibited.** Blots of three independent experiments were

quantified. The mean values ± SD of cdh1, normalized to the loading control protein, are shown in the histogram. The results are statistically significant ($p < 0,05$; $p < 0,05$).

5.1.5. mRNA levels of cdh1 and APC/C2 when treated with Aβ

In the previous experiments we had observed a proteasome-dependent decrease in cdh1 when treated with Aβ. Next, we tested whether there was a change in mRNA expression of cdh1 and in the catalytic subunit APC/C2 of the protein complex. We measured the mRNA levels of cdh1 and of APC/C2 using qPCR in control conditions and upon Aβ treatment. We observed no statistically significant differences in the expression levels in the two conditions and concluded therefore that changes in cdh1 protein levels when treated with Aβ occurred exclusively post-translational (Figure 5.10).

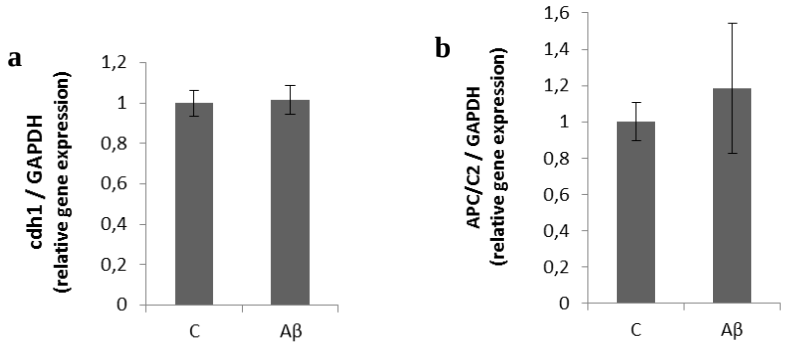

Figure 5.10 | **mRNA levels of APC/C2 and cdh1 in neurons.** Neurons in primary culture were treated with Aβ. After 24 h, the cells were collected and mRNA was isolated and retro-transcribed to cDNA. Relative expression levels were determined by real time qPCR using specific primers. Mean values ± SD of cdh1 and APC/C2 are shown in the histograms. There is no statistically significant difference (n=3).

5.2. Cdc20 protein level upon Aβ treatment in neurons

We also tested the protein level of cdc20, another co-activator subunit of APC/C, in control conditions and upon Aβ treatment. We identified a band of cdc20 at the corresponding molecular weight of 51 kDa (Figure 5.11 a). In three independent experiments we showed that there was a tendency of cdc20 decrease upon Aβ treatment, which was however not statistically significant (Figure 5.11 b-e).

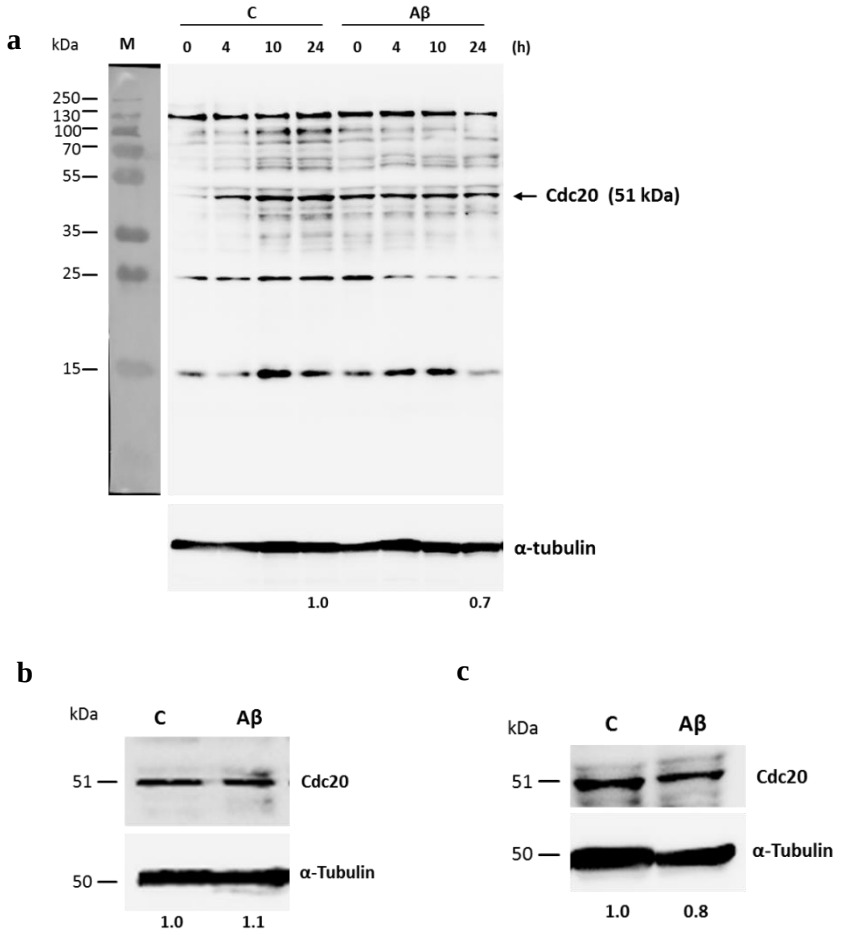

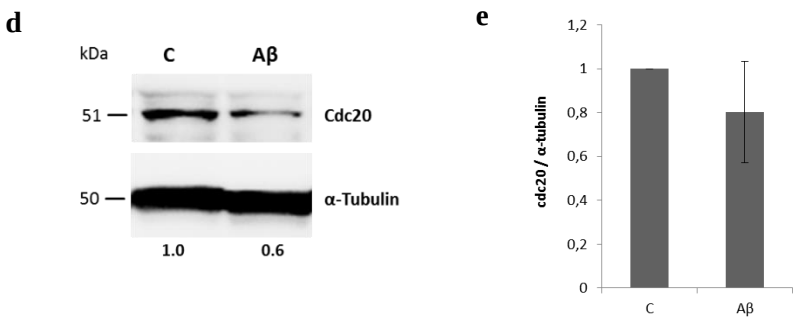

Figure 5.11 | **Cdc20 levels in neurons after Aβ treatment.** (a) Neurons in primary culture were treated with Aβ and collected after different time points (b-c) or after 24 hours. Cdc20 and α-tubulin levels were determined in whole-cell lysates by immunoblotting using specific antibodies for cdc20 (dilution 1:1000) and α-tubulin (dilution 1:1000). (e) Blots were quantified by densitometry and normalized with α-tubulin. Mean values ±SD are shown in the histogram. There was no statistically significant difference.

5.3. Analysis of APC/C-Cdh1 Substrates Cyclin B1 and Pfkfb3

To test the regulation of APC/C of its substrates in neurons, we either directly inhibited APC/C using the specific inhibitor proTAME and measured the protein levels of AD-related APC/C substrates or tested if those proteins accumulated after Aβ treatment, as we had observed that this treatment reduces cdh1. The APC/C-Cdh1 substrates (King et al., 1995, Maestre et al., 2008, Colombo et al., 2010) that we measured here were: Cyclin B1, Pfkfb3 and glutaminase 1.

5.3.1. Cyclin B1 accumulation upon APC/C inhibition by proTAME or Aβ

Cyclin B1 has been identified as a target of APC/C and was shown to be involved in neuronal survival (King et., 1995; Maestre et al., 2008).

For APC/C inhibition, the culture medium was changed for all neurons and either standard culture medium (for controls) or standard culture medium containing proTAME (12 µM) was added. Then the cells were collected at different time points between 3 and 30 h after the inhibition. The samples were subjected to western blotting and we detected cyclin B1 at the corresponding molecular weight of 60 kDa by a specific antibody (Figure 5.12 a). Results of three independent experiments showed a significant increase of cyclin B1 with proTAME treatment in a time-dependent manner (Figure 5.12 a-b, 5.13).

a

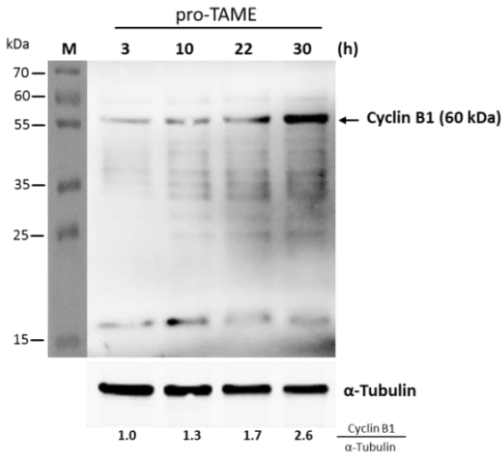

b

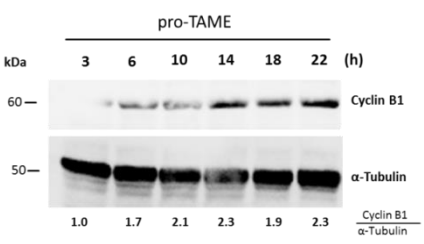

c

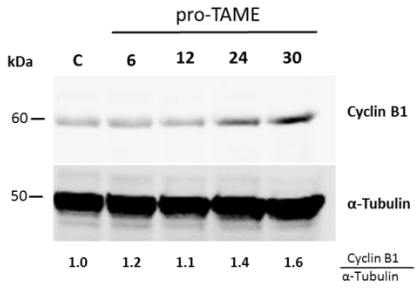

Figure 5.12 | **Cyclin B1 increases when APC/C is inhibited in neurons by proTAME.** (a-b) Neurons in primary culture were treated with proTAME. Cdh1 and α-tubulin levels were determined in whole-cell lysates by immunoblotting using specific antibodies for cyclin B1 (dilution 1:1000) and α-tubulin (dilution 1:1000). Western blot images show a time-dependent increase in cyclin B1 compared to control conditions. Blots were quantified by densitometry and normalized with α-tubulin; values are indicated below the blots.

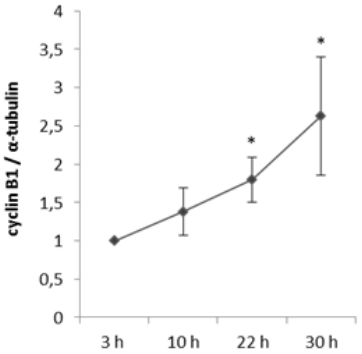

Figure 5.13 | **Quantification of cyclin B1 shows a significant increase after 22 h and 30 h of proTAME treatment.** Blots of three independent experiments were quantified. The mean values ± SD of cyclin B1, normalized to the loading control protein, are shown in the histogram. The result is statistically significant ($p < 0,05$).

After we observed an accumulation of cyclin B1 in neurons by direct APC/C inhibition, we tested if the treatment with Aβ, which had previously induced a decrease of cdh1, also led to an accumulation of cyclin B1. The Aβ treatments were accomplished as described above. Neurons were collected 20 h after the treatment and cyclin B1 protein levels were determined. It was shown in three independent experiments that cyclin B1 accumulates significantly in Aβ-treated cells (Figure 5.14 a-d).

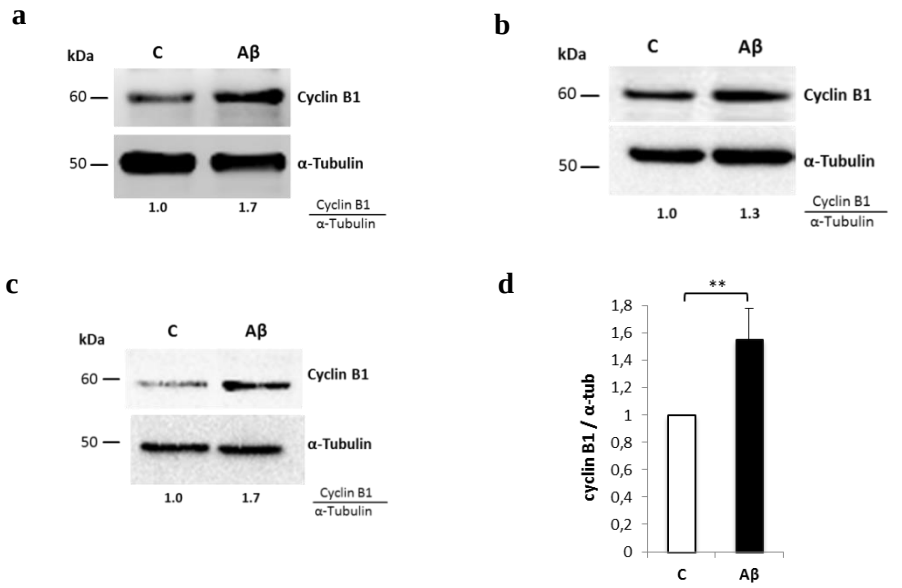

Figure 5.14 | **Cyclin B1 increases upon Aβ treatment.** (a-c) Neurons in primary culture were treated with Aβ for 20 h. Cyclin B1 and α-tubulin levels were determined in whole-cell lysates by immunoblotting using specific antibodies for cyclin B1 (dilution 1:1000) and α-tubulin (dilution 1:1000). Blots were quantified by densitometry and normalized with α-tubulin; values are indicated below the blots. (d) The mean values ± SD of cyclin B1 normalized to α-tubulin increased significantly upon treatment ($p < 0,01$).

5.3.2. No increase in pfkfb3 protein level upon Aβ treatment

Pfkfb3 has been described as a target of APC/C and unregulated accumulation of pfkfb3 in neurons has been shown to be involved in oxidative stress in AD (Rodriguez et al., 2012).

Here, we measured protein levels of pfkfb3 after treatment with Aβ in neuron primary culture. The Aβ treatment was accomplished as described above and pfkfb3 protein level was determined by western blotting. We detected pfkfb3 at the corresponding molecular weight of 60 kDa by a specific antibody (Figure 5.15 a).

We could not observe differences in the protein level of pfkfb3 in neurons under control conditions and after the treatment (Figure 5.15, a-c). A possible reason for this result might be that the basal expression of pfkfb3 is not sufficient to observe an accumulation after 20 h of treatment. It might also be possible that pfkfb3 is regulated by additional mechanisms independent from APC/C-Cdh1.

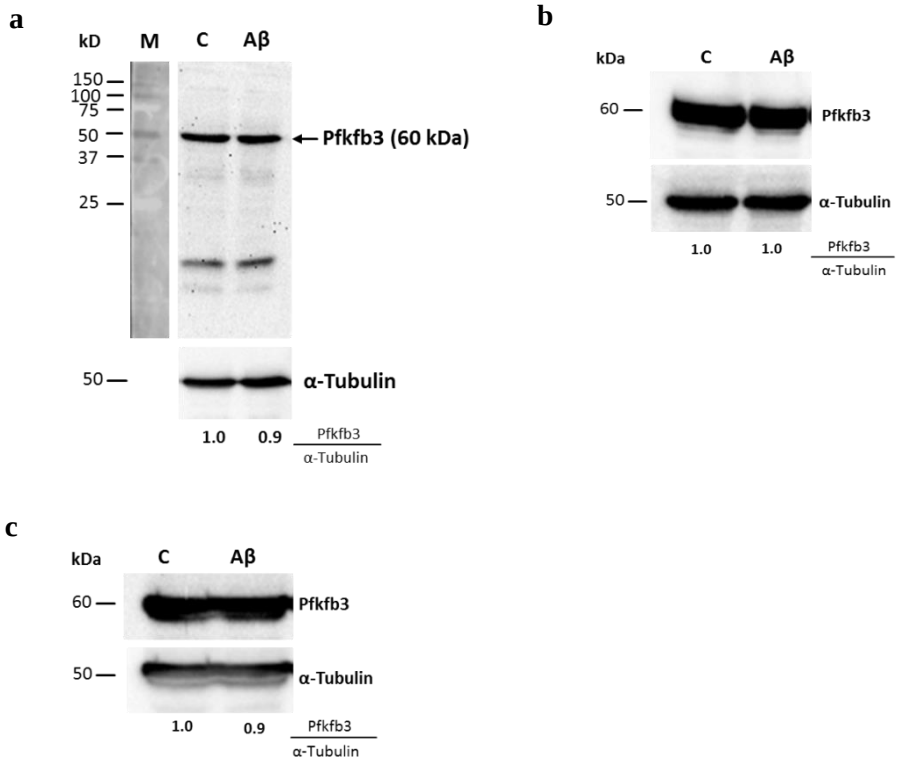

Figure 5.15 | **Protein level of pfkfb3 did not change after Aβ treatment.** (a-c) Neurons in primary culture were treated with Aβ for 20 h. Pfkfb3 and α-tubulin levels were determined in whole-cell lysates by immunoblotting using specific antibodies for Pfkfb3 (dilution 1:1000) and α-tubulin (dilution 1:1000). Blots were quantified by densitometry and normalized with α-tubulin; values are indicated below the blots. There was no detectable difference in protein levels between the controls and after the treatment.

5.4. Analysis of APC/C-Cdh1 Substrate Glutaminase

Glutaminase was identified as a substrate of APC/C-Cdh1 in lymphocytes (Colombo et al., 2010). To the best of our knowledge no studies had investigated its regulation by the ubiquitin ligase in neurons before. In the following sections the results of glutaminase as a target of APC/C-Cdh1 in neurons are summarized.

5.4.1. Glutaminase accumulation upon inhibition of APC/C

Here, we measured glutaminase protein levels in neurons in primary culture after the inhibition of APC/C by proTAME. The treatment was accomplished as described above.

The cells were collected at different time points between 0 and 24 h after the inhibition of APC/C or in control conditions. The samples were subjected to western blotting and we detected glutaminase at the corresponding molecular weight of 65 kDa by a specific antibody (Figure 5.16 a). We observed that glutaminase accumulates significantly when APC/C is inhibited (Figure 5.17 a-d, 5.18). We concluded that APC/C is involved in the regulation of glutaminase in neurons.

a

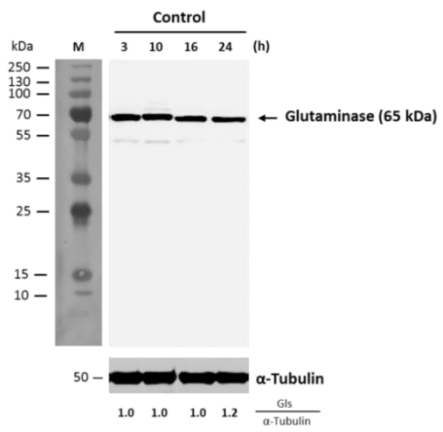

Figure 5.16 | Glutaminase level in neurons in primary culture in control conditions. The glutaminase band was detected at 65 kDa.

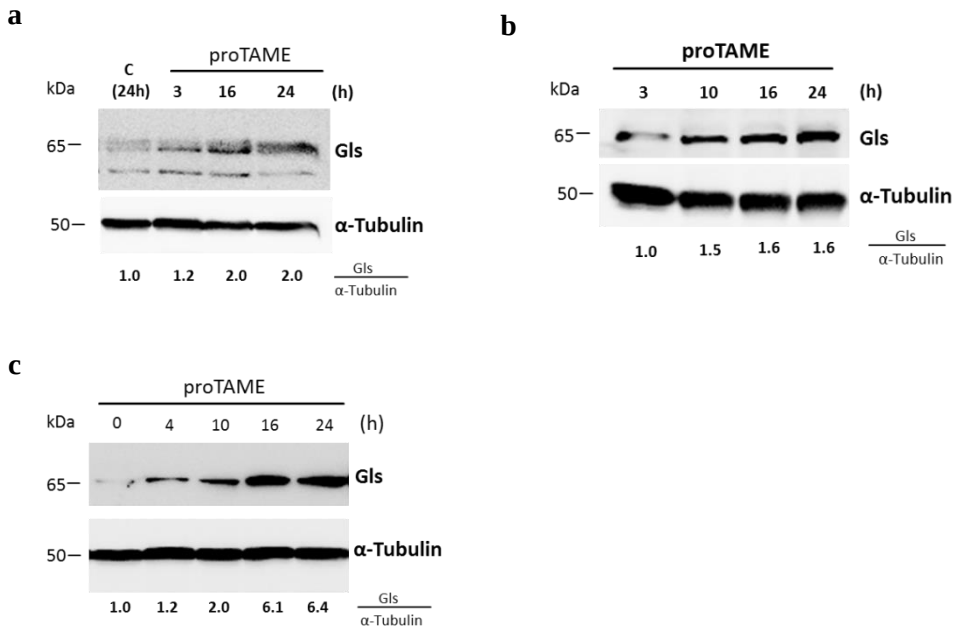

Figure 5.17 | **Glutaminase increases upon APC/C inhibition.** (a-e) Neurons in primary culture were treated with proTAME and collected at different time points between 0 and 24 h. Glutaminase and α-tubulin levels were determined in whole-cell lysates by immunoblotting using specific antibodies for glutaminase (dilution 1:1000) and α-tubulin (dilution 1:1000).

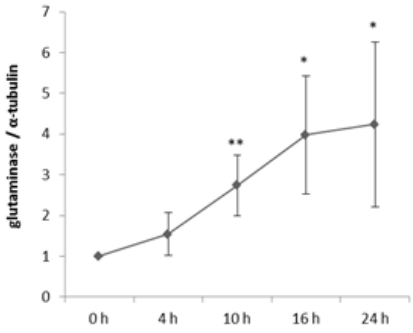

Figure 5.18 | **Quantification of glutaminase protein shows a significant increase after 10, 16 and 24 h of proTAME treatment.** Blots of three independent experiments were quantified. The mean values ± SD of cyclin B1, normalized to the loading control protein, are shown in the histogram. The result is statistically significant ($p < 0,01$; $p < 0,05$; $p < 0,05$).

5.4.2. Glutamate increases when APC/C is inhibited

We observed a significant increase of glutaminase in neurons when APC/C is inhibited and therefore next tested whether the levels of glutamate in the supernatants change after the treatment with proTAME. Before the treatments, cell culture medium was changed in all plates of controls and in proTAME treated cells. Supernatants were collected at different time points between 3 and 24 hours after the change. The samples were prepared as described in the method section and glutamate was measured. There was a significant increase in glutamate upon inhibition of APC/C in the supernatant of neurons (Figure 5.19).

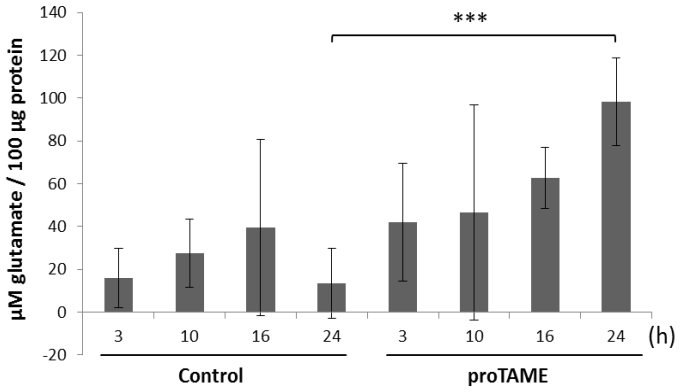

Figure 5.19 | **Extracellular glutamate increases when APC/C is inhibited by proTAME in neurons.** Glutamate levels in the extracellular culture medium of neurons after 3, 10, 16 and 24 h under control conditions or with proTAME (12 µM). Glutamate concentrations were normalized to

protein levels measured in neuron lysates from the corresponding cell culture plates. Mean values ± SD of three independent experiments are shown and are statistically significant ($p < 0,001$).

5.4.3. Glutaminase accumulates when treated with Aβ

We have previously observed a decrease in cdh1 levels upon Aβ treatment and then measured here glutaminase levels after the same treatment. The Aβ treatment was accomplished as described above and glutaminase protein levels were determined by western blotting. There was a significant increase in glutaminase after the treatment with Aβ in neurons (Figure 5.20 a-d).

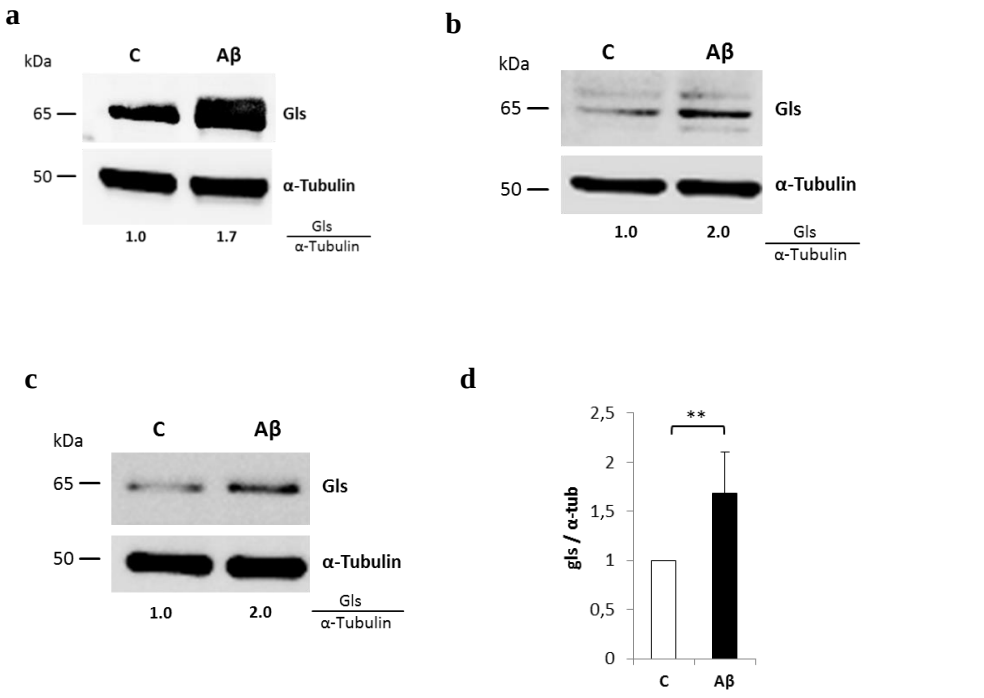

Figure 5.20 | **Glutaminase increases upon Aβ treatment.** (a-c) Neurons in primary culture were treated with Aβ for 24 h. Glutaminase and α-tubulin levels were determined in whole-cell lysates by immunoblotting using specific antibodies for glutaminase (dilution 1:1000) and α-tubulin (dilution 1:1000). Blots were quantified by densitometry and normalized with α-tubulin; values are indicated

below the blots. (d) The mean values ± SD of glutaminase, normalized to α-tubulin are shown in the histogram, and are statistically significant ($p < 0,01$).

5.4.4. mRNA expression levels of glutaminase upon Aβ treatment

In the previous experiment we have observed that glutaminase increases in neurons when treated with Aβ. Here we tested whether mRNA expression of glutaminase increases in this treatment conditions. We measured glutaminase mRNA level by qPCR and observed no statistically significant difference in controls or with Aβ (Figure 5.21). This result indicates that glutaminase accumulates with Aβ due to post-translational modifications (decreased degradation of glutaminase by APC/C-Cdh1) and not because of changes in mRNA expression.

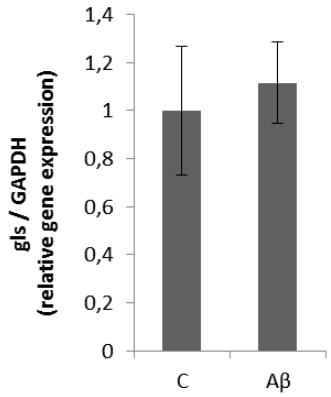

Figure 5.21 | **mRNA levels of glutaminase in neurons.** Neurons in primary culture were treated with Aβ. After 24 h the cells were collected and mRNA was isolated and retro-transcribed to cDNA. Relative expression levels were determined by real time qPCR using specific primers. Mean values ± SD of glutaminase normalized to GAPDH are shown in the histogram. There is no statistically significant difference (n=3).

5.4.5. Intracellular glutamate levels upon Aβ treatment

Primary neurons were treated with oligomeric Aβ (5 µM) for 16 or 20 h. The neurons were washed 3 times with 2 ml 1x PBS, collected in 1x PBS containing protease inhibitor and ortovanadate and stored at -80°C till use. The protein concentration was determined and glutamate was measured in whole cell lysates in duplicates. We could not detect a significant difference of glutamate in the cell lysates (Figure 5.22).

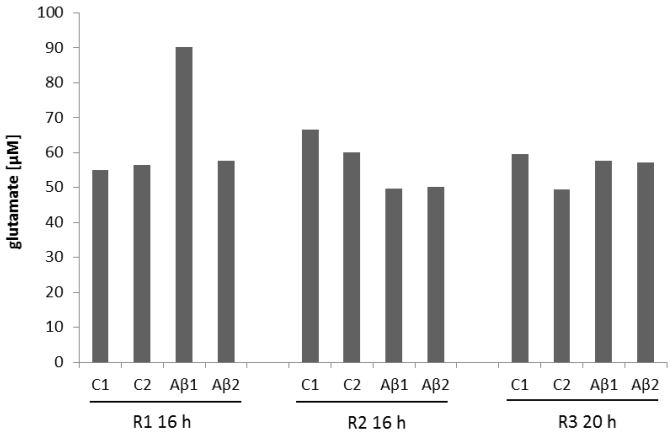

Figure 5.22 | **Glutamate concentration (µM) in neurons.** C1, C2 are duplicates of controls; Aβ1, Aβ2 are duplicates of neurons treated with Aβ. Samples from 3 animals (R1, R2, R3) with indicated times of Aβ incubation or in control conditions.

5.4.6. Extracellular glutamate levels upon Aβ treatment

We then measured extracellular glutamate levels in Aβ-treated samples. The Aβ treatment was accomplished as described above and supernatants were collected at different time points after the treatment. Glutamate levels were significantly

increased in samples treated with Aβ after 20 h in three independent experiments (Figure 5.23).

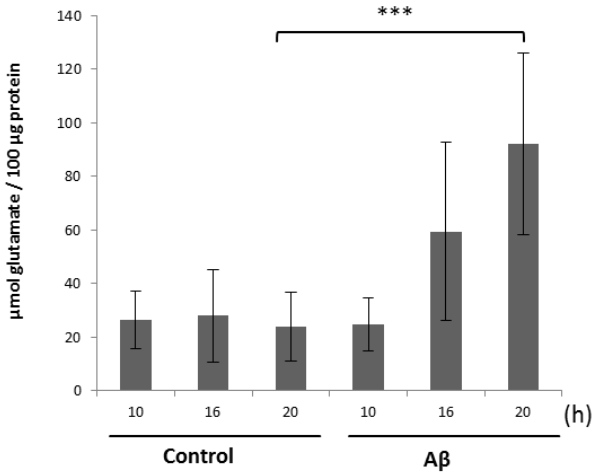

Figure 5.23 | **Extracellular glutamate increases upon Aβ treatment.** Glutamate levels in extracellular culture medium of neurons after 10, 16 and 20 h under control conditions or with Aβ. Glutamate concentrations were normalized to protein levels measured in neuron cell lysates from the same culture flasks. Mean values ± SD of three independent experiments are shown. There is a statistically significant increase when treated with Aβ.

5.4.7. Glutaminase accumulates in cdh1-silenced neurons

We have observed that glutaminase accumulates in neurons when APC/C is inhibited or when treated with Aβ. To determine whether the change in the glutaminase level occurs specifically due to a decrease of cdh1, we silenced cdh1 using smart pool on target siRNA. We observed a slight but significant increase in glutaminase in cdh1 silenced neurons (Figure 5.24).

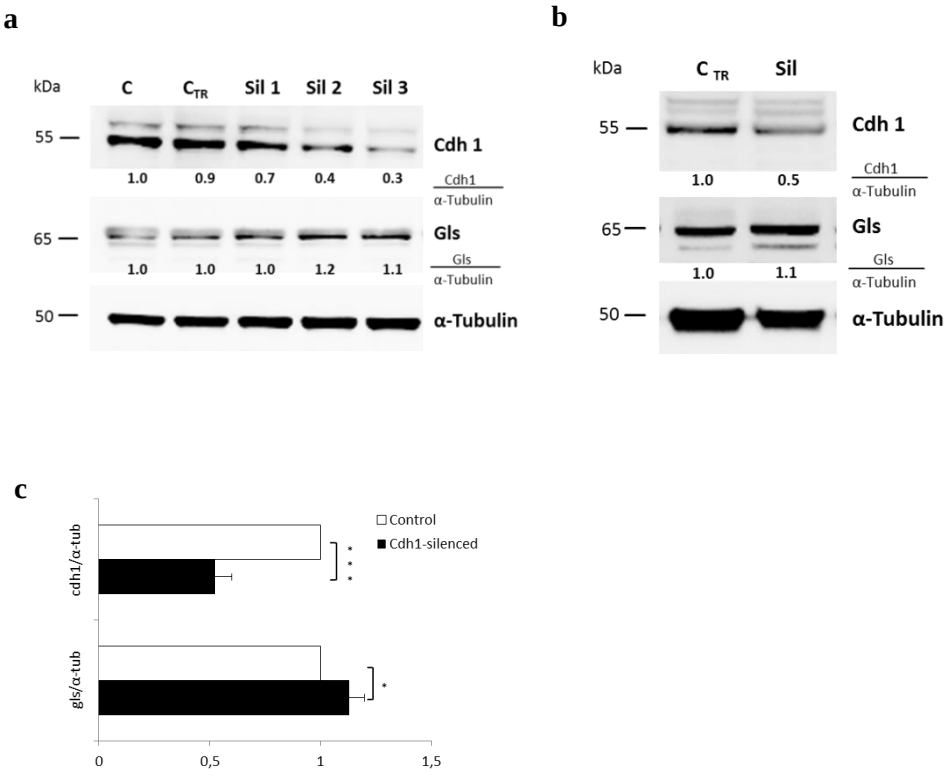

Figure 5.24 | **Glutaminase (gls) increases in cdh1-silencend neurons.** (a-b) Western blot image of cdh1 and gls in cdh1-silenced neurons. Cdh1, glutaminase and α-tubulin levels were determined in whole-cell lysates by immunoblotting using specific antibodies for cdh1 (1:1000), glutaminase (dilution 1:1000) and α-tubulin (dilution 1:1000). (c) Western blots were quantified by densitometry and normalized with α-tubulin, mean ± SD of three independent experiments are indicated.

We measured glutamate in the supernatants of cdh1-silenced neurons. We observed a tendency of glutamate increase, which was however not significant. Since there was only a small increase in glutaminase in cdh1-silencend neurons, we speculated that this increase was not sufficient to significantly increase extracellular glutamate levels (Figure 5.25).

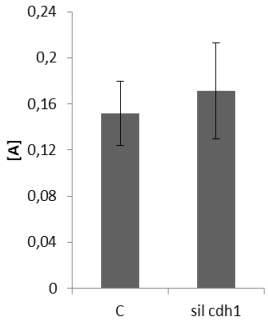

Figure 5.25 | **Extracellular glutamate levels in cdh1-silenced neurons.** Glutamate levels in the extracellular culture medium of neurons in control conditions or upon treatment with smart pool on target siRNA. Mean values ± SD of three independent experiments are shown. There is no statistically significant difference between the two groups.

In order to improve cdh1 silencing efficiency, we repeated cdh1 silencing using 'Accell siRNA', which is specialized siRNA for 'difficult-to-transfect' cells, like primary neurons. This siRNA does not require any transfection reagent but has to be used at higher concentrations (1 μM). Neurons were incubated in standard culture medium with reduced serum concentration (1%) for 96 hours with either control siRNA or cdh1 siRNA. The silencing of cdh1 was highly efficient and glutaminase significantly increased in cdh1-silenced neurons. When the cells were additionally treated with Aβ, it was added in the last 24 hours to the neurons upon silencing treatment. This caused a further increase in glutaminase in the samples (Figure 5.26 a-d).

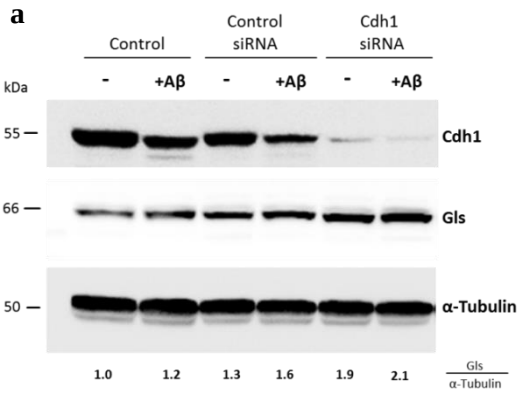
a
Control
Control siRNA
Cdh1 siRNA
kDa
-
+Aβ
-
+Aβ
-
+Aβ
55
Cdh1
66
Gls
50
α-Tubulin
1.0
1.2
1.3
1.6
1.9
2.1
Gls / α-Tubulin

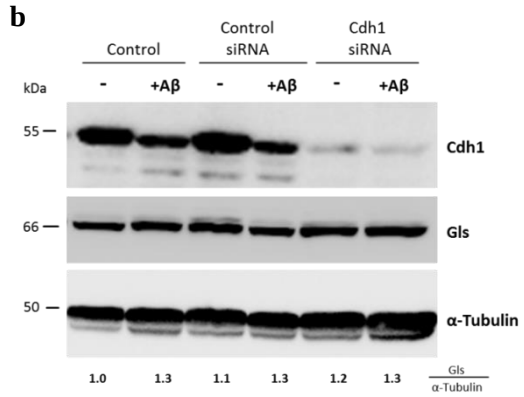
b
Control
Control siRNA
Cdh1 siRNA
kDa
-
+Aβ
-
+Aβ
-
+Aβ
55
Cdh1
66
Gls
50
α-Tubulin
1.0
1.3
1.1
1.3
1.2
1.3
Gls / α-Tubulin

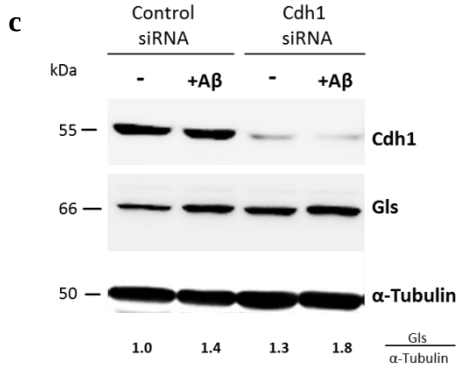
c
Control siRNA
Cdh1 siRNA
kDa
-
+Aβ
-
+Aβ
55
Cdh1
66
Gls
50
α-Tubulin
1.0
1.4
1.3
1.8
Gls / α-Tubulin

d

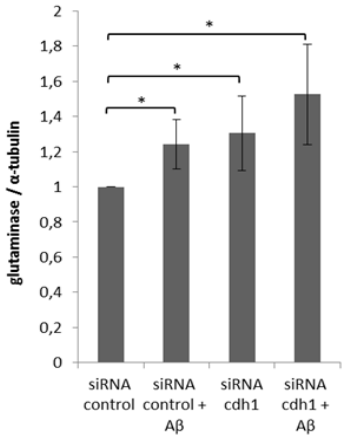

Figure 5.26 | **Glutaminase (gls) increases in cdh1-silencend (accell siRNA) neurons compared to control siRNA.** (a-c) Western blot image of cdh1 and gls in cdh1-silenced neurons with or without Aβ. Cdh1, glutaminase and α-tubulin levels were determined in whole-cell lysates by immunoblotting using specific antibodies for cdh1 (1:1000), glutaminase (dilution 1:1000) and α-tubulin (dilution 1:1000). (d) Glutaminase levels were quantified by densitometry and normalized with α-tubulin, mean ± SD of three independent experiments are indicated and are statistically significant ($p < 0,05$).

We measured glutamate in the supernatants in these cdh1-silenced neurons and observed an increase, which was however not significant due to high standard deviations.

The glutamate increase by APC/C inhibition using proTAME is higher than the glutamate increase caused by cdh1 depletion. The fact that inhibition of the whole ubiquitin ligase complex causes a more potent increase in glutamate than cdh1 depletion alone indicates that other coactivators (e.g. cdc20) might be involved in targeting glutaminase. It is also possible that the treatment conditions (96 h in low serum medium) leads to lower basal glutaminase expression levels. This would

cause that glutaminase and glutamate needed more time to accumulate upon a lack of degradation.

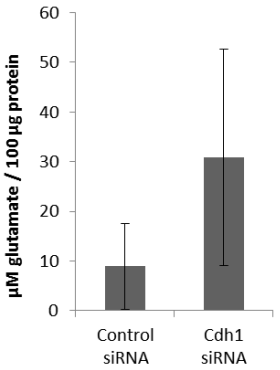

Figure 5.27 | **Extracellular glutamate levels in cdh1-silenced neurons.** Glutamate levels in extracellular culture medium of neurons with accell control siRNA or upon treatment with accel cdh1 siRNA. Mean values ± SD of three independent experiments are shown. There is a no statistically significant difference between the two groups.

5.4.8. Glutamate increase is caused by glutaminase accumulation

We observed a correlation between increasing glutaminase and glutamate levels when neurons were treated with proTAME or Aβ. To test if the glutamate increase induced by proTAME or Aβ is mediated by glutaminase, we inhibited glutaminase using 'compound 968', a cell permeable benzophenanthridinone that acts as an allosteric inhibitor of mitochondrial glutaminase activity. We inhibited glutaminase when treated with proTAME or Aβ for 24 hours and measured extracellular glutamate levels.

We observed that in neurons in which glutaminase was inhibited when treated with proTAME, the glutamate increase was completely abolished (Figure 5.28). This indicates that glutamate increase induced by APC/C inhibition is caused by

glutaminase accumulation. The glutamate increase in Aβ treated neurons was partially reduced when glutaminase is inhibited (Figure 5.29). This result suggests that glutaminase is involved in Aβ-induced glutamate increase.

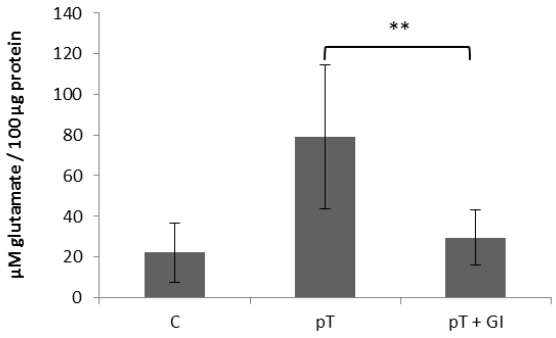

Figure 5.28 | **Extracellular glutamate increase upon APC/C inhibition is abolished when glutaminase is inhibited.** Neurons were treated with proTAME (pT) or pT and a glutaminase inhibitor (GI) for 24 h. Mean values ± SD of three independent experiments are shown. There is a statistically significant difference between the two groups.

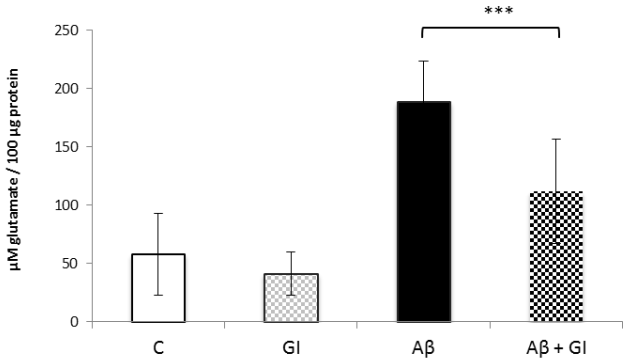

Figure 5.29 | **Extracellular glutamate increase upon Aβ treatment is reduced when glutaminase is inhibited.** Neurons were treated with Aβ alone or Aβ and a glutaminase inhibitor (GI) for 24 h. Mean values ± SD of three independent experiments are shown. There is a statistically significant difference between the two groups.

5.4.9. Glutaminase accumulation causes apoptosis

We then tested whether the glutaminase and glutamate increase, we observed upon APC/C inhibition cause excitotoxicity, inducing apoptosis.

First, we used flow cytometry analysis to determine whether inhibition of APC/C activity induced apoptosis in neuron cells. They were treated with proTAME for 0, 4, 10, 16 and 24 h and were carefully detached using trypsin and subjected to flow cytometry using an 'Annexin V-FITC Apoptosis Detection Kit'. We observed a significant increase in apoptosis upon the treatment after 24 h (Figure 5.30).

a

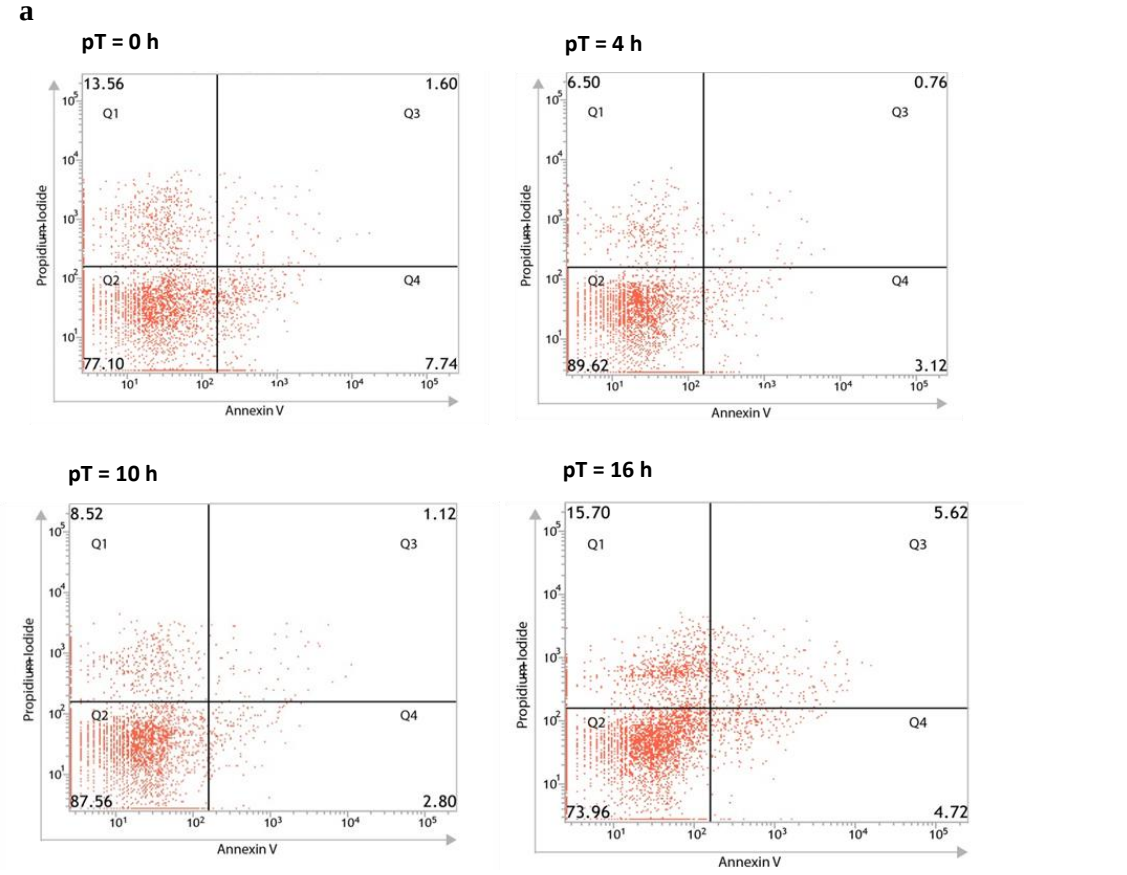

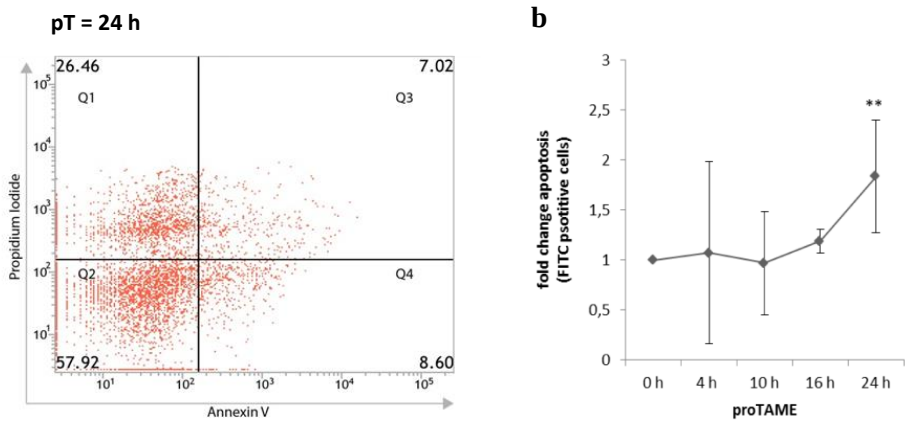

Figure 5.30 | **APC/C inhibition by proTAME causes apoptosis in primary neurons.** (a) Representative assays of flow cytometry analysis for apoptosis in neurons after 0, 4, 10, 16 and 24 hours. (b) Flow cytometry analysis for apoptosis of neurons shows the fold change ± SD of apoptotic cells level upon a time-course of pT treatment. Three independent experiments were quantified and were significant at 24 h of treatment ($p < 0,01$).

Moreover, neurons were next treated with proTAME alone or proTAME and the glutaminase inhibitor, as described above, for 20 h. Neurons were carefully detached using trypsin and subjected to flow cytometry using an 'Annexin V-FITC Apoptosis Detection Kit'. We observed proTAME treatment caused apoptosis in neurons, which was reduced when glutaminase was inhibited at the same time (Figure 5.31).

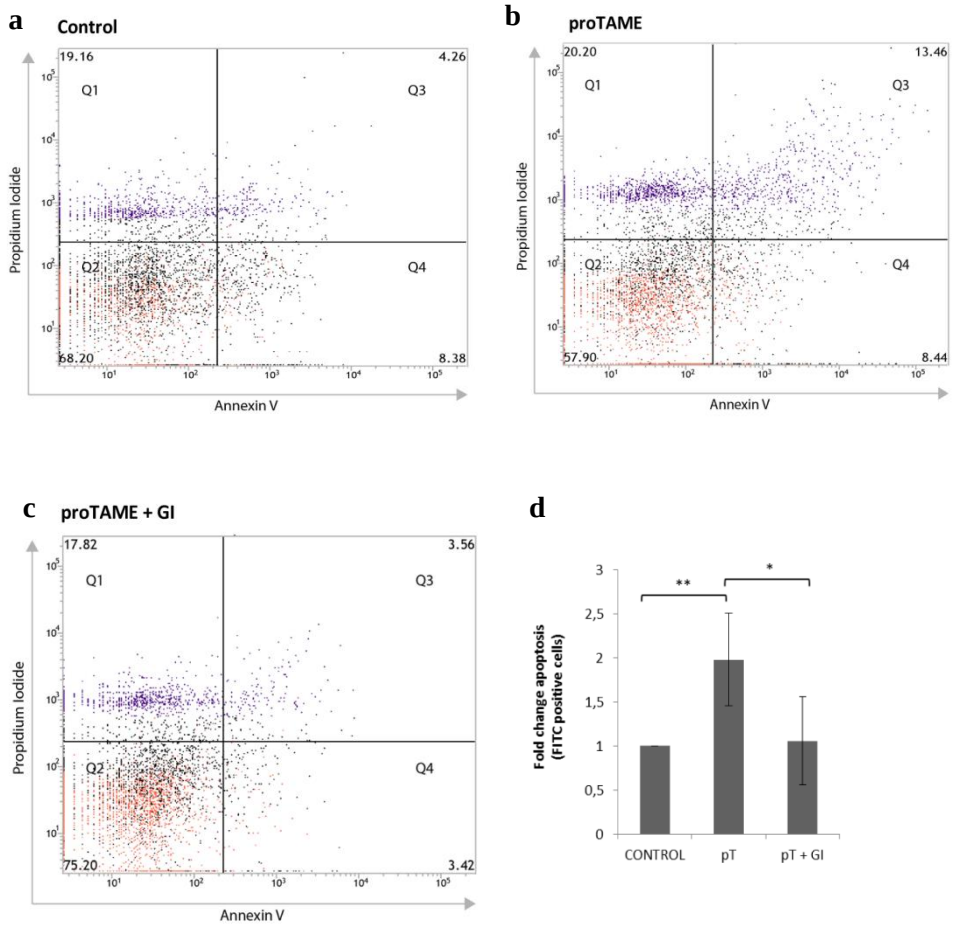

Figure 5.31 | **APC/C inhibition induces apoptosis, which is reduced when glutaminase is inhibited at the same time.** Representative assays of flow cytometry analysis of neurons under (a) control conditions, (b) treated with proTAME or (c) proTAME and glutaminase inhibitor 'compound 968' for 20 h. (d) Mean FITC values ± SD are shown and are statistically significant ($p < 0,005$, $p < 0,01$).

We also checked whether the inhibition of glutaminase alone affects the viability and apoptosis levels in neurons. There was no difference between the controls and neurons treated with the inhibitor (Figure 5.32).

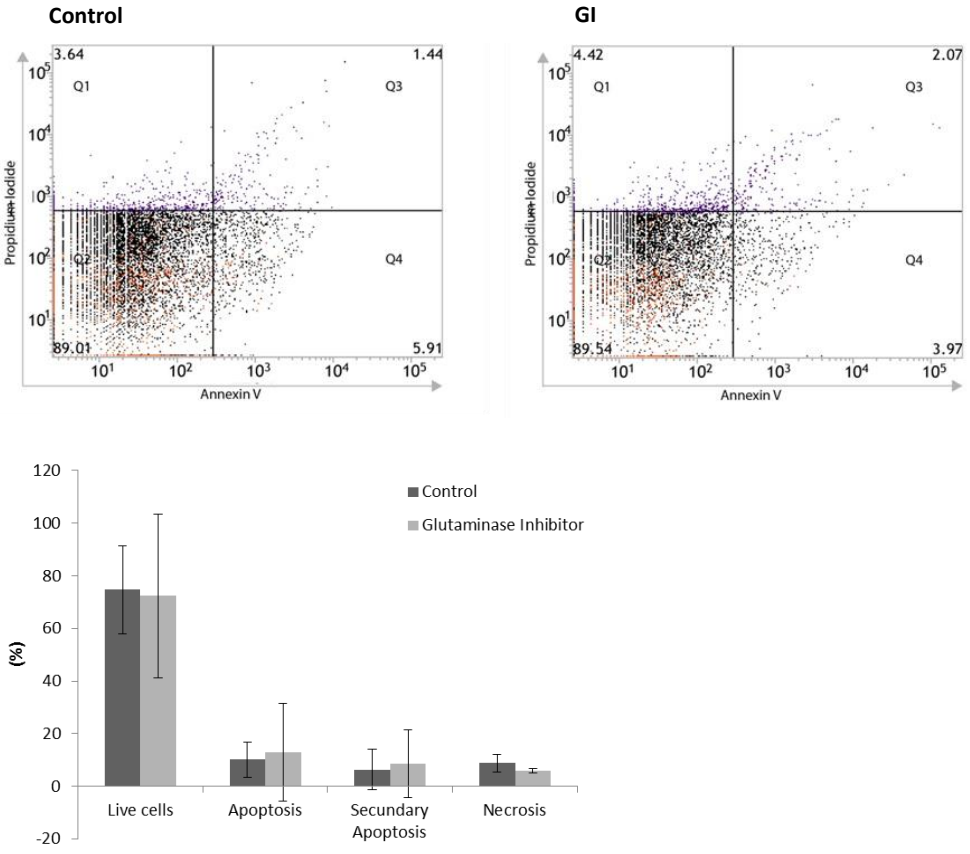

Figure 5.32 | **Glutaminase Inhibitor treatment in primary neurons. (a)** Representative assays of flow cytometry analysis for apoptosis of neurons under control conditions, or treated with the glutaminase inhibitor (GI) for 20 h. **(b)** Mean FITC values ± SD are shown from data of three independent experiments.

Next, we tested whether apoptosis induced by Aβ can be ameliorated by glutaminase inhibition. Neurons were treated with Aβ or Aβ and the glutaminase inhibitor for 20 h. Apoptosis was measured as described above by flow cytometry.

We observed Aβ treatment induced apoptosis, which was ameliorated by inhibition of glutaminase (Figure 5.33).

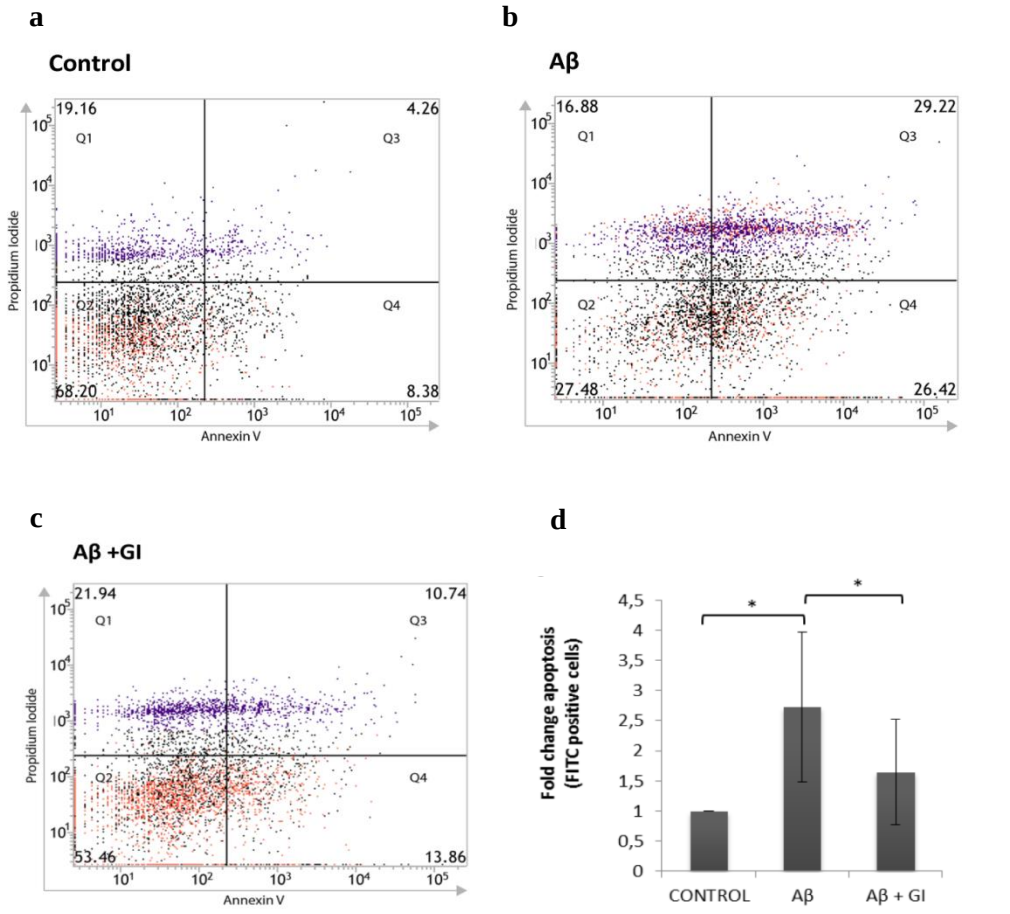

Figure 5.33 | **Aβ-induced apoptosis is ameliorated when glutaminase is inhibited.** Representative assays of flow cytometry analysis of neurons under (a) control conditions, (b) treated with Aβ (c) Aβ and glutaminase inhibitor 'compound 968' for 20 h. (d) Mean FITC values ± SD are shown and are statistically significant ($p < 0{,}001$; $p < 0{,}01$).

These results show that the glutamate increase induced by Aβ or proTAME causes apoptosis, mediated by glutaminase. The inhibition of glutaminase promotes cell viability in these toxic conditions.

5.4.10. Glutamine is required for glutamate increase

Glutaminase catalyses the reaction from glutamine to glutamate and ammonia. To test to which extend glutamate is metabolized from glutamine after the treatment with proTAME or Aβ, we tested if the removal of glutamine from the medium affects the glutamate levels in these treatment conditions.

Neurons were treated with proTAME or Aβ in control medium or glutamine-free medium for 24 h. We observed no increase of glutamate when glutamine was removed from the medium (Figure 5.34).

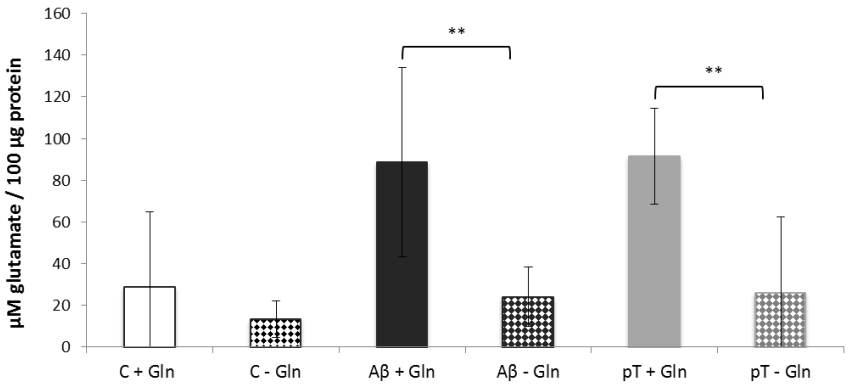

Figure 5.34 | **Extracellular glutamate increase observed upon proTAME (pT) or Aβ treatment is abolished when glutamine is removed from the medium.** Neurons were treated with pT or Aβ in medium with or without glutamine for 24 h. Mean values ± SD of three independent experiments are shown. There is a statistically significant difference between the two groups.

5.4.11. Ammonia increases when APC/C is inhibited by proTAME

We then tested if ammonia, the by-product of the transformation of glutamine to glutamate, also increases when APC/C is inhibited.

Neurons were treated with proTAME as described above for 24 h with or without glutamine in the medium. The supernatants were collected and ammonia was measured using an ammonia assay kit. We observed a significant increase of ammonia when APC/C was inhibited. The control condition, without glutamine, showed that there was no increase in ammonia when glutamine was removed from the medium (Figure 5.35).

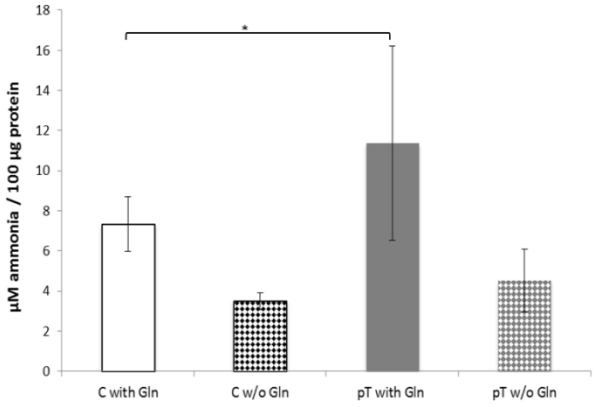

Figure 5.35 | **Extracellular ammonia increases upon APC/C inhibition.** Neurons were treated proTAME (pT) in medium with or without glutamine for 24 h. Mean values ± SD of three independent experiments are shown. There is a statistically significant difference between the two groups.

5.5. Intracellular Ca^{2+} Levels Increase Upon APC/C Inhibition

Excitotoxicity is characterized by increased Ca^{2+} influx through glutamate receptor channels. We had observed increased glutamate levels upon APC/C inhibition by proTAME or Aβ treatment. Here we tested whether the increased extracellular glutamate levels lead to an intracellular Ca^{2+} increase.

Neurons were isolated and cultured in chamber slides for microscope analysis as described in the method section. They were treated with Aβ, proTAME, or proTAME and glutaminase inhibitor 'compound 968' for 24 h. Glutamate treatment (500 µM) was used as a positive control. Cytochemical analysis using Fluo4 showed that there was a rise in the intracellular Ca^{2+} level after 24 h of treatment with Aβ or proTAME. Such levels were similar to those of cells treated directly with glutamate (500 µM). When glutaminase was inhibited in neurons, which were treated with proTAME, the increase in Ca^{2+} levels was abolished (Figure 5.36).

a

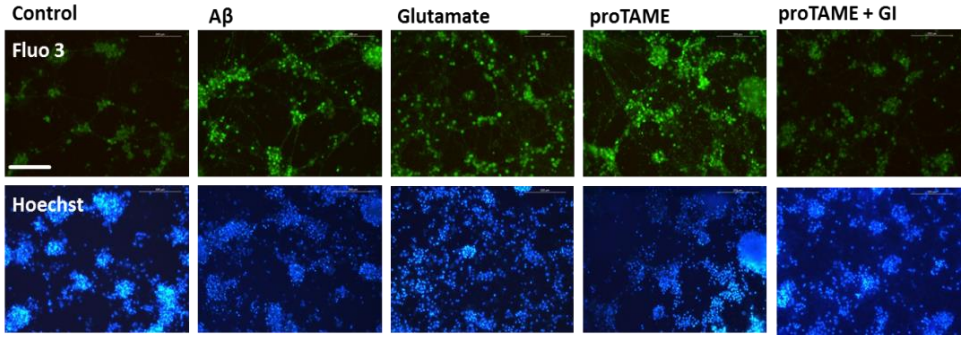

b

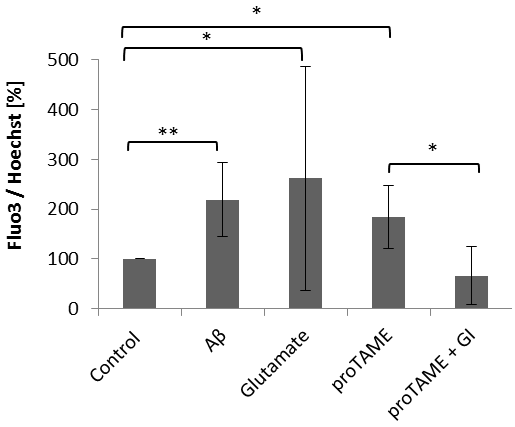

Figure 5.36 | **Ca^{2+} increases upon APC/C inhibition.** (a) Representative images of calcium by Fluo4 staining in neurons upon different treatments C, Aβ (5 µM), glutamate (500 µM), proTAME (12 µM), proTAME (12 µM) + GI (100 µM) for 24 h. Ca^{2+} staining intensities (Fluo4) were normalized to nuclei staining intensities (Hoechst). (b) The mean values ± SD from images of three independent experiments are shown and are statistically significant. Scale bar = 200 µM.

5.6. Upstream Regulators of Cdh1

5.6.1. Cdk5 increases with Aβ and glutamate treatment in neurons

It was shown that cdk5 phosphorylates cdh1 in excitotoxicity (Maestre et al., 2008). We observed that cdh1 decreases in neurons when treated with Aβ. It has been reported that Aβ causes dysregulation in Ca^{2+} homeostasis and that this leads an increase in cdk5. Here we tested whether cdk5 is affected by Aβ or glutamate, as we have previously observed increased levels of Ca^{2+} upon those treatments.

Neurons were treated with Aβ or glutamate as described above and cdk5 protein levels were measured by western blotting. We detected cdk5 at the corresponding molecular weight of 30 kDa by a specific antibody (Figure 5.37 a). In three

independent experiments we observed that cdk5 accumulates when treated with Aβ or glutamate (Figure 5.37 a-d).

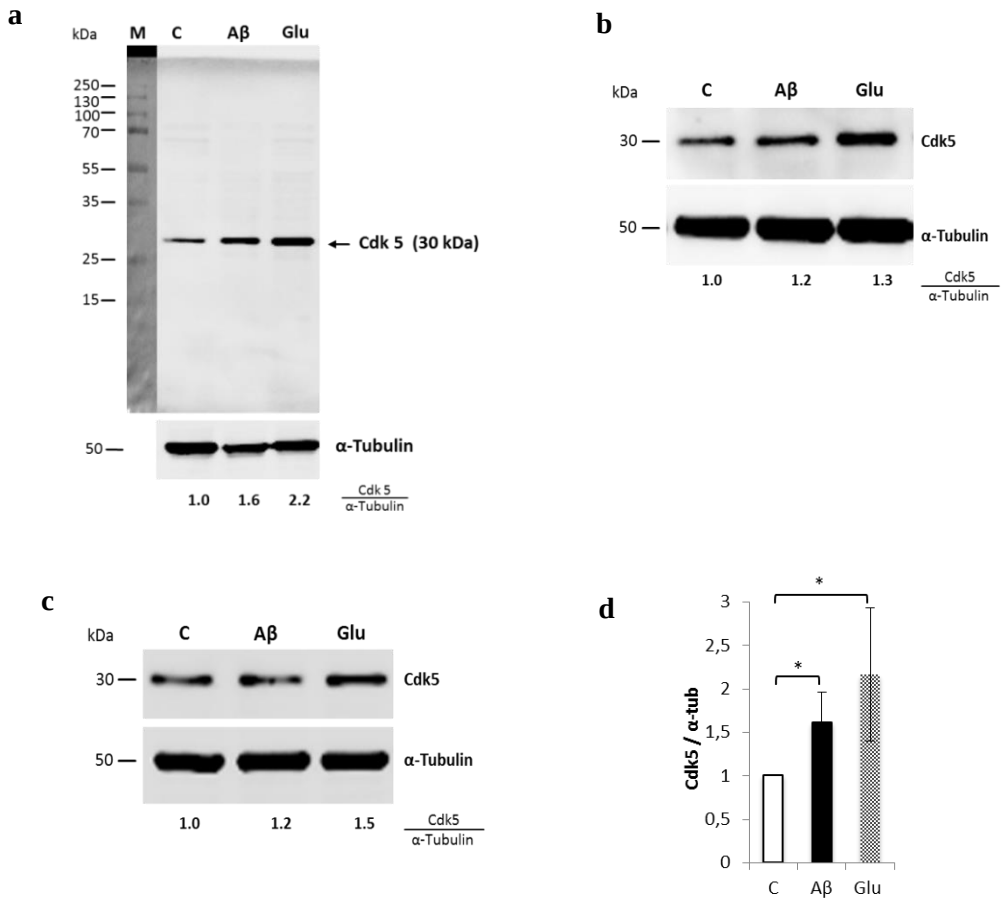

Figure 5.37 | **Cdk5 increases upon Aβ or glutamate treatment.** (a-c) Neurons in primary culture were treated with Aβ or glutamate for 24 h. Cdk5 and α-tubulin levels were determined in whole-cell lysates by immunoblotting using specific antibodies for cdk5 (dilution 1:1000) and α-tubulin (dilution 1:1000). Blots were quantified by densitometry and normalized with α-tubulin; values are indicated below the blots. (d) The mean values ± SD of cdk5, normalized to α-tubulin, showed a significant increase after the treatment ($p < 0,05$).

5.6.2. p25/p35 increases with Aβ and glutamate treatment in neurons

The activator of cdk5 is p35. The Ca^{2+} activated protease calpain cleaves p35 to p25, a more stable peptide. Therefore the increase in Ca^{2+} leads to a more stable Cdk5-p25 complex. We have observed that cdk5 increases when treated with Aβ or glutamate and tested here the protein levels of p35 and p25 upon these treatments. Neurons were treated as described above and p35 and p25 protein levels were measured by western blotting.

We detected p35 and p25 at the corresponding molecular weight of 35 and 25 kDa by a specific antibody (Figure 5.38 a). In three independent experiments we observed that p25 accumulates significantly when treated with Aβ or glutamate (Figure 5.38 a-c).

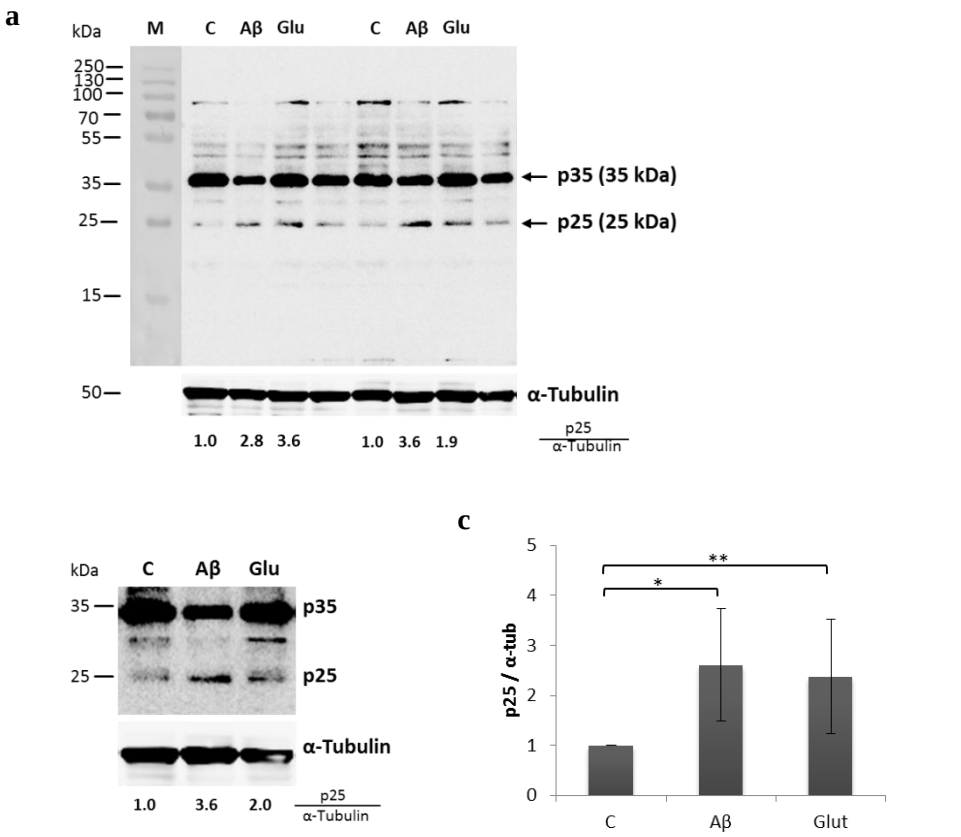

Figure 5.38 | **p25/p35 increases upon Aβ or glutamate treatment.** (a-b) Neurons in primary culture were treated with Aβ or glutamate for 24 h. p25/p35 and α-tubulin levels were determined in whole-cell lysates by immunoblotting using specific antibodies for p25/p35 (dilution 1:1000) and α-tubulin (dilution 1:1000). Blots were quantified by densitometry and normalized with α-tubulin; values are indicated below the blots. (c) The mean values ± SD of p25/p35, normalized to α-tubulin, showed a significant increase after the treatment.

5.6.3. Cdk5 mediates decrease of cdh1 and glutaminase accumulation

We have observed that cdk5 and its activator p25 increases upon treatment with Aβ. It is also known that it is a kinase that phosphorylates cdh1, leading to its inactivation and degradation. Here we tested if the inhibition of cdk5 by roscovitin leads to a stabilization of cdh1 when treated with Aβ. We also measured glutaminase levels upon cdk5 inhibition.

Neurons were treated with Aβ (5 µM) alone or Aβ and roscovitin (15 µM) for 24 h. After the treatment, neurons and their supernatants were collected. We observed that the Aβ-induced cdh1 decrease is partially reversed when cdk5 is inhibited. In the same line, glutaminase accumulation is limited upon inhibition of cdk5 in Aβ treated neurons (Figure 5.39).

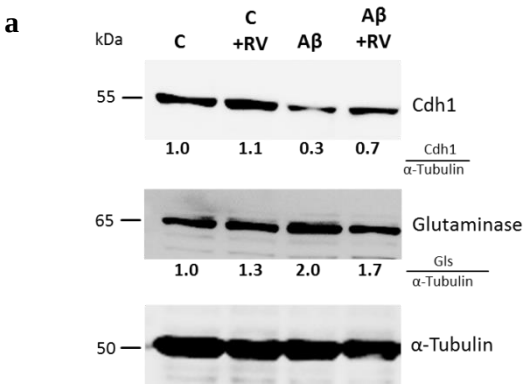

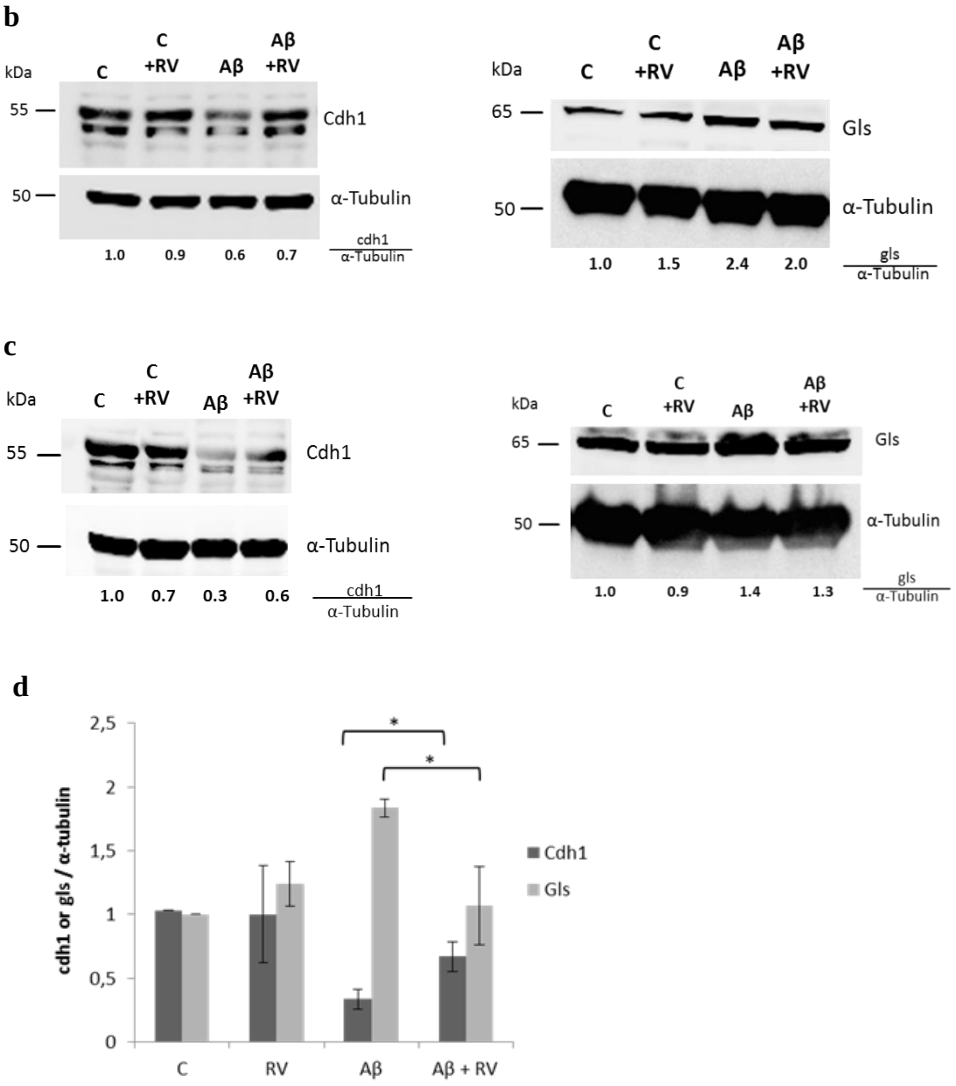

Figure 5.39 | **Cdk5 inhibition reduces Aβ-induced decrease of cdh1 and glutaminase accumulation.** (a-d) Neurons in primary culture were treated with roscovitine (RV), Aβ or Aβ and RV for 24 h. Cdh1, glutaminase (gls) and α-tubulin levels were determined in whole-cell lysates by immunoblotting using specific antibodies for cdh1 (dilution 1:1000), gls (dilution 1:1000) and α-tubulin (dilution 1:1000). Blots were quantified by densitometry and normalized with α-tubulin;

values are indicated below the blots. (d) The mean values ± SD are shown and the result demonstrates a significant change in cdh1 and glutaminase levels after the treatments.

5.6.4. Glutamate increase by Aβ is reduced upon cdk5 inhibition

We have observed that extracellular glutamate increases in neuron when treated with Aβ, mediated by cdh1 decrease and glutaminase accumulation. Furthermore, we showed that cdk5 mediates Aβ-induced alterations. Here we measured the extracellular glutamate levels of neurons treated with Aβ or Aβ and roscovitin, a cdk5 inhibitor. The treatments were accomplished as described above and supernatants were collected after 24 h. Glutamate increased significantly in samples treated with Aβ after 24 h and this was slightly reversed by cdk5 inhibition (Figure 5.40).

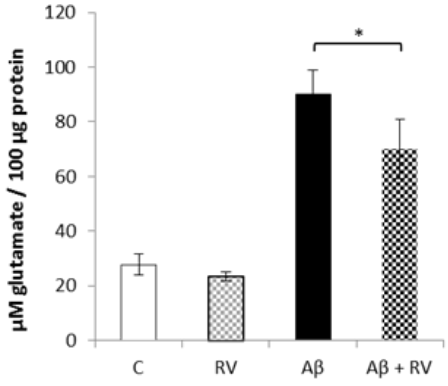

Figure 5.40 | **Extracellular glutamate increase induced by Aβ is reduced when cdk5 is inhibited.** Neurons were treated with roscovitine (RV), Aβ or Aβ and RV for 24 h and glutamate was measured in the supernatant. Mean values ± SD of three independent experiments are shown. There is a statistically significant difference between the two groups.

5.6.5. Pten decreases upon Aβ treatment

We have observed that cdk5-p25 regulates cdh1 upon Aβ treatment and consequently also, glutaminase and glutamate levels. We sought to identify whether there were other upstream regulators of cdh1. We looked for possible candidates in the literature according to the following criteria: (a) A protein that functions as a kinase or phosphatase, which has been related to cdh1 regulation and (b) that is known to be involved in AD. A protein fulfilling these criteria is the phosphatase and tensin homologue (Pten).

PTEN is another known upstream regulator of APC/C-Cdh1, responsible for assembly of APC/C with cdh1 in the nucleus (Garcia-Cao et al., 2012). Loss of PTEN negatively affects the activity of the E3 ligase APC/C-Cdh1 (Cordero-Espinoza et al., 2013). PTEN is one of the most frequently mutated/deleted tumor suppressors in human cancers. Moreover, PTEN deficiency results in hyperphosphorylation of tau (Kerr et al., 2006; Nayeem et al., 2007).

Neurons in primary culture were treated with Aβ (5 µM) for 20 h as described above. The samples were subjected to western blotting and we detected Pten at the corresponding molecular weight of 54 kDa by a specific antibody (Fig 5.41 a). We observed that Pten decreases when treated with Aβ (Figure 5.41 a-c).

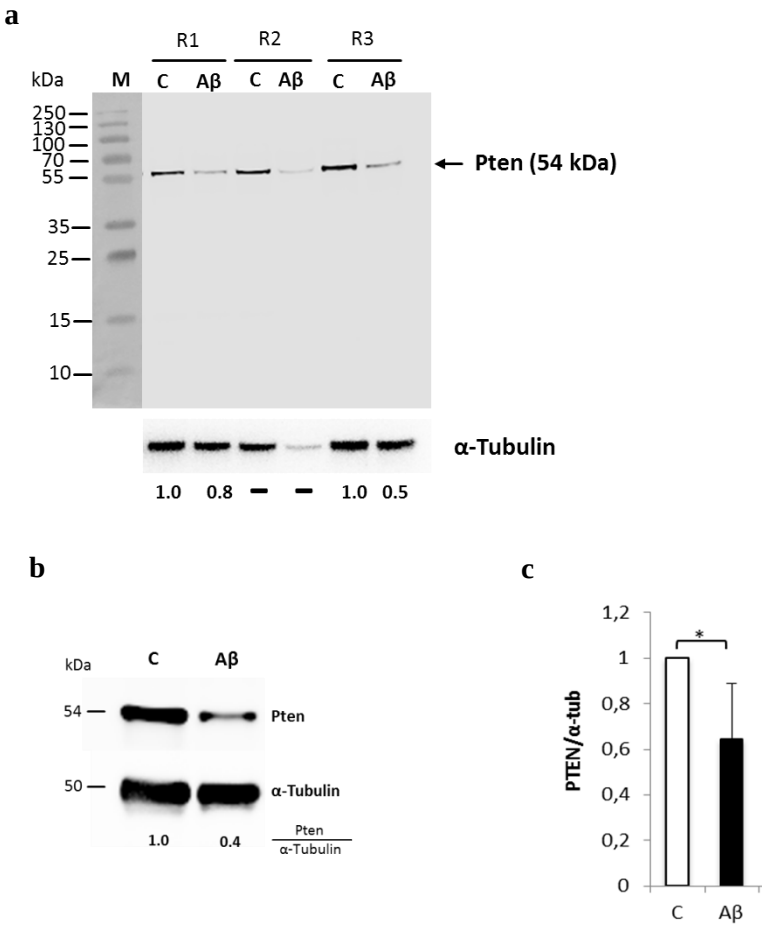

Figure 5.41 | **Pten decreases upon Aβ treatment**. (a-b) Western blot images of Pten under control conditions or with Aβ. Pten and α-tubulin levels were determined in whole-cell lysates by immuno-blotting using specific antibodies for Pten (dilution 1:1000) and α-tubulin (dilution 1:1000). Blots were quantified by densitometry and normalized with α-tubulin levels, values are indicated below the blots. (c) The mean values ± SD of three independent experiments are shown.

5.7. Glutamate Treatment in Neurons

Maestre et al. (2008) showed that cdh1 is phosphorylated by cdk5 in excitotoxicity. We observed that cdh1 decreases upon Aβ treatment, which has been shown to cause dysregulation in Ca^{2+} homeostasis. Therefore, we tested here whether glutamate, which induces an increase in intracellular Ca^{2+} levels, affects cdh1 and glutaminase levels.

Neurons in primary culture were treated with Aβ (5 µM) or glutamate (500 µM) for 24 h. We observed that glutamate treatment caused a decrease in the cdh1 protein level, similar to the one caused by Aβ (Figure 5.42 a-d).

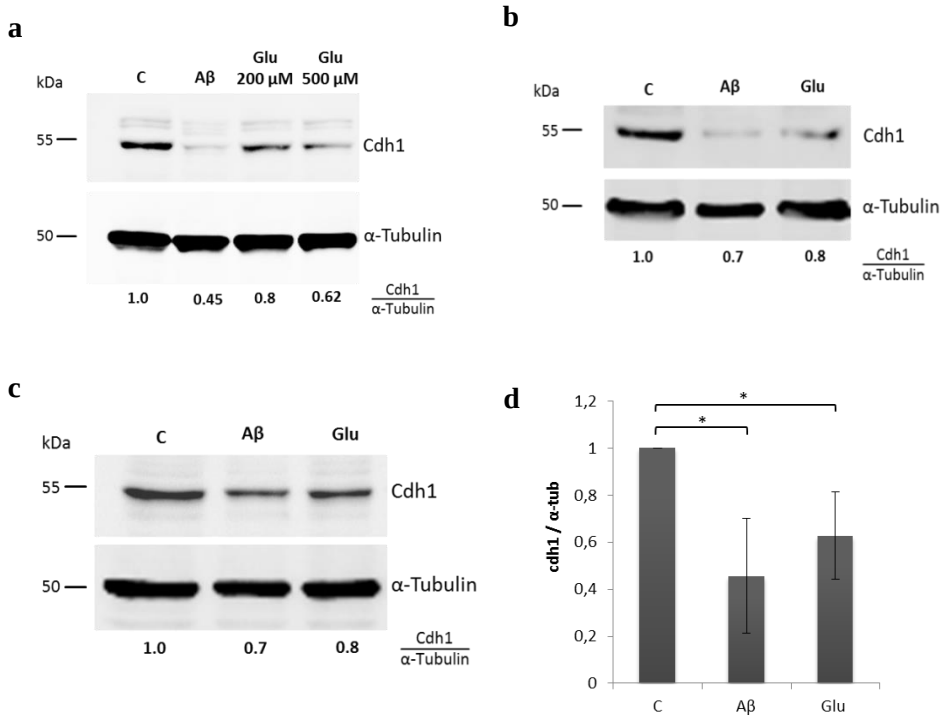

Figure 5.42 | **Cdh1 decreases upon treatment with glutamate.** (a-c) Western blot images of cdh1 and under control conditions, with Aβ or glutamate (a) 200 µM or 500 µM and (b-c) 500 µM treatment. Cdh1 and α-tubulin levels were determined in whole-cell lysates by immune-blotting using

specific antibodies for cdh1 (dilution 1:1000) and α-tubulin (dilution 1:1000). Blots were quantified by densitometry and normalized with α-tubulin levels, values are indicated below the blots. (d) The mean values ± SD of three independent experiments of controls, Aβ and glutamate (500 µM) are indicated.

Next, we measured the levels of glutaminase in these samples. We observed that the glutamate treatment caused an increase in glutaminase, similar to that caused by Aβ (Figure 5.43). The results indicate that glutamate affects cdh1-glutaminase levels in a similar way as Aβ. The next step was to analyse apoptosis upon glutamate treatment and if it can be prevented by glutaminase inhibition.

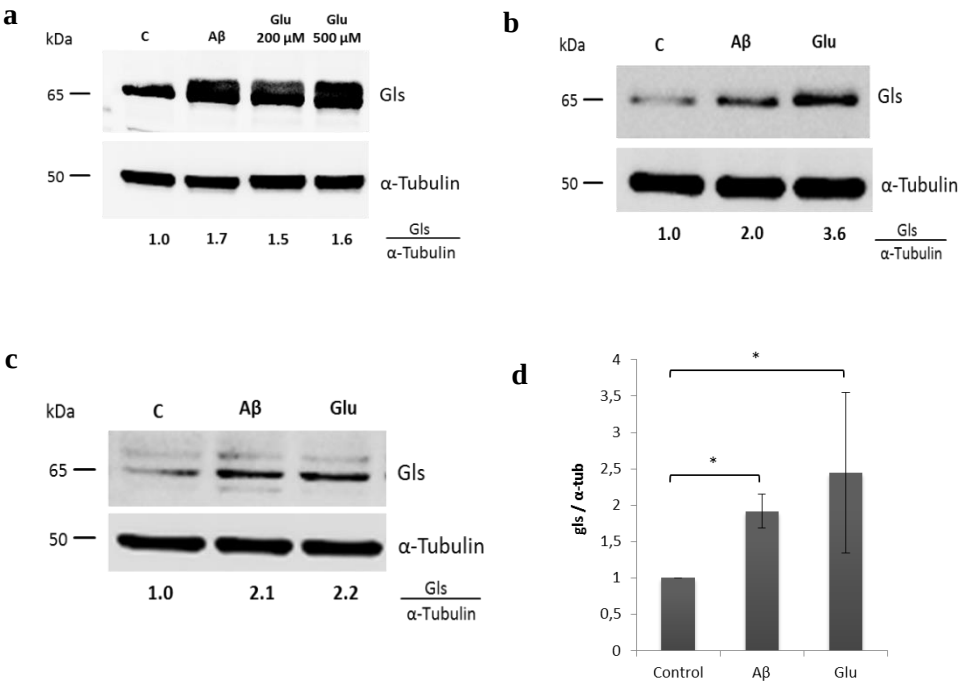

Figure 5.43 | **Glutaminase (gls) increases upon treatment with glutamate.** (a-c) Western blot images of gls and under control conditions, with Aβ or glutamate (a) 200 µM or 500 µM and (b,c) 500 µM treatment. Gls and α-tubulin levels were determined in whole-cell lysates by immune-

blotting using specific antibodies for gls (dilution 1:1000) and α-tubulin (dilution 1:1000). Blots were quantified by densitometry and normalized with α-tubulin levels, values are indicated below the blots. (d) The mean values ± SD of three independent experiments of controls, Aβ and glutamate (500 µM) are shown and are statistically significant.

5.7.1. Apoptosis in glutamate-treated neurons

First, we tested whether glutamate induced apoptosis in our experimental setting. Primary neurons were treated with Aβ (5 µM) or glutamate (500 µM) for 20 h and analysed by confocal microscopy using Annexin staining. We observed that apoptosis was induced at 500 µM glutamate comparable to apoptosis induced upon Aβ treatment (Figure 5.44). We continued the apoptosis analysis by flow cytometry.

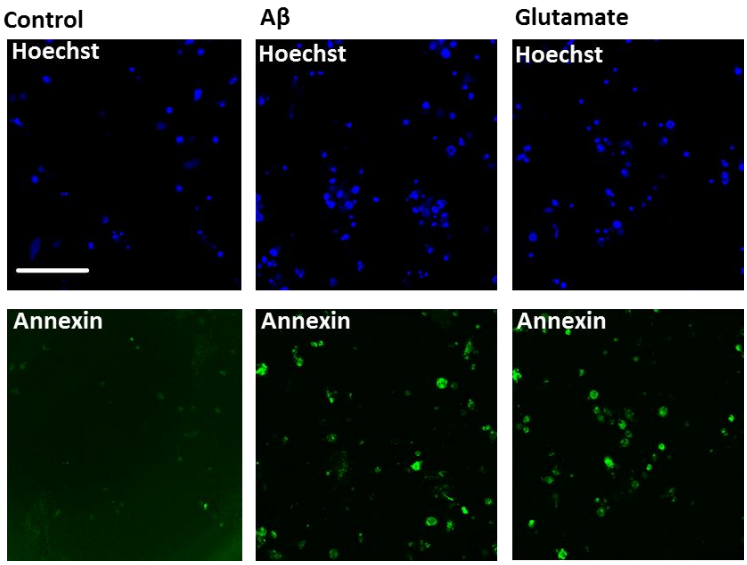

Figure 5.44 | **Apoptosis increases upon Aβ and glutamate treatment.** (a) Representative images of annexin stained neurons upon the treatments C, Aβ (5 µM), glutamate (500 µM).

5.7.2. Glutamate induces apoptosis mediated by glutaminase

Neurons were treated with glutamate (500 µM) alone or glutamate and glutaminase inhibitor for 20 h. Neurons were carefully detached using trypsin and subjected to flow cytometry using an 'Annexin V-FITC Apoptosis Detection Kit'. We observed glutamate treatment induced apoptosis in neurons, which was reduced by glutaminase inhibition (Figure 5.45).

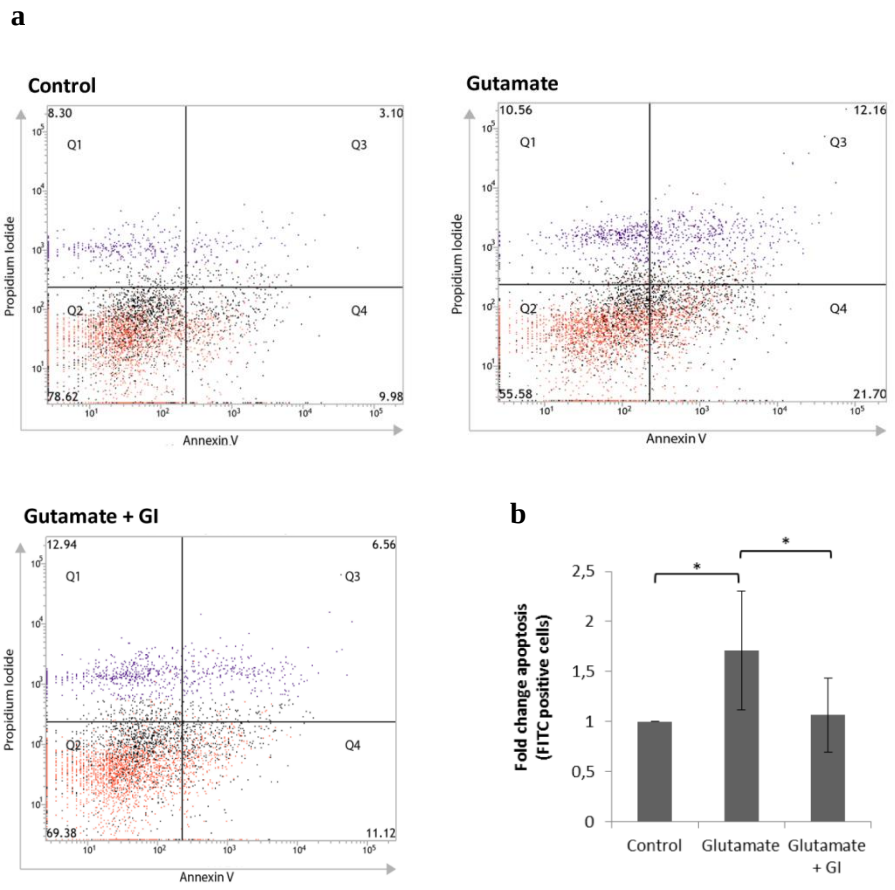

Figure 5.45 | **Glutamate induced apoptosis is ameliorated when glutaminase is inhibited.** Representative assays of flow cytometry analysis of neurons under (a) control conditions, (b) treated

with glutamate 500 µM (c) glutamate 500 µM and glutaminase inhibitor ‘compound 968‘ for 20 h. (d) Mean FITC values ± SD are shown.

5.8. APC/C-Cdh1 *in vivo*

The critical facts of the findings in neuron culture were then tested in *in vivo* models.

5.8.1. Aβ or glutamate microinjection in hippocampus affects cdh1 and glutaminase

We used microinjection in the brain of Wistar rats to test the effect of Aβ or glutamate on cdh1. We injected 10 µl volume of vehicle solution, Aβ (5 µM) or glutamate (1 mM) in the CA1 region of rat hippocampus according to stereotaxic adjustments and two days later the animals were sacrificed. The brains were prepared for immunohistochemical analysis. The result showed that cdh1 is located in the nucleus and in the cytoplasm in control conditions (vehicle injection) in CA1 neurons. Injection of Aβ or glutamate causes nuclear export of cdh1, which results in a 25% decrease of nuclear cdh1 (Figure 5.46 a-b). Both treatments also caused an increase in glutaminase in neurons in the pyramidal CA1 layer (Figure 5.46 a-b).

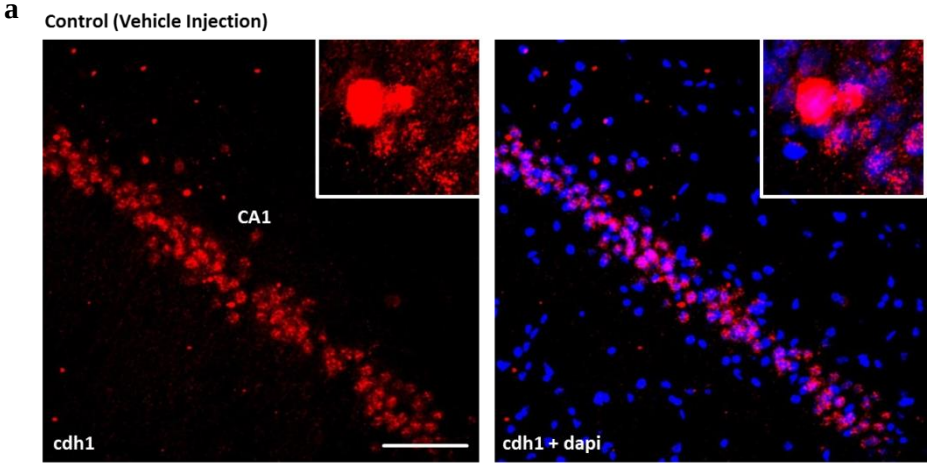

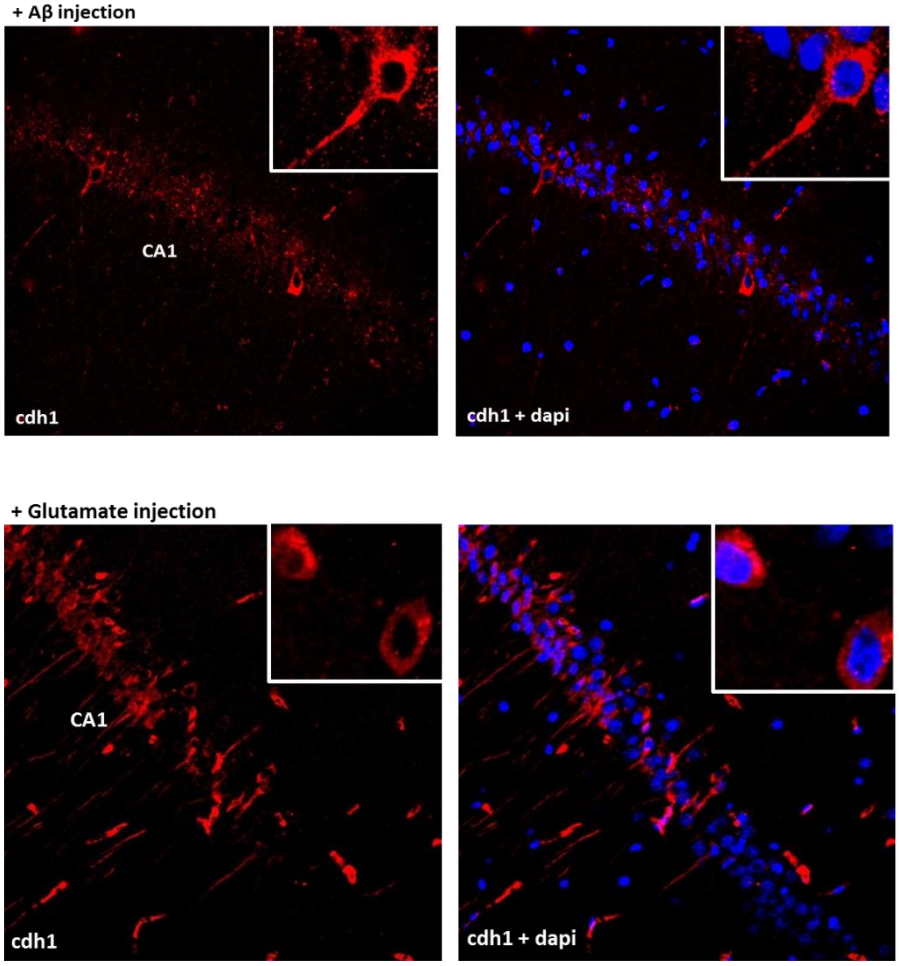
+ Aβ injection
CA1
cdh1
cdh1 + dapi
+ Glutamate injection
CA1
cdh1
cdh1 + dapi

b

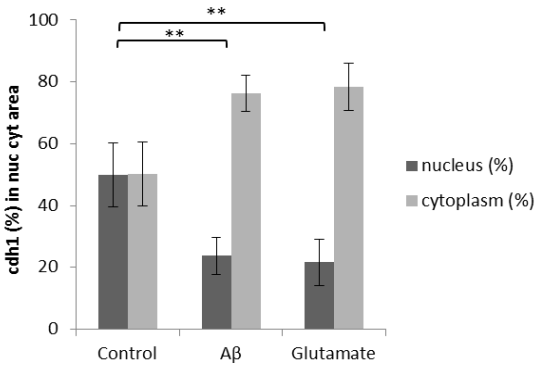
**
**
100
80
60
40
20
0
cdh1 (%) in nuc cyt area
Control
Aβ
Glutamate
nucleus (%)
cytoplasm (%)

Figure 5.45 | **Cdh1 in hippocampal CA1 brain slices (40 µm) after microinjection of Aβ or glutamate**. (a) Representative images of cdh1 and dapi stained (nucleus) hippocampal slices show nuclear export of cdh1 when treated with Aβ or glutamate compared to vehicle injection. (b) Results are show as mean ± SD of images of three independent experiments; percentages of nuclear and cytoplasmic cdh1 are shown ($p_{[C;\ A\beta]} < 0{,}01$; $p_{[C;Glut]} < 0{,}01$).

a

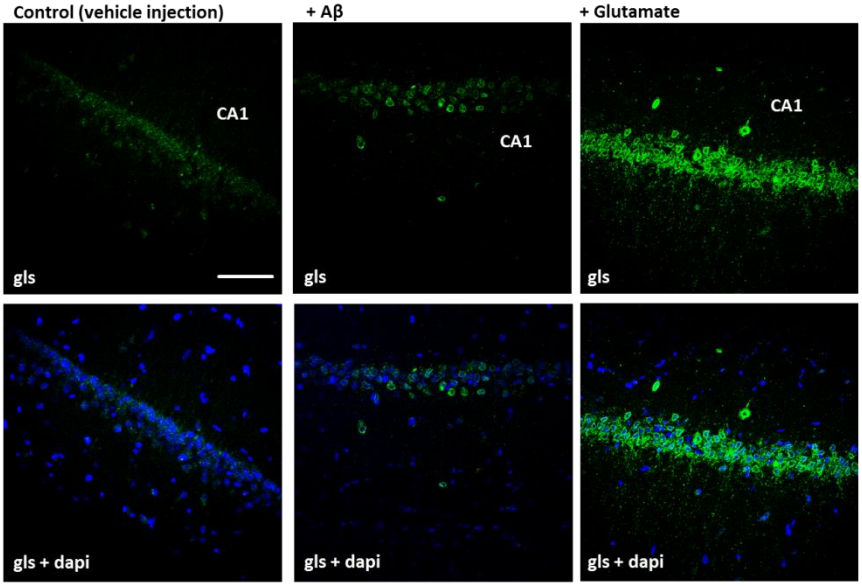

b

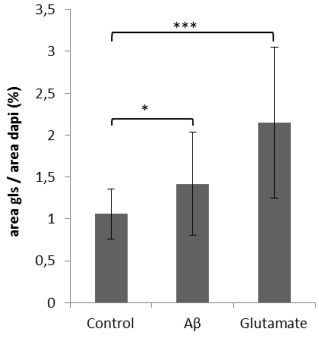

Figure 5.46 | G**lutaminase in hippocampal CA1 brain slices (40 µm) after microinjection of Aβ or glutamate**. (a) Representative images of glutaminase (gls) and dapi stained (nucleus) hippocampal slices show that glutaminase levels increase upon treatment with Aβ or glutamate. (b) Results are shown as mean ± SD of glutaminase area normalized to dapi area ($p_{[C;\ A\beta]} < 0{,}05$; $p_{[C;Glut]} < 0{,}001$). Scale bar = 75 µm.

5.8.2. Cdh1 and glutaminase in APP/PS1 mice by immunoblotting

After the *in vivo* study using acute Aβ or glutamate treatment, we tested the role of APC/C-Cdh1 in AD pathophysiology in the APP/PS1 mouse model of AD. APP/PS1 mice are subjected to chronic exposure to Aβ. We compared the protein levels of cdh1 and glutaminase in wild type (WT) and APP/PS1 mice at the age of 9 months (n=12).

Using western blot analysis, we observed lower levels of cdh1 in cortex homogenates of APP/PS1 compared to WT mice. Analysis of glutaminase in the same samples showed higher levels in APP/PS1 than in the WT mice (Figure 5.47).

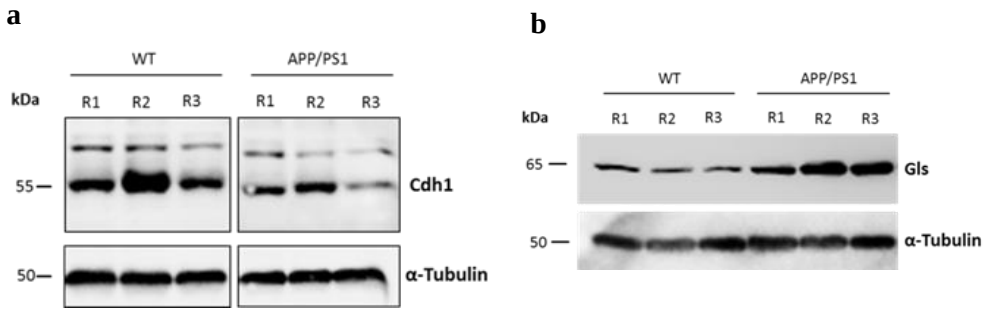

c

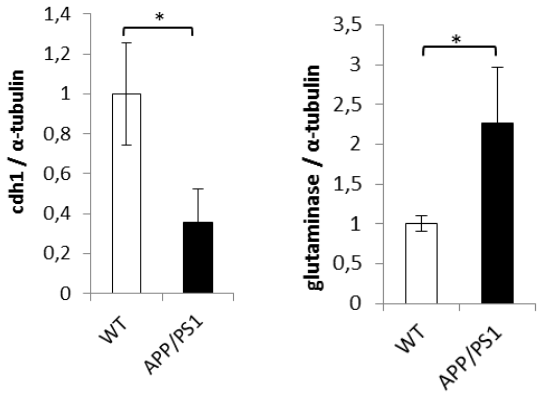

Figure 5.47 | **Cdh1 and glutaminase in APP/PS1 mice.** (a) Western blot analysis of cdh1 and glutaminase protein levels were measured in homogenates of mouse cerebral cortex of 3 wild type (WT) and 3 transgenic APP/PS1 mice. Cdh1 is decreased in APP/PS1 mice compared to WT [images of cdh1 bands are from the same western blot]. Glutaminase (gls) is increased in APP/PS1 mice compared to WT. (b) Cdh1 and gls western blot were quantified by densitometry and normalized with α-tubulin levels, mean ± SD of three independent samples are shown in the histogram.

5.8.3. mRNA levels of cdh1, APC/C2 and glutaminase in WT and APP/PS1 mice

In the previous experiments we have observed a difference in the protein levels of cdh1 and glutaminase in WT and APP/PS1 mice. Next, we tested whether there is there a difference in mRNA expression of cdh1, APC/C2 or glutaminase in WT and APP/PS1 cortex homogenates using qPCR. We observed no statistical significant difference in the expression of these genes. This result indicates that differences in cdh1 and glutaminase protein levels occur due to post-translational modifications (Figure 5.48).

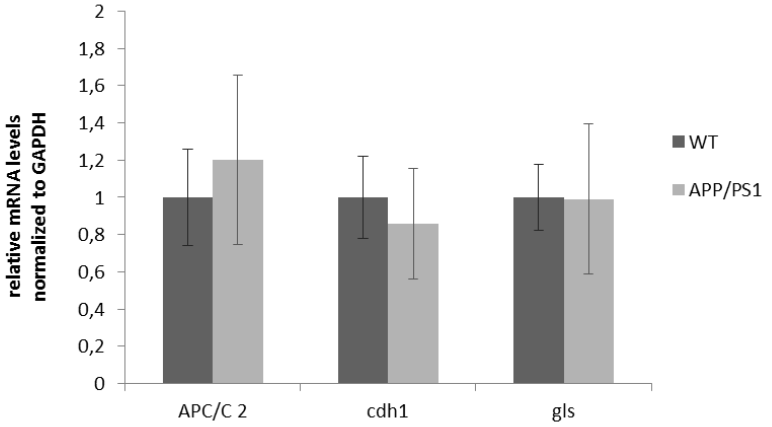

Figure 5.48 | **mRNA levels of APC/C2, cdh1 and glutaminase in mouse brain homogenates.** RNA was isolated from cortex samples using Trizol and was then retro-transcribed to cDNA. Specific primers were used to determine APC/C, cdh1, glutaminase and GAPDH levels by real time qPCR. Mean values ± SD of cdh1, APC/C2 and glutaminase normalized to GAPDH are shown in the histogram. There is no statistically significant difference (n=3).

5.8.4. Cdh1 and glutaminase in APP/PS1 mice by immunohistochemistry

For immunohistochemical analysis we isolated hippocampi of 6 animals (3 WT, 3 APP/PS1 mice). They were fixed in 4% PFA, embed in paraffin and 5 µm slices were prepared. The slices were mounted on chamber glass, incubated with cdh1 or glutaminase antibodies and stained using DAB-peroxidase. Nuclei were stained with hematoxylin. We observed less cdh1 in slices from APP/PS1 mice compared to slices prepared from WT (Figure 5.49 a-c). In slices of the same animals we observed more glutaminase staining (Figure 5.50 a-b).

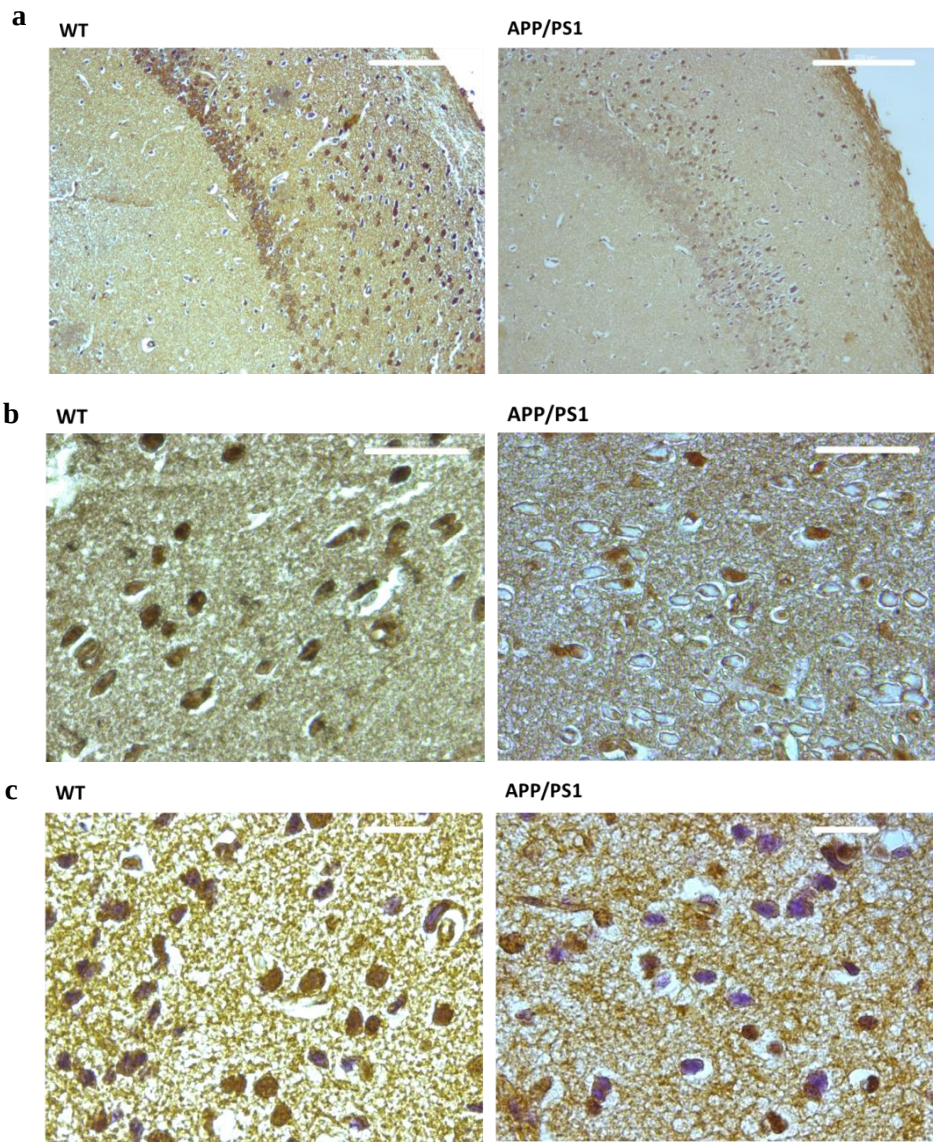

Figure 5.49 a-c | **Immunohistochemical staining of cdh1 in WT and APP/PS1 mice**. Paraffin embed hippocampus slices (5 µm) of wildtype (WT) and APP/PS1 mice were stained with cdh1 (1:100) (brown). Nuclei were stained with hematoxylin (blue). **(a)** Cdh1 and hematoxylin. Scale bar = 20 µm. **(b)** Cdh1 without hematoxylin staining. Scale bar = 50 µm. **(c)** Cdh1 and hematoxylin. Scale bar = 20 µm.

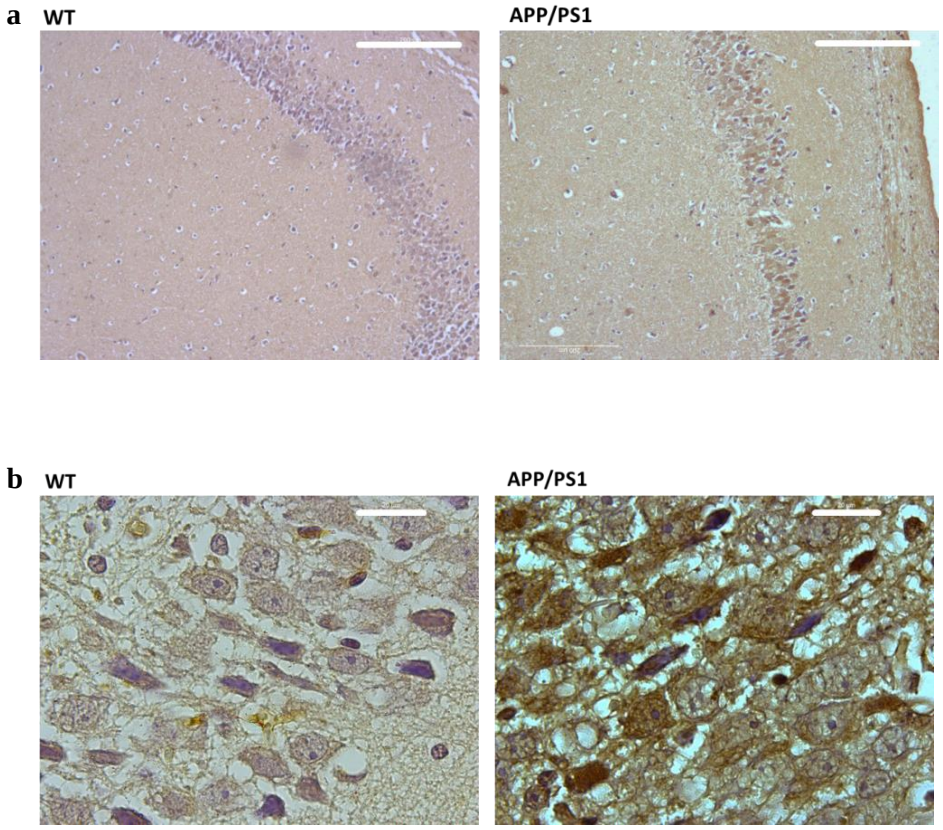

Figure 5.50 | **Immunohistochemical staining of glutaminase (gls) in WT and APP/PS1 mice**. Paraffin embed hippocampus slices (5 µm) of wildtype (WT) and APP/PS1 mice were stained with glutaminase (1:100) (brown). Nuclei were stained with hematoxylin (blue). **(a)** Scale bar = 200 µm. **(b)** Scale bar = 50 µm.

Once we had observed these differences in WT and APP/PS1 animals, we did additional analysis using fluorescent antibodies for cdh1 and glutaminase. Perfusion of six animals was carried out for immunohistochemical analysis. We observed a significantly lower cdh1 signal in the nucleus in transgenic animals compared to WT in the hippocampal CA1 region (Figure 5.51 a-b). Measurement

of glutaminase showed significantly increased levels in APP/PS1 compared to WT animals (Figure 5.52 a-b).

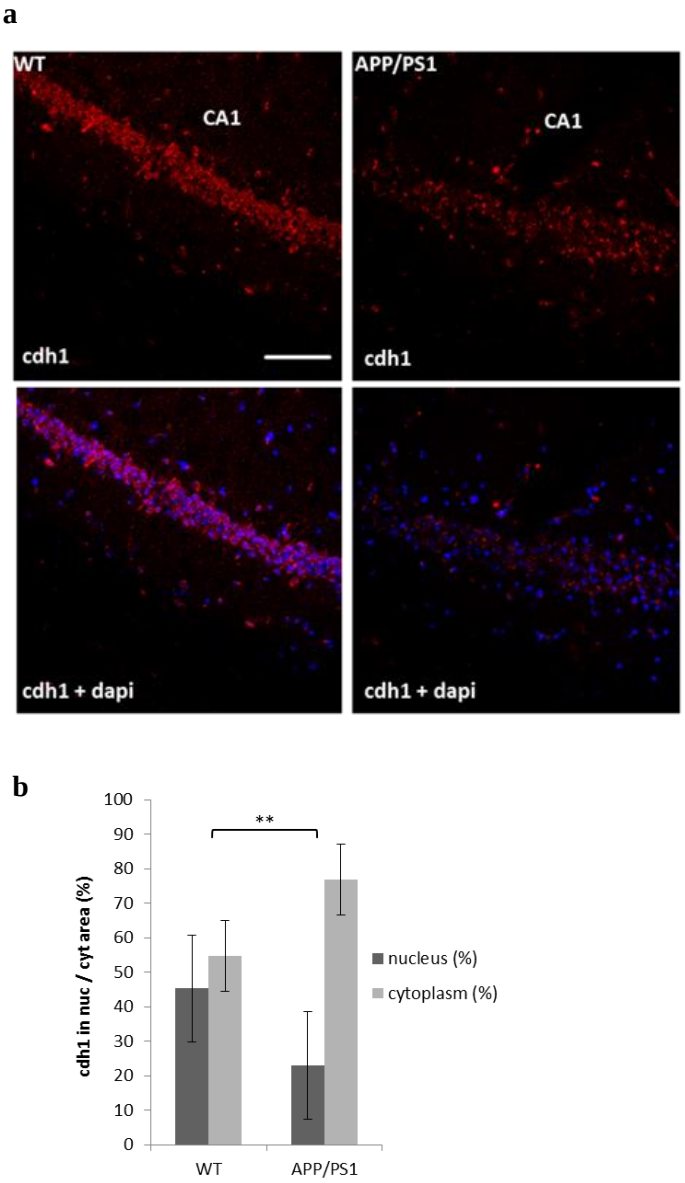

Figure 5.51 | **Immunohistochemical analysis of cdh1 in APP/PS1 mice. (a)** Representative images of cdh1 and nucleus (dapi) stained hippocampal slices of wild type (WT) and transgenic APP/PS1

mice. Results are show as mean ± SD of the percentage of nuclear and cytoplasmic cdh1 ($p_{[WT;\ TG]} < 0{,}01$). Scale bar = 75 µm.

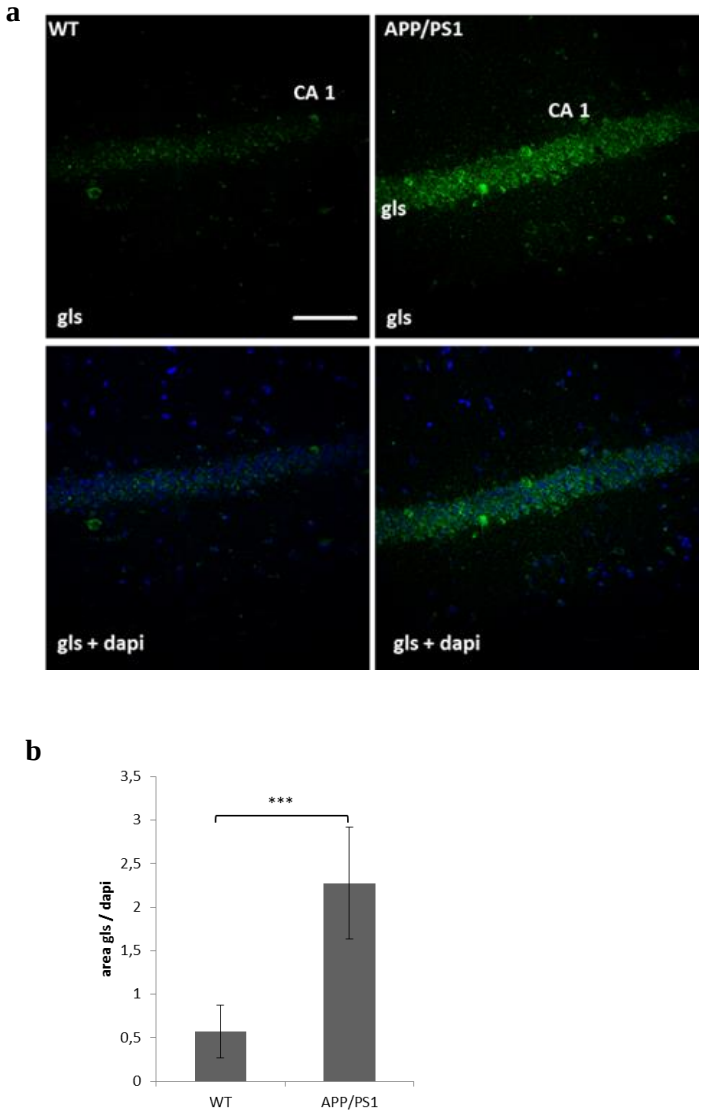

Figure 5.52 | **Immunohistochemical analysis of glutaminase in APP/PS1 mice.** Representative images of glutaminase (gls) and nucleus (dapi) stained hippocampal slices of WT and APP/PS1

animals. Results are show as mean ± SD of glutaminase area normalized to dapi ($p_{[WT;\ TG]} < 0.001$). Scale bar = 75 μm.

6. DISCUSSION

In this work we studied the role of APC/C-Cdh1 in AD. Previous studies have reported an increased abundance of APC/C substrates in AD brains, which suggests a dysregulation of the protein complex in the disorder. We report for the first time results that show a direct implication of APC/C-Cdh1 in the disease. We found that Aβ reduces the steady state levels and nuclear localization of the APC/C coactivator subunit cdh1 in primary cortical neurons *in vitro* and in the hippocampus *in vivo*. Reduced cdh1 levels lead to an accumulation of the enzyme glutaminase, an APC/C-Cdh1 substrate. This causes enhanced glutamate generation, an increase in intracellular calcium levels, and apoptosis in neurons in culture. Similar results were observed following the treatment of cells with the APC/C inhibitor proTAME.

A major conclusion of this study is that maintaining normal APC/C-Cdh1 activity may be a useful target in AD treatment.

6.1. Aβ alters Cdh1 in Neurons

While cdh1 levels oscillate during the cell cycle, in post-mitotic neurons cdh1 levels are maintained in a steady state.

It has been well documented that phosphorylation of cdh1 abolishes its ability to activate APC/C (Zachariae et al., 1998; Kotania et al., 1999). Cell cycle-related studies showed that cdh1 phosphorylation is controlled by cyclin dependent kinases and phosphatases (Jaspersen et al., 1999; Lukas et al., 1999). Phosphorylation of cdh1 promotes nuclear export (Jaquenoud et al., 2002) and it also inhibits its nuclear import (Zhou et al., 2003). Thus, phosphorylation of cdh1 has dual effects

on nuclear export and import, both of which lead to cytoplasmic retention of cdh1. It has been shown that phosphorylated cytoplasmic cdh1 is inactive, and it was suggested that nuclear decrease of cdh1 therefore contributes to the inactivation of APC/C (Jaquenoud et al., 2002). Furthermore, the SCF complex is involved in the degradation of phosphorylated cdh1 in the cytoplasm (Benmaamar and Pagano, 2005; Almeida, 2012), which may lead to decreased cdh1 levels after phosphorylation.

In our study we tested whether Aβ affects total cdh1 levels in neurons in culture and we also analyzed nuclear and cytoplasmic cdh1 levels. We observed a proteasome-dependent cdh1 decrease in total cell lysates in neurons in primary culture after Aβ treatment. Furthermore, cdh1 was completely abolished in the nucleus when treated with Aβ, which suggests that nuclear export of cdh1 occurred. Other studies reported that nuclear export of cdh1 occurs after cdh1 phosphorylation, which led us hypothesize that cdh1 might have been phosphorylated in neurons when treated with Aβ. We could not analyze phosphorylation of cdh1 directly, since there is no commercially available phospho-cdh1 antibody.

Analysis of cdh1 protein half-life with and without Aβ treatment showed that the protein half-life of cdh1 is shorter when treated with Aβ. This suggests that Aβ acts on cdh1 in a post-translational manner.

mRNA levels of cdh1 and APC/C2 did not change in response to Aβ treatment. We confirmed that mRNA expression is not affected by the treatment and concluded that the cdh1 decrease depends only on post-transcriptional modifications. Also the core subunit, APC/C2 with catalytic function, did not show a significant difference in expression, which allows us to conclude that the activity of APC/C is not affected by Aβ through downregulation of the expression this subunit.

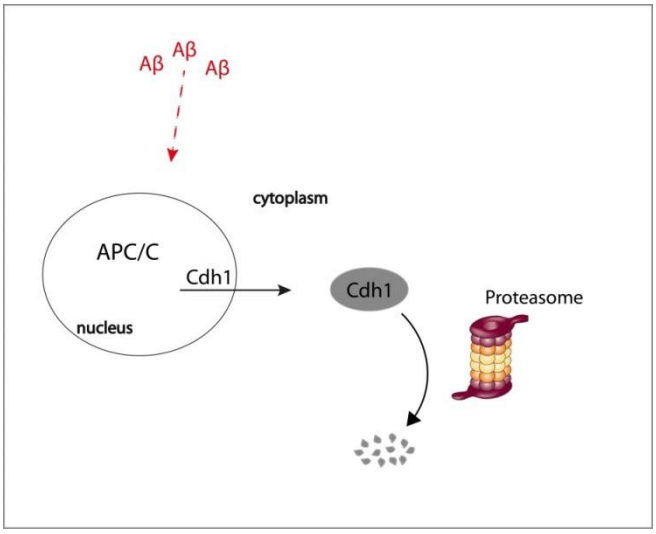

Figure 6.1 | **Schematic representation of the results and conclusions summarized in this section.** Aβ induces cdh1 nuclear export (effect direct or indirect, indicated by dashed line). Cdh1 is then degraded in the cytoplasm by the proteasome.

Maestre et al. (2008) showed that cyclin dependent kinase 5 (cdk5) phosphorylates cdh1 in excitotoxic conditions in neurons. Therefore we analyzed if cdk5 was involved in Aβ-mediated degradation of cdh1.

6.2. The Upstream Regulators of APC/C-Cdh1: Cdk5-p25 and PTEN

Cdk5 is a serine/threonine kinase which has an important role in postmitotic neurons. It is considered to be a non-traditional cdk, since it has no established role as a cell-cycle regulator protein. However, in neurons it was shown to be involved in cell cycle arrest (Zhang et al., 2008; Cicero and Herru, 2005).

Among the set of substrates of the kinase activity of cdk5 are cytoskeletal proteins and it was shown that cdk5 catalyses the phosphorylation of Tau proteins and

neurofilaments (Lew et al., 1995). Lee et al. found elevated cdk5 kinase activity in human AD brains compared to controls, thus it is an attractive target in AD research (Lee et al., 1999).

Cdk5 forms a complex with one of its regulatory activators p35 or p39, which activates the enzymatic function of cdk5. Neurotoxic insults, like ischemia or the presence of Aβ that induce Ca^{2+} dysregulation, lead to an over-activation of the calcium-dependent protease calpain which cleaves p35 into a 25 kDa fragment termed 'p25'. The shorter peptide p25 has a longer half-life than p35, because it cannot be properly degraded. Cdk5-p25 forms a stable complex leading to constitutive activation of the kinase. It has been shown that this leads to neurodegeneration (Patrick et al., 2000). Here we showed that Aβ treatment in neurons in culture causes an increase in cdk5-p25, and that inhibition of cdk5 partially rescued the Aβ-induced decrease of cdh1. Taking our results and the previous findings together, there is strong evidence for an Aβ-induced Ca^{2+} – cdk5-p25 – cdh1 signalling aberration in AD.

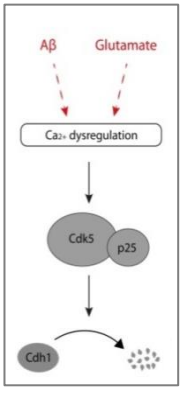

Figure 6.2 | **Schematic representation of results summarized from this section.** Aβ and glutamate treatments cause intraneuronal Ca^{2+} dysregulations. Cdk5-p25 increases and mediates cdh1 degradation.

Phosphatase and Tensin Homolog (PTEN) promotes APC/C-Cdh1 assembly in the nucleus, probably in a manner independent of its phosphatase activity (Song et al., 2011). Loss of PTEN negatively affects the activity of the E3 ligase APC/C-Cdh1, resulting in the stabilization of glutaminase and pfkfb3 in proliferating cells (Cordero-Espinoza et al, 2013; Garcia-Cao et al., 2012). PTEN is one of the most frequently mutated/deleted tumor suppressors in human cancers. Loss of PTEN in the cerebellum results in hyperphosphorylation of tau and in cdk5 activation (Kerr et al., 2006; Nayeem et al., 2007). We reported here that Aβ decreases PTEN levels. We suspect that cdh1 becomes phosphorylated by cdk5 and cannot re-assemble with APC/C properly due to low levels of PTEN, and this might be the reason why cdh1 remains in the cytoplasm, where it becomes degraded.

6.3. Accumulation of APC/C-Cdh1 Substrates in Neurons is Related to AD

Once we had observed the decrease of cdh1 in neurons after the treatment with Aβ, we analysed protein levels of substrates of APC/C-Cdh1 in these samples. We looked for APC/C substrates in the literature, which were expressed in neurons and that were known to be dysregulated in AD. Three proteins that met these characteristics were cyclin B1, pfkfb3 and glutaminase.

Elevated levels of cyclin B1 in neurons are involved in the re-entry into an ectopic cell cycle in neurons in AD (Vicent et al., 1997; Bonda et al., 2009). We have observed that direct APC/C inhibition or cdh1 downregulation by Aβ treatment, led to an accumulation of cyclin B1. Since this protein is a well-described target of APC/C in neurons, we used it as a “positive control” for testing APC/C degradation activity. Next, we tested pfkfb3, a protein that is targeted by APC/C in neurons to keep basal level of glycolysis low. The controlled degradation of pfkfb3 is responsible to keep up an antioxidant status in neurons. Therefore the accumulation of this enzyme can lead to oxidative stress and apoptosis in neurons (Herrero-

Mendez et al., 2009). However, in our experimental conditions we could not observe an increase in pfkfb3 upon treatment with Aβ after 20 h. It is possible that the basal expression level of pfkfb3 is too low to detect an accumulation of pfkfb3 within 20 h of treatment. Pfkfb3 might also be co-regulated by other mechanisms and its protein level might not only depend on the degradation of APC/C-Cdh1.

It has been reported that glutaminase is a target of APC/C-Cdh1in lymphocytes (Colombo et al., 2010). Glutaminase has important functions in neurons, as it a main source for the production of the neurotransmitter glutamate. When glutamine enters the mitochondria, glutaminase converts it to glutamate and ammonia. Alterations of glutaminase levels in AD were first reported in 1989 by Akiyama et al., who described a loss of glutaminase-positive neurons in late stages of AD. Furthermore, neurons immunoreactive to glutaminase and glutamate have been correlated with the formation of neurofibrillary tangles in AD (Kowall and Beal, 1991). Burbaeva et al. (2005) reported increased levels of glutaminase in the prefrontal cortex of AD patients.

First, we tested whether glutaminase is targeted for degradation by APC/C-Cdh1 in neurons, using siRNA to silence cdh1. We confirmed that it accumulated in neurons when cdh1 was depleted. Additionally, we inhibited the whole APC/C complex using the specific inhibitor proTAME, and observed that glutaminase accumulated upon that treatment. In the same line, we observed an accumulation of glutaminase in neurons when they were treated with Aβ. In the following parts of this project we analysed downstream effects of glutaminase accumulation in neurons.

6.4. Increased Glutamate Levels in AD

We showed that Aβ treatment induced an increase in glutamate levels in the extracellular medium of neurons and that this was mediated by accumulation of glutaminase. Direct inhibition of APC/C was also sufficient to increase the glutamate concentration to similar levels as those found after Aβ treatment. The glutamate increase after both treatments with Aβ or proTAME was reduced when glutaminase was inhibited. Furthermore, removal of glutamine from the culture medium completely abolished the Aβ- or proTAME-induced glutamate increase. Our findings are relevant in AD research, as they describe a novel signalling way to induce excitotoxitiy, an event that occurs in AD.

In the cerebrospinal fluid of AD patients, high levels of glutamate have been observed compared to healthy individuals of similar age (Pomara et al., 1992; Csernansky et al., 1996; Jiménez-Jiménez et al., 1998; Kaiser et al., 2010). Currently, glutamatergic systems are one of the main therapeutic targets in AD treatment (Zádori et al., 2014). Aβ synaptic toxicity can be partially ameliorated by the NMDAR antagonist memantine (Lipton, 2005; Tu et al., 2014). Studies related to AD, which focused on molecular mechanisms of excitotoxicity, reported that the glutamate increase was attributed to failure in the glutamate recycling system. Glutamate cannot be properly taken up by astrocytes because there is a decrease of the glutamate transporter GLT1 and thus the neurotransmitter remains in the synaptic cleft (Lauderback et al., 1999; Scimemi et al., 2013). We postulate here that excitotoxicity in AD does not only result from perturbations in the glutamate reuptake system, but also from aberrantly increased glutamate generation by glutaminase.

Interestingly, Maestre et al. (2008) reported that an excitotoxic glutamate stimulus causes APC/C-Cdh1 inactivation. In this work, we have confirmed the previous

finding that glutamate reduces cdh1 protein levels and have shown that this also leads to glutaminase accumulation.

It has been reported that an excitotoxic glutamate insult causes sustained NMDA receptor activation underlying a positive feedback loop (Norris et al., 2006; Rodriguez-Rodriguez et al., 2013). Our findings suggest that glutamate-induced glutaminase accumulation may contribute to a positive feedback loop of glutamate generation resulting in excitotoxicity, and thereby maintaining the down-regulation of APC/C activity. This would lead to the accumulation of APC/C-Cdh1 targets, of which some are related to neurodegenerative processes. An aberrant cyclin B1 increase in neurons causes an ectopic cell cycle re-entry and high levels of pfkfb3 induce oxidative stress (Maestre et al., 2008; Herrero-Mendez et al., 2009). Moreover, gene profiling has shown that excitotoxicity favors neuronal pathways that induce cell cycle re-activation and oxidative stress and that these events, together, accelerate neurodegeneration (Chen et al., 2013). We found that glutamate induced apoptosis can be ameliorated by glutaminase inhibition. We suggest these events, which all occur in AD, are linked through deficient APC/C activity.

6.5. Increased Ammonia Levels in AD

When glutamine enters the mitochondria, glutaminase converts it to glutamate and to ammonia. Excessive amounts of ammonia can have a neurotoxic effect by destroying the neuron's mitochondria, because it opens gates/pores in the mitochondrial membrane and creates reactive oxygen species (ROS) (Norenberg et al., 2004; Halim et al., 2014). Furthermore, ammonia is elevated in blood and in the CSF of AD patients (Fisman et al., 1985; Branconnier et al., 1986; Kaiser et al., 2010). Moderate chronic increase of ammonia concentration impairs NMDA receptor dependent long-term potentiation in the hippocampus and has therefore been related to neurological imbalance and memory impairment (Seiler, 2002).

We observed that inhibition of APC/C-Cdh1 increases ammonia in the extracellular medium of neurons. Since excess ammonia impairs glutamatergic synapses, and both glutamate and ammonia are overly produced in neurons in AD, these events together could seriously contribute to the pathogenesis of the disease.

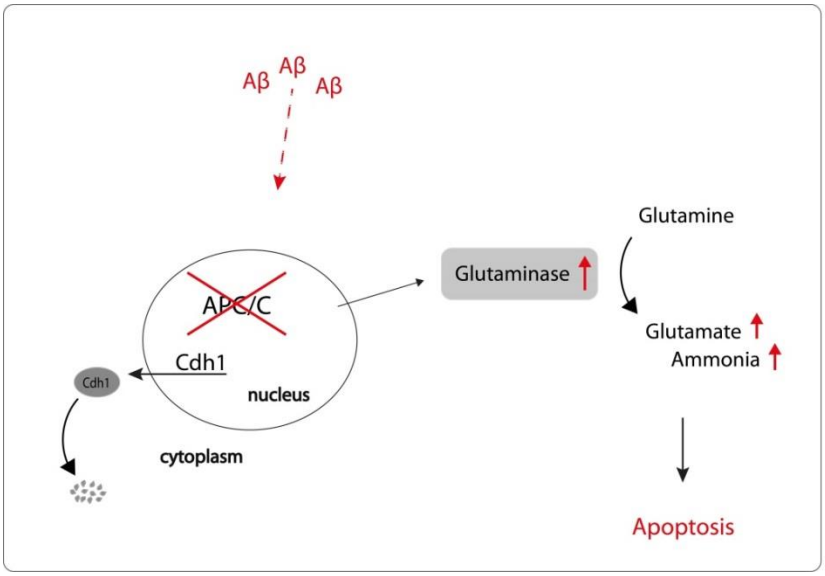

Figure 6.3 | **Schematic representation of the results and conclusions summarized in these sections.** Decreased APC/C activity (either by direct inhibition through proTAME or through cdh1 decrease by Aβ) leads to an accumulation of glutaminase. This leads to an increase of glutamate and ammonia in the extracellular medium of neurons causing apoptosis.

6.6. APC/C Inhibition and Ca^{2+} Dysregulation

Glutamate activates NMDA receptors, leading to a subsequent intracellular increase of Ca^{2+}. This is a central event for neuronal activity. However, increased glutamate levels lead to an overload of intracellular Ca^{2+} levels, which causes the main excitotoxic damage in neurons. Aβ causes a dysregulation in the Ca^{2+} homeostasis which leads to the stabilization of p25, the activator of cdk5 (La Ferla,

2002). Furthermore, Maestre et al. (2008) showed that cdk5-p25 phosphorylates cdh1 by over-activation of glutamate receptors through a Ca^{2+} mediated mechanism.

We observed that in neurons in culture in which glutamate was increased by Aβ or APC/C inhibition, also intracellular Ca^{2+} levels were higher compared to basal levels. Moreover, we found that Aβ- or proTAME treatment induced neuronal apoptosis, which was ameliorated by the inhibition of glutaminase. This indicates that increased glutaminase levels, and resultant glutamate levels, induced excitotoxicity after the treatments with Aβ or proTAME.

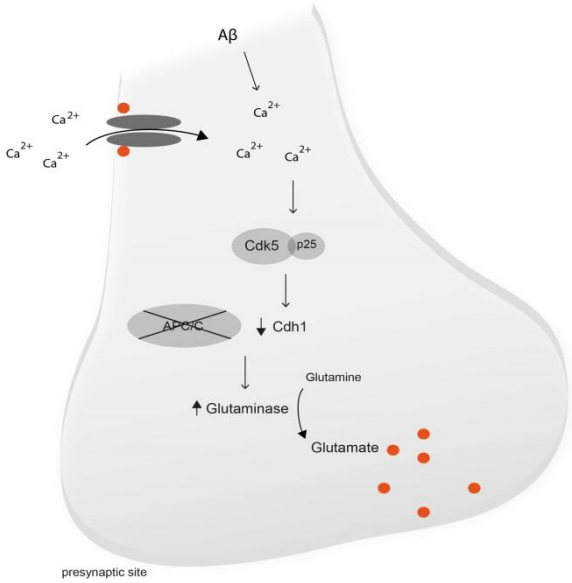

Figure 6.4 | **Schematic representation of results and conclusions of the signalling cascade described in this project.** Ca^{2+} dysregulation induced by Aβ or high glutamate levels, lead to a stabilization of cdk5-p25. This kinase phosphorylates cdh1 and inactivates the ubiquitin ligase. This leads to an accumulation of the APC/C-Cdh1 target, glutaminase, which leads to increased glutamate levels.

6.7. Aβ and Glutamate Reduce Cdh1 Levels *in vivo*

We then turned to *in vivo* studies using acute insults (injections). Microinjection of $A\beta_{1-42}$ oligomers in the CA1 field of the rat hippocampus caused nuclear export of cdh1 and increased glutaminase levels. It has been reported in a study using similar experimental setups, that intra-hippocampal microinjection of $A\beta_{1-42}$ oligomers impaired spatial working memory in rats (Pearson-Leary and Mc, 2012).

Similar to the effects of Aβ injection, a glutamate stimulus (by injection) caused nuclear export of cdh1 in the hippocampus, and also glutaminase was increased compared to controls. These findings might also be relevant for other neurodegenerative diseases, like ischemia. It has been reported that global ischemic injury induces downregulation of APC/C-Cdh1 in the CA1 field of the hippocampus in rat brain, and this was related to neuronal apoptosis (Zhang et al., 2011). Ischemic injury causes an increase in the extracellular glutamate concentration leading to over-stimulation of the NMDA receptors in extrasynaptic sites. Proteins involved in this excitotoxic cascade are, among others, PTEN, calpain, cdk5, p25. These events cause delayed and progressive neuronal damage and neuronal death (damage appears three days post-ictus and continues progressively for months) (Lai et al., 2014). Our observation of the effect of glutamate on cdh1 suggests that cdh1 down-regulation in ischemia observed by Zhang et al., might have been induced by glutamate excitotoxicity. Moreover, APC/C-Cdh1 down-regulation and subsequent glutaminase accumulation may contribute to the generation of excitotoxic environments in ischemia.

6.8. Cdh1 and Glutaminase in the Transgenic Mouse Model APP/PS1

We then analysed cdh1 protein levels in the APP/PS1 mouse model of AD, in which neurons are chronically exposed to Aβ. This is a widely used model for AD,

as the amyloid plaque-pathology occurs in a very similar manner as in the human AD pathology. This model was developed to alter both, the presenilins and the human APP. In the mouse model there is a strong positive correlation between Aβ accumulation and cognitive decline. However, APP/PS1 mutant mice do not have formation of neurofibrillary tangles, neuronal loss or larger ventricles, which are other major hallmarks of AD in humans. Since in our study we analysed in particular the effect of Aβ on APC/C-Cdh1, we believe this mouse model was suitable for our study.

We found lower levels of cdh1 (and predominantly less cdh1 in the nucleus) than in WT mice in the CA1 layer of the hippocampus. Glutaminase was increased in the same brain areas. Thus we confirmed our results in an *in vivo* model of AD.

6.9. Our Findings in a Systemic View for AD

Finally, our findings allow us to speculate about their possible involvement in the onset of the disease in a systemic view. In physiological conditions, glutaminase is present in high concentrations in hippocampus and the entorhinal cortex (Altschuler et al., 1985; Akiyama et al., 1989). Recently, the lateral entorhinal cortex has been identified as the primary area affected in preclinical phases of AD. This area projects to the CA1 region of the hippocampus in the lateral perforant pathway (LPP), which is the base of the declarative memory. The LPP is mostly composed of glutamatergic connections (Khan et al., 2014). The Aβ-induced glutamate toxicity could have deleterious effects specifically in these areas of the brain that are first affected in AD, because of the high basal glutaminase level. Therefore we postulate that excitotoxicity could be a crucial event in the onset of the disease and in memory impairment.

6.10. Outlook: APC/C-Cdh1 in AD research

Substantial evidence has been provided that APC/C-Cdh1 and the downstream target glutaminase could have a major role in the pathophysiology of AD. Further indications suggest that some targets of APC/C are involved in processes related to AD. Nevertheless, it would be crucial to determine if cdh1 dysregulation occurs in the human AD brain. Indeed, loss of glutaminase-positive neurons has been observed, which suggests impaired glutaminase regulation in the disorder. However, studies in human AD brains are difficult to perform, most of all when a dysregulation occurs at the onset of a disease.

We can, however, speculate about possible consequences of APC/C-Cdh1 downregulation in AD. The altered activity of the ubiquitin ligase would affect a whole set substrates and several independent processes would be impaired. Among these are cell cycle regulation and neurogenesis, oxidative regulation, LTP and glutamate metabolism. High levels of cyclin B1 have been related in ectopic cell cycle reentry, accumulation of pfkfb3 induces oxidative stress in neurons and increased glutaminase levels causes excitotoxicity (Fig. 6.5). However, several other (unidentified) targets of APC/C might be involved either directly or indirectly in the pathophysiology of AD. In various knock-out models of cdh1, impaired in LTP and LTD were observed. Therefore, it would be reasonable to think, that impaired LTP in AD occurs due to the dysregulation of APC/C-Cdh1. Further analysis of APC/C substrates or related proteins involved in LTP and LTD (EphA4, GluR, Liprin alapha, FRMP) could give more insights of protein dysregulation in the disorder.

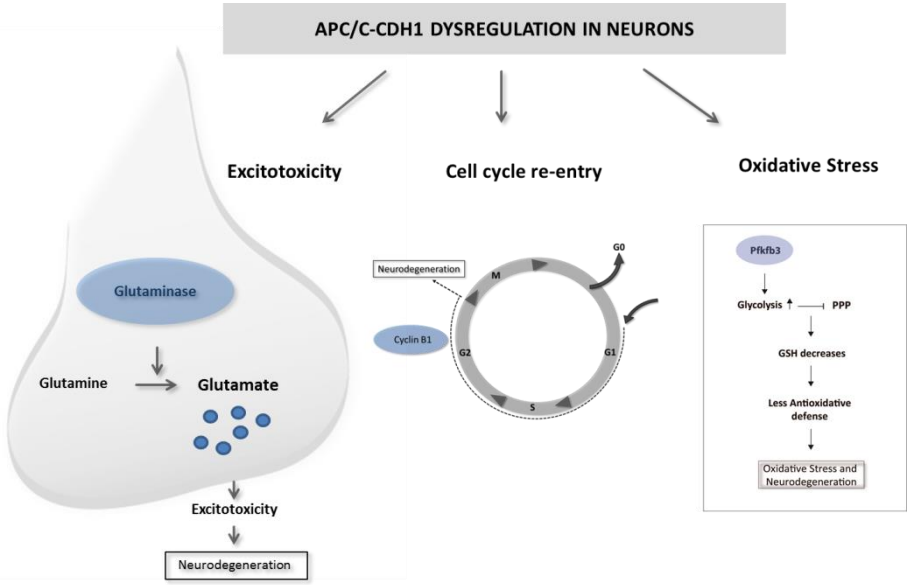

Figure 6.5 | **Schematic representation of impaired processes related to AD caused by APC/C-Cdh1 dysregulation.** The accumulation of glutaminase, cyclin B1 and pfkfb3 are involved in excitotoxicity, cell cycle re-entry and oxidative stress, respectively.

7. CONCLUSIONS

1. Aβ induces a decrease in total cdh1 and strongly reduces nuclear cdh1 levels. The degradation occurs in a proteasome-dependent manner, while mRNA levels of cdh1 are not affected by the treatment.

2. Cdk5-p25 meditates the decrease of cdh1 when treated with Aβ in neurons.

3. Cyclin B1 and glutaminase accumulate in neurons upon Aβ treatment in neurons.

4. When glutaminase is not properly degraded in neurons by APC/C-Cdh1, glutamate, ammonia and Ca^{2+} levels increase.

5. The dysregulation of APC/C-Cdh1 and glutaminase induces neurodegeneration.

6. Reduced nuclear and increased glutaminase cdh1 levels *in vivo* in APP/PS1 mice, and after microinjection of Aβ and glutamate in rat hippocampus.

8. APPENDIX: RESUMEN DE LA TESIS

La enfermedad de Alzheimer (EA) es la causa más común de demencia entre las personas de edad avanzada mayores de 65 años. Las estimaciones sugieren que en la actualidad hay aproximadamente 47,5 millones de personas en todo el mundo que sufren de demencia, de los cuales el 60-70% son casos de EA (Wolrd Health Organization, 2015). Es una enfermedad irreversible de naturaleza progresiva, que conduce a un deterioro de las funciones cognitivas más allá de lo que es normal en un proceso de envejecimiento saludable. Entre las funciones cognitivas afectadas se encuentran la memoria, las habilidades de pensamiento y la orientación.

La EA es una de las principales causas de discapacidad entre las personas mayores y tiene un gran impacto socio-económico. Actualmente no existe tratamiento para curar EA y es un campo muy activo en la investigación biomédica. Gran cantidad de nuevos tratamientos se están probando en diferentes etapas de la enfermedad para alterar su curso progresivo.

Las principales lesiones que se encuentran en los cerebros de los pacientes de EA son las placas seniles extraneuronales y los ovillos neurofibrilares (NFTs) intraneuronales. Las primeras están formadas fundamentalmente por depósitos de péptido beta-amiloide (Aβ), un péptido que puede tener 40 ó 42 aminoácidos y que tiende mucho a la agregación y precipitación. Los NFTS están constituidos principalmente por agregados de la proteína tau asociada a microtúbulos, en un estado de hiperfosforilación. Estas acumulaciones causan daño a las células y provocan la pérdida neuronal progresiva, difusa y masiva. Las zonas más afectadas son la corteza cerebral, hipocampo, amígdala, y sus cortezas asociadas. Además, diversas moléculas y vías de señalización se alteran en la EA, lo que podría contribuir sustancialmente a la aparición y / o el progreso de la enfermedad. En

este trabajo se analiza la implicación de una ubiquitina ligasa E3, la llamada anaphase promoting complex/cyclosome (APC/C) en la EA.

APC/C es un gran complejo de proteínas que forma un 'ring finger' ligasa de ubiquitina E3. Es considerada como uno de los principales reguladores del ciclo celular en células proliferantes. APC/C reconoce proteínas gracias a motivos de aminoácidos específicos, como secuencias KEN-BOX o D-BOX y las marca para su degradación. En la última década, se han descubierto importantes funciones neurobiológicas de APC/C, así como también de sus activadores Cdh1 y Cdc20. Se demostró que APC/C está implicada en el control de mantenimiento de la fase G0 neuronal, en el crecimiento axonal, que coordina la neurogénesis y también en el desarrollo sináptico. Hasta la fecha, 15 sustratos han sido identificados, todos ellos directamente involucrados en procesos ubicados en el sistema nervioso central. La acumulación de algunas de estas proteínas diana de APC/C se ha asociado con la neurodegeneración. Por ello, en este trabajo se ha probado la hipótesis de que APC/C o más bien la inactivación de APC/C, podría tener un papel fisiopatológico relevante en la EA.

Objetivos

En primer lugar, estábamos interesados en la evaluación de si el péptido Aβ afectaba a los niveles de la proteína Cdh1 y a la actividad de la ubiquitina ligasa *in vitro*. A continuación, quisimos determinar si estaba mediada por cdk5 y si otras quinasas o fosfatasas regulan el Cdh1 en las neuronas.

El segundo objetivo principal fue la descripción de la posibilidad de una regulación correspondiente de APC/C-Cdh1 sobre la glutaminasa en neuronas. La glutaminasa ha sido descrita anteriormente como un sustrato de la ubiquitina ligasa en los linfocitos. La regulación de la glutaminasa por APC/C podría ser de gran

importancia potencial, ya que esto sería vincular la actividad del APC/C con el metabolismo del glutamato en las neuronas. Las alteraciones en el metabolismo del glutamato y la excitotoxicidad juegan un papel importante en la EA. Y nosotros nos centramos en observar si la señalización de APC/C y sus sustratos deteriorada causaba neurodegeneración.

Esto se llevó a cabo mediante estudios *in vitro*, y también se probó en el modelo de ratón APP/PS1, que se utiliza ampliamente en la investigación de la EA.

Los objetivos concretos fueron:

1. Comprobar si el péptido Aβ en neuronas en cultivo cambia la expresión de cdh1 y/o en los niveles de proteina de cdh1.
2. Comprobar si el tratamiento con Aβ en neuronas afecta a la eficacia en la degradación de APC/C-Cdh1 y por tanto, produce la acumulación de sustratos de la ubiquitin ligasa.
3. Comprobar si la glutaminasa es regulada por APC/C-Cdh1 en neuronas y si fuera así, si esto lleva a la alteración en los niveles de glutamato y Ca^{2+}.
4. Determinar qué quinasas y fosfatasas regulan APC/C-Cdh1 en neuronas tratadas con Aβ.
5. Comrobar si la desregulación de APC/C-Cdh1 causa neurodegeneración.

Metodología

Cultivo celular, transfección y tratamientos

Se prepararon cultivos primarios de neuronas corticales de cerebro de feto de rata Wistar a los 14 días de gestación. Las cortezas se diseccionaron mecánicamente y se dispersaron en un medio de cultivo libre de suero y el tejido se filtró a través de una red de nylon (90 micras de poro). Las neuronas se sembraron en frascos de cultivo T25 cubiertos con poli-L-lisina (superficie de 25 cm^2), para los análisis de las muestras por Western blot, para las medidas de glutamato y para los análisis por citometría de flujo. Para microscopía de fluorescencia se sembraron neuronas en portaobjetos con cámaras de recubrimiento de vidrio, tratadas con poli-L-lisina (área superficial de 0,7 cm^2).

Las neuronas se cultivaron en ambos casos en medio DMEM suplementado con suero bovino fetal (10% v / v) y como antibióticos una mezcla de penicilina y de estreptomicina (1%). Se incubaron a 37°C en una atmósfera que contenía el 5% de CO_2. A las 72 h después de la siembra, se añadió citosina-arabinósido (10 mM) al medio de cultivo, y un día más tarde fue sustituido el medio por medio de cultivo fresco que contiene la mitad de la cantidad de citosina-arabinósido. Al día siguiente, se retiró el medio y se sustituyó por otro medio de cultivo estándar. Después de 6 días, se obtuvo un cultivo puro del 95% de neuronas, que se utilizó para los tratamientos.

El medio de cultivo fue sustituido por otro medio de cultivo fresco en el momento de los tratamientos, que se realizaron en las siguientes concentraciones: oligómeros Aβ (5 M), glutamato (500 mM) (G-1251, Sigma, St. Louis, EE.UU.), proTAME (12 M) (I-440, BostonBiochem, Cambridge, MA, EE.UU.), compuesto 968 (100 M) (352010, Calbiochem, Nottingham, Reino Unido), roscovitina (15 M) (R 7772, Sigma, Missouri, ESTADOS UNIDOS), cicloheximida (3,5 M) (Sigma C7698,

Missouri, EE.UU.), MG132 (10 M) (M7449, Sigma, Missouri, EE.UU.). Los tiempos de incubación se indican en las leyendas de las figuras.

Para los experimentos de silenciamiento de Cdh1 utilizamos Accell SmartPool Fzr1 siRNA (E-100432-00-0050, Dharmacon), y Accell 'non-target' siRNA (D-001910-01-20, Dharmacon): 1 M siRNA por ml de medio de cultivo con suero reducido a 1% durante 96 h. Entonces se recogieron las células y se utilizaron para el tratamiento.

Animales transgénicos

Se utilizaron en este estudio ratones APPswe, PSEN1dE9-85Dbo / J dobles transgénicos y ratones de tipo salvaje de la misma colonia (de nueve meses de edad). Los ratones se mantuvieron en un ciclo de luz-oscuridad de 12:12 h a 23 ± 1°C y 60% de humedad relativa, y se les proporcionó una dieta estándar Chow (PANLAB SL) y agua *ad libitum*.

Infusión Intrahipocampal

Un grupo de nueve ratas Wistar (hembras) fueron tratadas con nitrato de atropina de metilo (0,4 mg/kg, i.p.), anestesiadas con una mezcla de ketamina (60 mg/kg i.p.) (Imalgen, 0,05 g/ml; Rhône Mérieux, Lyon, Francia) y xilazina (10 mg/kg i.p.) (Xilagesic, 20 mg/ml; Lab.Calier, Barcelona, España). Los animales se colocaron en un aparato estereotáxico Kopf (Kopf Instruments, Tujunga, EE.UU.). Con el fin de minimizar el sufrimiento de los animales, fue inyectada lidocaína subcutánea en el área de la cirugía. En el cuero cabelludo se realiza una incisión y se retrae, y la posición del cabezal se ajustó a colocar bregma y lambda en el mismo plano horizontal. A continuación fueron realizadas perforaciones de trépano pequeñas (1 mm de diámetro) en el cráneo de forma unilateral.

Las infusiones en el hipocampo se hicieron usando un sistema de cánula de acero inoxidable (Plastics One, Roanoke, VA) que consiste en un tubo exterior de guía (calibre 24) y un tubo de infusión interior (31 gauge). Las cánulas se colocaron estereotáxicamente 4,36 mm posterior al bregma, 1,4 mm lateral desde la línea media sagital, y se implantaron 3,4 mm por debajo de la superficie exterior del cráneo en la región del hipocampo CA1 del lado izquierdo, de acuerdo con el atlas de Paxinos y Watson 1998. La cánula de infusión se conectó a una microjeringa 10 µl (Hamilton) mediante un tubo de polietileno.Un volumen total de 10 µl de soluciones de infusión (glutamato 1 mM en 1 x PBS; 5 µM Aβ disueltos en DMSO al 0,5% en 1x PBS) se inyectaron en el hipocampo a 0,5 µl/min controlada por una bomba de infusión. Las ratas control recibieron solución de vehículo (PBS) al mismo volumen y la misma velocidad.

Preparación y fijación del tejido

Después de 48 h de tratamiento, los animales se anestesiaron con una dosis letal de pentobarbital de sodio (100 mg/kg 20%) (Dolethal Vetoquinol Madrid, España) y se perfundió de modo trans-cardíaco con solución salina heparinizada (0,1%, pH 7), seguido de paraformaldehído (4%) en tampón de fosfato (PBS) (0,1 M, pH 7,4). Los cerebros se post-fijaron durante 24 h en paraformaldehído (4%) en PBS a 4°C y se mantuvieron durante 2 días en sacarosa (30%) a 4°C para crioprotección. Se obtuvieron secciones coronales de 40 micras por microtomía por congelación (Leica) y se almacenaron en tampón de fosfato (0,1 M, pH 7,4) a 4°C.

Análisis de las muestras

Para el análisis de las muestras obtenidas se utilizaron los siguientes métodos: marcaje por inmunohistoquímica, marcaje por inmunocitoquímica, adquisición de imágenes por microscopía confocal, Western Blot, medición de glutamato basado en un ensayo enzimático, medición de amoníaco en base a un ensayo enzimático, citometría de flujo para el análisis de la apoptosis y la determinación de la expresión de mRNA por rtPCR cuantitativa (para más detalles véase la sección Métodos).

Número de muestras y análisis estadístico

Los resultados se expresan como valores medios de los datos de al menos tres experimentos independientes; las barras de error representan la desviación estándar. En general, los experimentos se realizaron como duplicados, en cada experimento independiente. Sólo cuando el número de la muestra fue alta (en experimentos en que se mide tras un tratamiento a distintos tiempo), no se llevaron a cabo repeticiones, sin embargo en este caso, las muestras se analizaron por duplicado por Western Blot. Todas las reacciones de PCR se llevaron a cabo por triplicado. Para el análisis inmunohistoquímico, las secciones de cada cerebro se recogieron en series de tres a cinco muestras independientes. De estos, al menos dos series se analizaron por animal (por duplicado).

Para el cálculo de la vida media de la proteína se supuso que la degradación de proteínas sigue una cinética de descomposición de primer orden. Inicialmente se hizo una transformación logarítmica de los datos de la medida de la intensidad de proteína. A continuación, se determinó la velocidad de disminución constante k, obteniéndose un coeficiente de determinación (R-cuadrado). Por otra parte, se estimó el error estándar de la pendiente. Para evaluar las diferencias de

significación se utilizó una prueba z. Se sabe que, bajo hipótesis de normalidad de los errores de ajuste, la diferencia entre las estimaciones de pendiente dividido por la raíz cuadrada media de su error estándar sigue una distribución normal estándar. Por último, a partir de la constante de velocidad de desintegración, se calculó la vida media ($T(1/2) = \ln(2) / k$).

Para otros análisis estadísticos, se utilizó la prueba t-test de una cola o el análisis del Mann-Whitney U-test. Los p-valores se clasificaron en las unidades de significación que se establecieron de la siguiente manera: $p > 0,05$, no significativo (NS), $p < 0,05$ significativo (*), $p < 0,01$ muy significativo (**), $p < 0,001$ altamente significativa (***).

Conclusiones y Discusión

Aβ disminuye los niveles de cdh1

Mientras los niveles de Cdh1 oscilan durante el ciclo celular, en las neuronas post-mitóticas los niveles Cdh1 se mantienen en un estado estacionario. Se ha documentado que la fosforilación de Cdh1 suprime su capacidad de activar APC/C (Zachariae et al, 1998;. Kotania et al., 1999). Estudios relacionados con el ciclo celular mostraron que la fosforilación de Cdh1 es controlado por quinasas y fosfatasas dependientes de ciclina (Jaspersen et al., 1999; Lukas et al., 1999). La fosforilación de Cdh1 promueve la exportación nuclear (Jaquenoud et al., 2002) y también inhibe su importación nuclear (Zhou et al., 2003). Por lo tanto, la fosforilación de Cdh1 tiene efectos duales de exportación nuclear y de importación, los cuales conducen a la retención citoplásmica de Cdh1. Se ha demostrado que Cdh1 citoplásmica fosforilada está inactiva, y se sugirió que la disminución nuclear de Cdh1, por tanto, contribuye a la inactivación de APC/C (Jaquenoud et al., 2002). Además, se sabe que el complejo SCF está implicado en la degradación de Cdh1 fosforilada en el citoplasma (Benmaamar y Pagano, 2005; Almeida, 2012), lo que puede conducir a la disminución de los niveles de Cdh1 después de la fosforilación.

En nuestro estudio hemos probado si Aβ afecta a los niveles de Cdh1 tanto totales en las neuronas en cultivo y como los niveles de Cdh1 nucleares y citoplasmáticos. Se ha observado una disminución de Cdh1 en lisados de células totales en las neuronas en cultivo primario después del tratamiento con Aß. Además, los niveles de Cdh1 fue completamente disminuidos en el núcleo después del tratamiento con Aß, lo que sugiere que Cdh1 se ha translocado del núcleo al citosol. Así mismo, hemos comprobado que la degradación de Cdh1 era dependiente del proteasoma. Otros estudios han demonstrado que la exportación nuclear de Cdh1 se produce después de la fosforilación Cdh1, lo que nos ha llevado a la hipótesis de que Cdh1 podría haber sido fosforilada en las neuronas cuando son tratados con Aβ. No

pudimos analizar la fosforilación de Cdh1 directamente, ya que no hay anticuerpo fosfo-Cdh1 disponible comercialmente. Por ello, analizamos los niveles de una posible quinasa como es Cdk5. Maestre et al. (2008) demostraron que la quinasa dependiente de ciclina 5 (cdk5) fosforila Cdh1 en condiciones de excitotoxicidad en neuronas. Por lo tanto, analizamos si cdk5 estuvo implicado en la degradación de cdh1 tras el tratamiento con Aß.

Análisis de niveles de proteina total de Cdh1, la vida media con y sin tratamiento de Aß mostró que la semivida de la proteína de Cdh1 es más corta cuando se trata con Aß. Esto sugiere que Aß actúa sobre Cdh1 de una manera posterior a la transcripcion (de mRNA). Los niveles de mRNA de Cdh1 y APC/C2 no cambiaron en respuesta al tratamiento Aß. Se confirmó que la expresión de mRNA no se ve afectada por el tratamiento y concluimos que la disminución de Cdh1 sólo depende de modificaciones post-transcripcionales. También una de las subunidades principales, APC/C2 con la función catalítica, no mostró una diferencia significativa en la expresión, lo que nos permite concluir que la actividad de APC/C no se ve afectada por Aß a través de la regulación de la expresión de esta subunidad.

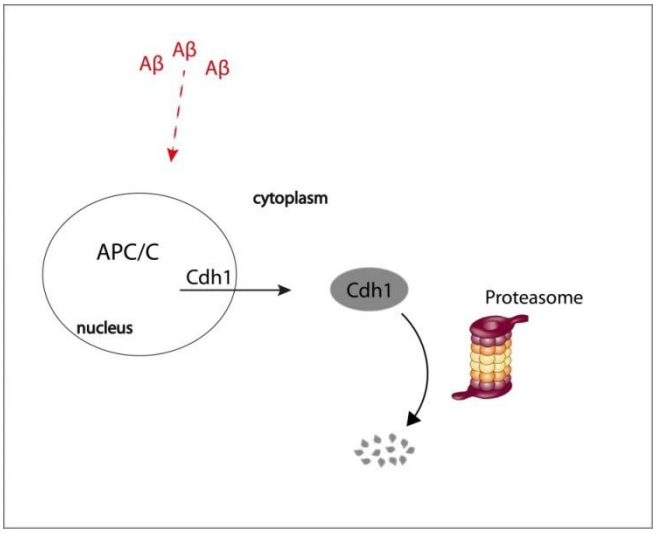

Figura 1 | Representación esquemática de los resultados y conclusiones que se resumen en esta sección. Aß induce la exportación nuclear de Cdh1 (efecto directo o indirecto, indicado por la línea discontinua). Cdh1 es luego degradado en el citoplasma por el proteasoma.

Los reguladores de APC/C-Cdh1: Cdk5-p25 y PTEN

Cdk5 es una serina/treonina quinasa que tiene un papel importante en neuronas postmitóticas. Se considera que es una cdk no tradicional, ya que no tiene funciones como regulador de proteínas del ciclo celular. Sin embargo, en neuronas se demostró que esta involucrada en la detención del ciclo celular (Zhang et al., 2008; Cicerón y Herru, 2005). Entre los sustratos de la actividad quinasa de cdk5 encontramos proteínas del citoesqueleto y concretamente, se ha demostrado que cdk5 cataliza la fosforilación de proteínas y neurofilamentos de tau (Lew et al., 1995). Lee et al. demostraron que hay una actividad de cdk5 elevada en cerebros humanos de pacientes de EA en comparación con los controles, por lo que es un objetivo atractivo en la investigación de esta enfermedad (Lee et al., 1999).

Cdk5 forma un complejo con uno de sus reguladores p35 o p39, que activan la función enzimática de la misma. Agresiones neurotóxicas, como la isquemia o la presencia de Aβ que inducen una desregulación de Ca^{2+}, conducen a una activación de la proteasa calpaína, que es dependiente de calcio y que escinde p35 en un fragmento 25 kDa denominado 'p25 '. El péptido p25 tiene una vida media más larga que p35, ya que no puede ser degradado correctamente. Cdk5-p25 forman un complejo estable que conduce a la activación constitutiva de la quinasa. Se ha demostrado que esto esta involucrado en a la neurodegeneración (Patrick et al., 2000). En la presente tesis demostramos que el tratamiento con Aβ en neuronas en cultivo, provoca un aumento de cdk5-p25, y que la inhibición de cdk5 rescata parcialmente la disminución de cdh1 inducida por Aβ. Analizando los resultados

anteriormente descritos, podemos concluir que existe una fuerte evidencia de que Aβ induzca una alteración en la señalización de Ca^{2+} - cdk5-p25 - cdh1 en la EA.

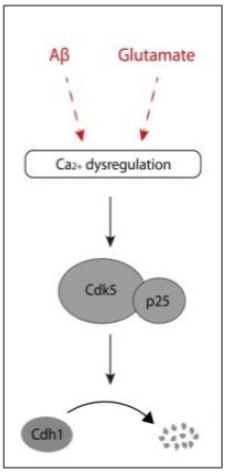

Figura 2 | Representación esquemática de los resultados que se resumen en esta sección. Tratamientos de Aβ y glutamato provocan una desregulación intraneuronal de Ca^{2+}. Cdk5-p25 causa la degradación de cdh1.

La acumulación de sustratos de APC/C-Cdh1en las neuronas se relaciona con EA

Una vez demostrada la disminución de cdh1 en las neuronas después del tratamiento con Aβ, se analizaron los niveles de proteína de otros sustratos de APC/C-Cdh1 en las mismas muestras. Buscamos sustratos de APC/C en la literatura, que se expresaran en neuronas y que se sabe que estuvieran alterados en la EA. Tres proteínas que cumplían estas características fueron: ciclina B1, pfkfb3 y glutaminasa.

Los niveles elevados de ciclina B1 en las neuronas están involucrados en la re-entrada en un ciclo celular ectópico en las neuronas en la EA (Vicent et al., 1997; Bonda et al., 2009). Hemos observado que tanto la inhibición de APC/C directa,

como la disminuición de cdh1 por tratamiento con Aβ, condujeron a una acumulación de la ciclina B1. Dado que esta proteína es un sustrato bien descrito de APC/C en las neuronas, lo usamos como un "control positivo" para la actividad de la degradación de APC/C. A continuación, medimos pfkfb3, una proteína que está controlada por la actividad de APC/C en neuronas con el fin de mantener un nivel basal bajo en la glucolisis. La degradación controlada de pfkfb3 es responsable también de mantener un nivel estable de antioxidantes en las neuronas. Por lo tanto, la acumulación de esta enzima puede conducir a estrés oxidativo y a apoptosis en neuronas (Herrero-Méndez et al., 2009). Sin embargo, en nuestras condiciones experimentales, no se observó un aumento en pfkfb3 tras el tratamiento con Aβ después de 20h. Es posible que el nivel de expresión basal de pfkfb3 sea demasiado baja para detectar una acumulación de pfkfb3 dentro de las 20h de duración del tratamiento. Pfkfb3 podría también ser co-regulado por otros mecanismos y su nivel de proteínas no sólo depender de la degradación de APC/C-Cdh1.

Por otro lado, se ha demostrado que la glutaminasa es un sustrato de APC/C-Cdh1 en linfocitos (Colombo et al., 2010). La glutaminasa tiene funciones importantes en las neuronas, ya que es una fuente principal para la producción del neurotransmisor glutamato. Cuando la glutamina entra en la mitocondria, la glutaminasa cataliza la reacción que lo convierte en glutamato y amoníaco. Las alteraciones de los niveles de glutaminasa en la EA se vieron por primera vez en 1989 por Akiyama et al., los cuales describen una pérdida de neuronas 'glutaminasa-positivas', en las últimas etapas de la EA. Además, las neuronas inmunorreactivas a la glutaminasa y glutamato se han correlacionado con la formación de ovillos neurofibrilares en EA (Kowall y Beal, 1991). Burbaeva et al. (2005) reportaron mayores niveles de glutaminasa en la corteza prefrontal de pacientes con EA.

En primer lugar, hemos probado si la glutaminasa está destinada a la degradación por APC/C-Cdh1 en las neuronas, utilizando siRNA para silenciar cdh1. Se

confirmó que se acumulaba en las neuronas cuando cdh1 esta disminuido. Adicionalmente, se inhibió todo el complejo APC/C utilizando el proTAME como inhibidor específico, y observamos que la glutaminasa se acumulaba tras el tratamiento. En la misma línea, se observó una acumulación de glutaminasa en las neuronas cuando se trataban con péptido Aβ. En los siguientes apartados de este proyecto se analizaron los efectos de la acumulación de glutaminasa en las neuronas.

El aumento de los niveles de glutamato en la EA

Hemos demostrado que el tratamiento con péptido Aβ induce un aumento en los niveles de glutamato en el medio extracelular de las neuronas y que esto es mediado por la acumulación de glutaminasa. La inhibición directa de APC/C también era suficiente para aumentar la concentración de glutamato a niveles similares a los de después del tratamiento con Aβ. El aumento de glutamato, después de ambos tratamientos bien con Aβ o proTAME, se reducía al inhibir la glutaminasa. Además, la eliminación de la glutamina del medio de cultivo revertió completamente el aumento de glutamato inducido por Aβ o proTAME. Nuestros resultados son relevantes en la investigación de EA, ya que describen una forma novedosa de señalización para inducir la excitotoxicidad, un evento que se produce en la EA.

En el líquido cefalorraquídeo de pacientes con EA, se han observado altos niveles de glutamato en comparación con individuos sanos de edad similar (Pomara et al., 1992; Csernansky et al., 1996; Jiménez-Jiménez et al., 1998;. Kaiser et al., 2010). Actualmente, los sistemas glutamatérgicos son una de las principales dianas terapéuticas en el tratamiento de EA (Zádori et al., 2014). El fármaco es la memantina, un antagonista del receptor de NMDA, que se ha demostrado mejora parcialmente la toxicidad sináptica causada por Aβ (Lipton, 2005; Tu et al., 2014). Estudios relacionados con la EA, que se centraron en los mecanismos moleculares

de la excitotoxicidad, informaron de que el aumento de glutamato se debía a un fallo en el sistema de reciclaje de mismo. El glutamato no puede ser internalizado adecuadamente por los astrocitos al haber una disminución de su transportador GLT1, y por lo tanto el neurotransmisor aumenta su concentración en la hendidura sináptica (Lauderback et al, 1999. Scimemi et al, 2013). Postulamos aquí que la excitotoxicidad en la EA no sólo resulta de perturbaciones en el sistema de la recaptación de glutamato, sino también por aumento de la generación de glutamato por la glutaminasa.

Curiosamente, Maestre et al. (2008) demostraron que un estímulo de excitotoxicidad causado por el glutamato inactiva APC/C-Cdh1. En nuestro trabajo, hemos confirmado estos resultados, ya que hemos visto que el glutamato reduce los niveles de la proteína cdh1 y hemos demostrado que esto también conduce a la acumulación de glutaminasa.

Se ha demostrado que una agresión excitotóxica con glutamato causa la activación constante del receptor de NMDA y ello lleva a un bucle de retroalimentación positivo (Norris et al, 2006; Rodríguez-Rodriguez et al, 2013).

Nuestros resultados sugieren que la acumulación de glutaminasa inducida por el glutamato podría contribuir a este bucle de retroalimentación positivo en la generación de glutamato, que resultaría en excitotoxicidad, y eso mantendría la actividad de APC/C baja. Además, esto llevaría a la acumulación de sustratos de APC/C-Cdh1, de las cuales algunos estarían relacionados con procesos neurodegenerativos. Un aumento de la ciclina B1 por ejemplo, provoca la reentrada en el ciclo celular en las neuronas, dando lugar a un ciclo celular ectópico y altos niveles de pfkfb3 inducen estrés oxidativo (Maestre et al, 2008;. Herrero-Méndez et al., 2009). Por otra parte, perfiles de expresión génica han indicado que la excitotoxicidad favorece vías neuronales que inducen la re-activación del ciclo celular y estrés oxidativo y que estos eventos juntos aceleran la neurodegeneración

(Chen et al., 2013). Nosotros hemos encontrado que la apoptosis inducida por glutamato se puede mejorar inhibiendo la glutaminasa. Sugerimos que estos eventos en conjunto tienen lugar en el proceso fisiopatológico asociado a la EA y que todos están vinculados a través de una actividad deficiente de APC/C.

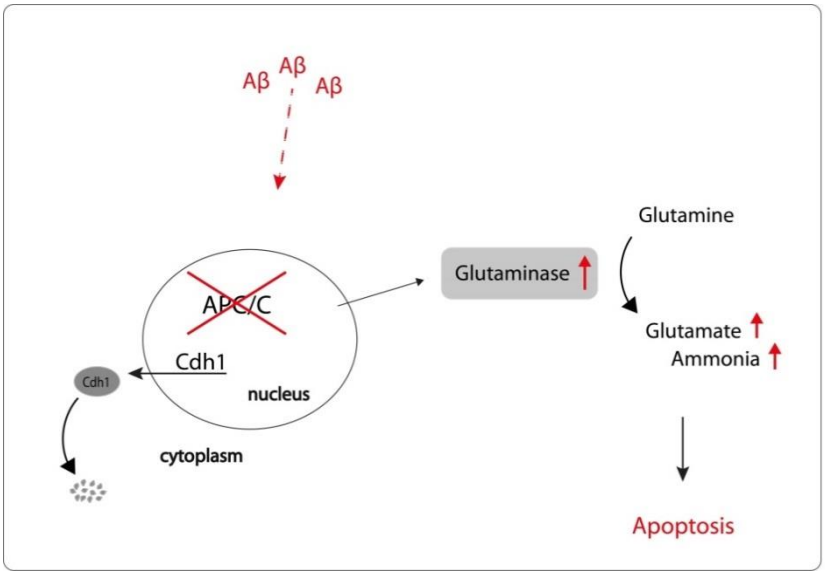

Figura 3 | Representación esquemática de los resultados y conclusiones que se resumen en estas secciones. Disminución de la actividad APC/C (ya sea mediante la inhibición directa a través de proTAME o mediante por la disminución de cdh1 por Aβ) conduce a una acumulación de la glutaminasa. Esto conduce a un aumento del glutamato y amoníaco en el medio extracelular de las neuronas lo cual causa apoptosis.

La inhibición de APC/C y la desregulación de Ca^{2+}

El glutamato activa receptores de NMDA, lo que lleva a un aumento del Ca^{2+} intracelular. Este es un evento central para la actividad neuronal. Sin embargo, el aumento alterado de los niveles de glutamato conducen a una sobrecarga en los niveles de Ca^{2+} intracelular, que causa un daño de excitotoxicidad en las neuronas.

Sabemos que el péptido Aβ causa una desregulación en la homeostasis de Ca^{2+} que conduce a la estabilización de p25, el activador de cdk5 (La Ferla, 2002). Además, Maestre et al. (2008) demostraron que cdk5-p25 fosforila a cdh1 acompañado de un exceso de activación de los receptores de glutamato, a través de un mecanismo mediado por Ca^{2+}.

Hemos observado que en las neuronas en cultivo en el que el glutamato se incrementó tras un tratamiento con Aβ o inhibición de APC/C (con proTAME), los niveles intracelulares de Ca^{2+} fueron incrementados también en comparación con los niveles basales. Por otra parte, se encontró que el tratamiento con Aβ o proTAME indujo apoptosis neuronal, que mejoraba si inhibíamos la glutaminasa. Esto indica que el aumento de los niveles de glutaminasa, y los niveles de glutamato después de los tratamientos con Aβ o proTAME inducen excitotoxicidad.

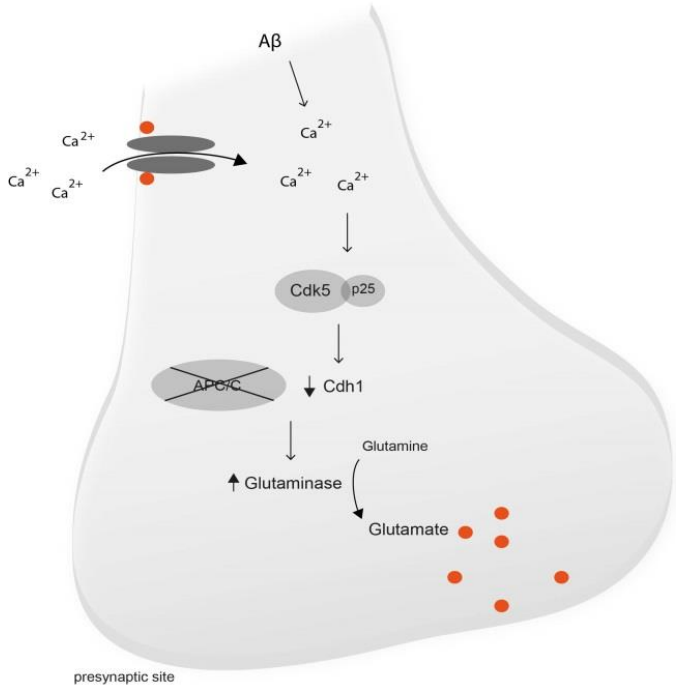

Figura 4 | Representación esquemática de los resultados y conclusiones de la cascada de señalización que se describe en este proyecto. Una desregulación de Ca^{2+} inducida por Aβ o por niveles elevados de glutamato, conducen a una estabilización de cdk5-p25. Esta quinasa fosforila cdh1 e inactiva a la ubiquitina ligasa. Esto conduce a una acumulación del sustrato de APC/C-Cdh1, la glutaminasa, lo que conduce a un aumento de los niveles de glutamato.

Aβ y glutamato reducen los niveles de Cdh1 *in vivo*

A continuación, quisimos comprobar nuestros resultados en un modelo *in vivo.* Para ello, utilizamos lesiones agudas por medio de microinyecciones intracerebrales. La infusión de oligómeros $A\beta_{1-42}$ en el área CA1 del hipocampo de la rata causó exportación nuclear de cdh1 y un aumento de los niveles de glutaminasa. Se ha demostrado en un estudio previo en el que se utilizaron condiciones experimentales similares, que la microinyección de oligómeros de $A\beta_{1-42}$ dentro de hipocampo provocaba un deterioro de la memoria de trabajo espacial en ratas (Pearson-Leary y Mc, 2012).

De forma similar a los efectos de la inyección de Aβ, la infusión de glutamato monosódico causó la exportación nuclear de cdh1 en el hipocampo. Además, ambos tratamientos aumentaron los niveles de glutaminasa en comparación con los controles microinyectados con vehículo. Estos resultados también podrían ser relevantes para otras enfermedades neurodegenerativas, como la isquemia. Se ha demostrado que una lesión isquémica global induce la disminución de APC/C-Cdh1 en la región CA1 hipocampal en el cerebro de rata, y esto además, estaba relacionado con la apoptosis neuronal (Zhang et al., 2011). La lesión isquémica provoca un aumento en la concentración de glutamato extracelular que conduce a la sobre-estimulación de los receptores de NMDA extrasinápticos. Las proteínas

implicadas en esta cascada de excitotoxicidad son entre otras PTEN, calpaína, cdk5 y p25. El daño aparece tres días post-ictus y continúa progresivamente a lo largo de meses (Lai et al., 2014). Por lo que se concluye que estos eventos causan daño neuronal retardado y progresivo, que al final resultan en la muerte neuronal. Nuestra observación del efecto del glutamato sobre cdh1 sugiere que la disminución de cdh1 en la isquemia observado por Zhang et al., podría haber sido inducido por la excitotoxicidad del glutamato. Por otra parte, la disminuición de APC/C-Cdh1 y la acumulación de glutaminasa subsiguiente puede contribuir a la generación de entornos de excitotoxicidad en la isquemia.

Cdh1 y glutaminasa en el ratón transgénico APP/PS1

A continuación, analizamos los niveles de la proteína cdh1 en el modelo murino de la EA, el doble transgénico APP/PS1, en el que las neuronas están expuestos crónicamente a Aβ. Este es un modelo ampliamente utilizado para el estudio de la EA, ya que desarrollan la principal lesión encontrada en el cerebro humano, las placas de Aβ. En el modelo de ratón hay una fuerte correlación positiva entre la acumulación de Aβ y el deterioro cognitivo. Sin embargo, los ratones mutantes de APP/PS1 no tienen formación de ovillos neurofibrilares, pérdida neuronal o ventrículos más grandes, que son otras características principales de la AD en el ser humano. Dado que en nuestro estudio hemos analizado en particular el efecto de Aβ sobre APC/C-Cdh1, creemos que éste es el modelo adecuado para nuestro trabajo.

Los estudios inmunohistológicos muestran niveles inferiores de cdh1 (y predominantemente menos cdh1 en el núcleo) en los ratones transgénicos comparados con los ratones salvajes, en la capa CA1 del hipocampo. La

glutaminasa tambien se encuentra aumentada en las mismas áreas del cerebro. De este modo se confirmó nuestros resultados en un modelo de EA *in vivo.*

Nuestros resutados en una visión global para la EA

Por último, nuestros resultados nos permiten especular sobre su posible implicación en la aparición de la enfermedad en una visión global. En condiciones fisiológicas, la glutaminasa está presente en altas concentraciones en el hipocampo y la corteza entorrinal (Altschuler et al, 1985;. Akiyama et al., 1989). Recientemente, la corteza entorrinal lateral ha sido identificada como la principal área afectada en fases preclínicas de la EA. Este área proyecta a la región CA1 del hipocampo por la vía perforante lateral (LPP), que es parte de uno de los circuitos implicados en la memoria declarativa. La LPP está compuesta principalmente de conexiones glutamatérgicos (Khan et al., 2014). La toxicidad del glutamato inducida por Aβ podría tener efectos deletéreos específicamente en estas áreas del cerebro que se ven afectados en fases preclínicas de la EA, debido al alto nivel de glutaminasa basal. Por lo tanto postulamos que la excitotoxicidad podría ser un evento crucial en la aparición de la enfermedad y en deterioro de la memoria.

Perspectivas: APC/C-Cdh1 en la investigación en la EA

La evidencia sustancial nos dice que APC/C-Cdh1 y la glutaminasa podrían tener un papel importante en la fisiopatología de la EA. Otras indicaciones sugieren que algunos de los sustratos de APC/C están implicados en procesos relacionados con la EA. Sin embargo, sería crucial determinar si la desregulación de cdh1 se produce en el cerebro humano de los pacientes de EA. De hecho, se ha observado pérdida de neuronas 'glutaminasa-positivas', lo que sugiere un deterioro de la regulación de

la glutaminasa en la enfermedad. Sin embargo, los estudios en los cerebros de humanos de EA son difíciles de realizar, sobre todo si la desregulación se produce en el inicio de la enfermedad.

Podemos sin embargo, especular sobre las posibles consecuencias de una alteración en la regulación de APC/C-Cdh1 en la EA. La modificación de la actividad de la ubiquitina ligasa afectaría a un conjunto de sustratos y varias vías patológicas independientes pudieran verse perjudicadas a la vez. Entre ellas se encuentran la regulación del ciclo celular y la neurogénesis, la regulación oxidativa, el LTP y el metabolismo del glutamato. Los altos niveles de ciclina B1 han sido relacionados en una reentrada del ciclo celular ectópica, la acumulación de pfkfb3 induce estrés oxidativo en las neuronas y el aumento de los niveles de glutaminasa causan excitotoxicidad (Figura 6). Sin embargo, otros sustratos de APC/C aún no identificados, podrían estar involucrados directa o indirectamente en la fisiopatología de la EA. En varios modelos knock-out de cdh1, se ve afectado el proceso de long-term potentiation (LTP). Por lo tanto, sería razonable sugerir, que la alteración del LTP en la EA se produce debido a la desregulación de la APC/C-Cdh1. Un análisis más detallado de los sustratos de APC/C o proteínas relacionadas que participan en la LTP (EphA4, GluR, Liprina alfa, FRMP) podría dar más puntos de vista de la desregulación de proteínas en la EA.

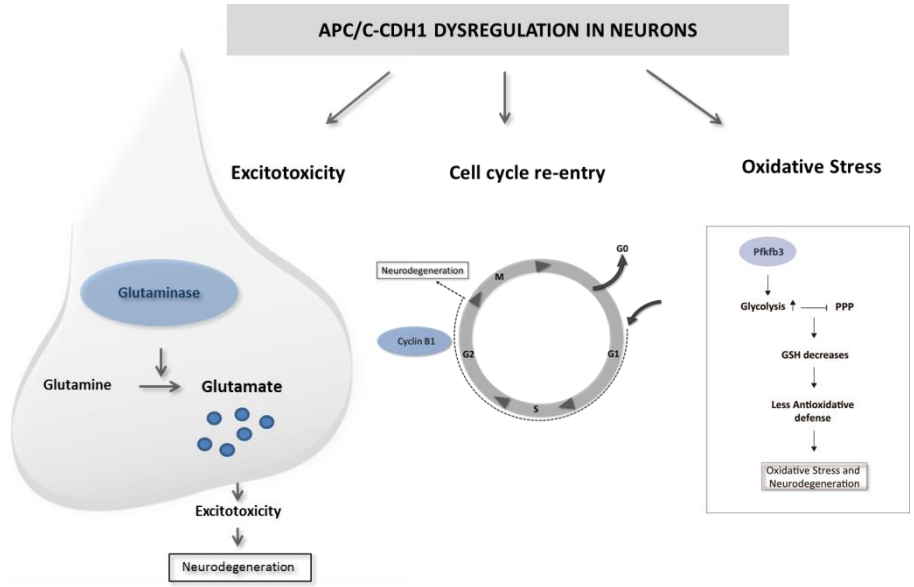

Figura 5 | Representación esquemática de los procesos alterados en la EA causado por una desregulación de APC/C-Cdh1. La acumulación de glutaminasa, la ciclina B1 y pfkfb3 están involucrados en la excitotoxicidad, el la reentrada en el ciclo celular de y el estrés oxidativo, respectivamente.

9. REFERENCES

Akiyama H, McGeer PL, Itagaki S, McGeer EG, Kaneko T (1989) Loss of glutaminase-positive cortical neurons in Alzheimer's disease. *Neurochemistry Research* **14**: 353-358.

Almeida A (2012) Regulation of APC/C-Cdh1 and Its Function in Neuronal Survival. *Molecular Neurobiology* **46**: 547–554.

Almeida A, Bolaños JP, Moncada S (2010) E3 ubiquitin ligase APC/C-Cdh1 accounts for the Warburg effect by linking glycolysis to cell proliferation. *PNAS* **107**: 738-41.

Almeida A, Bolanos JP, Moreno S (2005) Cdh1/Hct1-APC Is Essential for the Survival of Postmitotic Neurons. *The Journal of Neuroscience* **25**: 8115-8121.

Altschuler RA, Monaghan DT, Haser WG, Wenthold RJ, Curthoys NP, Cotman CW (1985) Immunocytochemical localization of glutaminase-like and aspartate aminotransferase-like immunoreactivities in the rat and guinea pig hippocampus. *Brain Research* **25**: 225-233.

Bashir T, Dorrello NV, Amador V, Guardavaccaro D, Pagano M (2004) Control of the SCF(Skp2-Cks1) ubiquitin ligase by the APC/C(Cdh1) ubiquitin ligase. *Nature* **428**: 190-3.

Benmaamar R and Pagano M (2005) Involvement of the SCF complex in the control of Cdh1 degradation in S-phase. *Cell Cycle* **4**: 1230-2.

Bertram L, Lange C, Mullin K, Parkinson M, Hsiao M, Hogan MF, Schjeide BM, Hooli B, Divito J, Ionita I, Jiang H, Laird N, Moscarillo T, Ohlsen KL, Elliott K, Wang X, Hu-Lince D, Ryder M, Murphy A, Wagner SL, Blacker D, Becker KD, Tanzi RE (2008) Genome-wide association analysis reveals putative Alzheimer's disease susceptibility loci in addition to APOE. *American Journal of Human Genetics* **83**: 623-632.

Bloom J, Amador V, Bartolini F, DeMartino G, Pagano M. (2003) Proteasome-mediated degradation of p21 via N-terminal ubiquitinylation. *Cell* **115:** 71–82.

Bonda DJ, Evans TA, Santocanale C, Llosá JC, Viña J, Bajic V, Castellani RJ, Siedlak SL, Perry G, Smith MA, Lee HG (2009) Evidence for the progression through S-phase in the ectopic cell cycle reentry of neurons in Alzheimer disease. *Aging* **1**: 382–388.

Bordji K, Becerril-Ortega J, Buisson A (2011) Synapses, NMDA receptor activity and neuronal Aβ production in Alzheimer's disease. *Reviews in the Neurosciences* **22**: 285-294.

Bosu DR and Kipreos ET (2008) Cullin-RING ubiquitin ligases: global regulation and activation cycles. *Cell Division* **3**:7.

Branconnier RJ, Dessain EC, McNiff ME, Cole JO (1986) Blood ammonia and Alzheimer disease. *American Journal of Psychiatry* **143**: 13-14.

Burbaeva GS, Boksha IS, Tereshkina EB, Savushkina OK, Starodubtseva LI, Turishcheva MS (2005) Glutamate metabolizing enzymes in prefrontal cortex of Alzheimer's disease patients. *Neurochemistry Research* **30**: 1443-51.

Buxbaum JD, Thinakaran G, Koliatsos V, O'Callahan J, Slunt HH, Price DL Sisodia SS (1998) Alzheimer amyloid protein precursor in the rat hippocampus: Transport and processing through the perforant path. *The Jounal of Neuronscience* **4**: 233-234.

Chang LF, Zhang Z, Yang J, McLaughlin SH, Barford D (2014) Molecular architecture and mechanism of the anaphase-promoting complex. *Nature* **513**: 388-93.

Chang LF, Zhang Z, Yang J, McLaughlin SH, Barford D (2015) Atomic structure of the APC/C and its mechanism of protein ubiquitination. *Nature* **522**: 450-4.

Chen MJ, Ng JM, Peng ZF, Manikandan J, Yap YW, Llanos RM, Beart PM, Cheung NS (2013) Gene profiling identifies commonalities in neuronal pathways in excitotoxicity: evidence favouring cell cycle re-activation in concert with oxidative stress. *Neurochemistry International* **5**: 719-30.

Chen QS, Wei WZ, Shimahara T, Xie CW (2002) Alzheimer amyloid beta-peptide inhibits the late phase of long-term potentiation through calcineurin-dependent mechanisms in the hippocampal dentate gyrus. *Neurobiology of Learning and Memory* **77**: 354-71.

Cheng PL, Lu H, Shelly M, Gao H, Poo MM (2011) Phosphorylation of E3 ligase Smurf1 switches its substrate preference in support of axon development. *Neuron* **69**: 231-243.

Cicero S and Herru K (2005) Cyclin-dependent kinase 5 is essential for neuronal cell cycle arrest and differentiation. *Journal of Neuroscience* **25**: 9658-9668.

Ciechanover A, Heller H, Elias S, Haas AL and Hershko A (1980) ATP-dependent Conjugation of Reticulocyte Proteins with the Polypeptide Required for Protein Degradation. *PNAS* **77**: 1365–1368.

Ciechanover A, Hod Y and Hershko A (1978). A Heat-stable Polypeptide Component of an ATP-dependent Proteolytic System from Reticulocytes. *Biochemical and Biophysical Research Communications* **81**, 1100–1105.

Colombo SL, Palacios-Callender M, Frakich N, De Leon J, Schmitt CA, Boorn L, Davis N, Moncada S (2010) Anaphase-promoting complex/cyclosome-Cdh1 coordinates glycolysis and glutaminolysis with transition to S phase in human T lymphocytes. *PNAS* **107**: 18868-73.

Copani A, Caraci F, Hoozemans JM, Calafiore M, Sortino MA, Nicoletti F (2007) The nature of the cell cycle in neurons: Focus on a "non-caconical" pathway of DNA replication causally related to death. *Biochimica et Biophysica Acta* **1772**: 409-412.

Cordero-Espinoza and Hagen T (2013) Increased concentrations of fructose 2,6-bisphosphate contribute to the Warburg effect in phosphatase and tensin homolog (PTEN)-deficient cells. *The Journal of Biological Chemistry* **288**: 36020–36028.

Crews L, Patrick C, Adame A, Rockenstein E, and Masliah E (2011) Modulation of aberrant CDK5 signaling rescues impaired neurogenesis in models of Alzheimer's disease. *Cell Death and Disease* **2**: e120.

Csernansky JG, Bardgett ME, Sheline YI, Morris JC, Olney JW (1996) CSF excitatory amino acids and severity of illness in Alzheimer's disease. *Neurology* **46**: 1715-20.

Dahlgren KN, Manelli AM, Stine WB Jr., Baker LK, Krafft GA, LaDu MJ (2002) Oligomeric and fibrillar species of amyloid-beta peptides differentially affect neuronal viability. *Journal of Biological Chemistry* **277**: 32046-53.

Delgado-Esteban M, García-Higuera I, Maestre C, Moreno S, Almeida A (2013) APC/C-Cdh1 coordinates neurogenesis and cortical size during development. *Nature Communications* **4**: 2879.

DiAntonio A & Hicke L (2004) Ubiquitin-dependent regulation of the synapse. *Annual Review of Neuroscience* **27**: 223-46.

Dong X, Wang Y, Qin ZH (2009) Molecular mechanisms of excitotoxicity and their relevance to pathogenesis of neurodegenerative diseases. *Acta Pharmacologica Sinica* **30**: 379–387.

Eguren M, Porlan E, Manchado E, García-Higuera I, Cañamero M, Fariñas I, Malumbres M (2013) The APC/C cofactor Cdh1 prevents replicative stress and p53-dependent cell death in neural progenitors. *Nature Communications* **4**: 2880.

Emanuele MJ, Elia AEH, Xu Q, Thoma CR, Izhar L, Leng Y, Guo A, Chen YN, Rush J, Hsu PWC, Yen HCS, Elledge SJ (2011) Global Identification of Modular Cullin-RING Ligase Substrates. *Cell* **147**: 459–474.

Fisman M, Gordon B, Feleki V, Helmes E, Appell E, Rabheru K (1985) Hyperammonemia in Alzheimer's disease. *American Journal of Psychiatry* **142**: 71–73.

Fonseca PCA, Kong EH, Zhang Z, Schreiber A, Williams MA, Morris EP, Barford D (2010) Structures of APC/CCdh1 with substrates identify Cdh1 and Apc10 as the D-box co-receptor. *Nature* **470**: 274–278.

Fu AK, Hung KW, Fu WY, Shen C, Chen Y, Xia J, Lai KO & Ip NY (2011) APC Cdh1 mediates EphA4-dependent downregulation of AMPA receptors in homeostatic plasticity. *Nature Neuroscience* **14**: 181- 191.

Garcia-Cao I, Song MS, Hobbs RM, Laurent G, Giorgi C, de Boer VC, Anastasiou D, Ito K, Sasaki AT, Rameh L, Carracedo A, Vander Heiden MG, Cantley LC, Pinton P, Haigis MC, Pandolfi PP (2012) Systemic Elevation of PTEN Induces a Tumor-Suppressive Metabolic State. *Cell* **149**: 1-14.

García-Higuera I, Manchado E, Dubus P, Cañamero M, Méndez J, Moreno S, Malumbres M (2008) Genomic stability and tumour suppression by the APC/C cofactor Cdh1. *Nature Cell Biology* **10**: 802-11.

Gengler S, Hamilton A, Hölscher C (2010) Synaptic plasticity in the hippocampus of a APP/PS1 mouse model of Alzheimer's disease is impaired in old but not young mice. *PLoS One* **5**: e9764.

Gieffers C, Peters BH, Kramer ER, Dotti CG, Peters JM (1999) Expression of the CDH1-associated form of the anaphase-promoting complex in postmitotic neurons. *PNAS* **96**: 11317-22.

Glotzer M, Murray AW, Kirschner MW (1991) Cyclin is degraded by the ubiquitin pathway. *Nature* **349**: 132–138.

Golde TE, Schneider LS, Koo EH (2011) Anti-aβ therapeutics in Alzheimer's disease: the need for a paradigm shift. *Neuron* **69**: 203-13.

Hainline SG, Rickmyre JL, Neitzel LR, Lee LA, Lee E (2014) The Drosophila MCPH1-B isoform is a substrate of the APCCdh1 E3 ubiquitin ligase complex. *Biology Open* **3**: 669-76.

Halim MA, Almatarneh MH, Poirier RA (2014) Mechanistic Study of the Deamidation Reaction of Glutamine: A Computational Approach. *The Journal of Physical Chemistry* **118**: 2316-2330.

Harmey D, Smith A, Simanski S, Moussa ZC, Ayad NG (2009) The Anaphase Promoting Complex Induces Substrate Degradation during Neuronal Differentiation. *The Journal of Biological Chemistry* **284**: 4317–4323.

Herrero-Mendez A, Almeida A, Fernández E, Maestre C, Moncada S, Bolaños JP (2009) The bioenergetic and antioxidant status of neurons is controlled by continuous degradation of a key glycolytic enzyme by APC/C-Cdh1. *Nature Cell Biology* **11**: 747-752.

Hershko A and Ciechanover A (1982) Mechanisms of intracellular protein breakdown. *Annual. Review of Biochemistry* **51**: 335–364.

Huang J, Ikeuchi Y, Malumbres M, Bonni A (2015) A Cdh1-APC/FMRP Ubiquitin Signaling Link Drives mGluR-Dependent Synaptic Plasticity in the Mammalian Brain. *Neuron* **86**: 1–14.

Hynd MR, Scott HL, Dodd PR (2004) Glutamate-mediated excitotoxicity and neurodegenerationin Alzheimer's disease. *Neurochemistry International* **45**: 583–595.

Jaquenoud M, van Drogen F, Peter M (2002) Cell cycle-dependent nuclear export of Cdh1p may contribute to the inactivation of APC/CCdh1. *The EMBO Journal* **21**: 6515-6526.

Jaspersen S L, Charles JF, Morgan DO (1999) Inhibitory phosphorylation of the APC regulator Hct1 is controlled by the kinase Cdc28 and the phosphatase Cdc14. *Current Biology* **9**: 227–236.

Jiménez-Jiménez FJ, Molina JA, Gómez P, Vargas C, de Bustos F, Benito-León J, Tallón-Barranco A, Ortí-Pareja M, Gasalla T, Arenas J (1998) Neurotransmitter amino acids in cerebrospinal fluid of patients with Alzheimer's disease. *Journal Neural Transmission* **105**: 269-277.

Juo P & Kaplan JM. (2004) The anaphase-promoting complex regulates the abundance of GLR-1 glutamate receptors in the ventral nerve cord of C. elegans. *Current Biology* **14**: 2057-62.

Kahn UA, Liu L, Provenzano FA, Berman DE, Proface CP, Sloan R, Mayeux R, Duff KE, Small SA (2014) Molecular drivers and cortical spread of lateral entorhinal cortex dysfunction in preclinical Alzheimer's disease. *Nature Neuroscience* **17**: 304-311.

Kaiser E, Schoenknecht P, Kassner S, Hildebrandt W, Kinscherf R, Schroeder J (2010) Cerebrospinal fluid concentrations of functionally important amino acids and metabolic compounds in patients with mild cognitive impairment and Alzheimer's disease. *Neurodegenerative Diseases* **7**: 251-259.

Kannan M, Lee SJ, Schwedhelm-Domeyer N, Stegmüller J (2012) The E3 ligase Cdh1-anaphase promoting complex operates upstream of the E3 ligase Smurf1 in the control of axon growth. *Development* **139**: 3600-3612.

Kerr F, Rickle A, Nayeem N, Brandner S, Cowburn RF, Lovestone S (2006) PTEN, a negative regulator of PI3 kinase signalling, alters tau phosphorylation in cells by mechanisms independent of GSK-3. *FEBS Letter* **580**: 3121-8.

Kim AH, Puram SV, Bilimoria PM, Ikeuchi Y, Keough S, Wong M, Rowitch D, Bonni A (2009) A centrosomal Cdc20-APC pathway controls dendrite morphogenesis in postmitotic neurons. *Cell* **136**: 322–336.

King RW, Glotzer M, Kirschner MW (1996) Mutagenic analysis of the destruction signal of mitotic cyclins and structural characterization of ubiquitinated intermediates. *Molecular Biology of the Cell* **7**: 1343-57.

King RW, Peters JM, Tugendreich S, Rolfe M, Hieter P, Kirschner MW (1995) A 20S complex containing CDC27 and CDC16 catalyzes the mitosis-specific conjugation of ubiquitin to cyclin B. *Cell* **81**: 279-88.

Koch G, Di Lorenzo F, Bonnì S, Ponzo V, Caltagirone C, Martorana A (2012) Impaired LTP- but not LTD-like cortical plasticity in Alzheimer's disease patients. *Journal of Alzheimers Dis*ease **31**: 593-9.

Konishi Y, Stegmuller J, Matsuda T, Bonni S, Bonni A (2004) Cdh1-APC controls axonal growth and patterning in the mammalian brain. *Science* **303**: 1026–1030.

Kotania S, Tanakab H, Yasudab H, Todokoro K (1999) Regulation of APC Activity by Phosphorylation and Regulatory Factors. *Journal of Cell Biology* **146**: 791-800.

Kowall NW & Beal MF (1991) Glutamate-, glutaminase-, and taurine-immunoreactive neurons develop neurofibrillary tangles in Alzheimer's disease. *Annals of Neurology* **29**: 162-167.

LaFerla FM (2002) Calcium dyshomeostasis and intracellular signalling in Alzheimer's Disease. *Nature Review Neuroscience* **3**: 862-872.

Lai TW, Zhang S, Wang YT (2014) Excitotoxicity and stroke: identifying novel targets for neuroprotection. *Progress in Neurobiology* **115**: 157-88.

Lambert MP, Barlow AK, Chromy BA, Edwards C, Freed R, Liosatos M, Morgan TE, Rozovsky I, Trommer B, Viola KL, Wals P, Zhang C, Finch CE, Krafft GA, Klein WL (1998) Diffusible, nonfibrillar ligands derived from Aβ_{1-42} are potent central nervous system neurotoxins. *PNAS* **95**: 6448-6453.

Lasorella A, Stegmüller J, Guardavaccaro D, Liu G, Carro MS, Rothschild G, de la Torre-Ubieta L, Pagano M, Bonni A, Iavarone A (2006) Degradation of Id2 by the anaphase-promoting complex couples cell cycle exit and axonal growth. *Nature* **442**: 471-4.

Lauderback CM, Harris-White ME, Wang Y, Pedigo NW, Carney JM, Butterfield DA (1999) Amyloid beta-peptide inhibits Na^+-dependent glutamate uptake. *Life Sciences* **65**: 1977-81.

Lee KY, Clark AW, Rosales JL, Chapman K, Fung T, Johnston R (1999) Elevated neuronal Cdc2-like kinase activity in the Alzheimer disease brain. *Neuroscience Research* **34**: 21-29.

Lew J, Qi Z, Huang Q, Paudel H, Matsuura I, Matsshita M, Zhu X, Wang JI (1995) Structure, function, and regulation of neuronal cdc2-like protein kinase. *Neurobiology of Aging* **16**: 263-270.

Li B, Yamamori H, Tatebayashi Y, Shafit-Zagardo B, Tanimukai H, Chen S, Iqbal K, Grundke-Iqbal I (2008) Failure of neuronal maturation in Alzheimer disease dentate gyrus. *Journal of Neuropathology & Experimental Neurology* **67**: 78-84.

Li M, Shin YH, Hou L, Huang X, Wie Z, Klann E, Zhang P (2008) The adaptor protein of the anaphase promoting complex Cdh1 is essential in maintaining replicative lifespan and in learning and memory. *Nature Cell Biology* **10**: 1083-1089.

Li M & Zhang P (2009) The function of APC/C-Cdh in cell cycle and beyond. *Cell division* **4**, doi: 10.1186/1747-1028-4-2.

Li R, Wan B, Zhou J, Wang Y, Luo T, Gu X, Chen F, Yu L (2012) APC/C(Cdh1) targets brain-specific kinase 2 (BRSK2) for degradation via the ubiquitin-proteasome pathway. *PLoS One* **7**: e45932.

Lipton SA (2005) The molecular basis of memantine action in Alzheimer's disease and other neurologic disorders: low-affinity, uncompetitive antagonism. *Current Alzheimer Research* **2**: 155-165.

Littlepage LE, Ruderman JV (2002) Identification of a new APC/C recognition domain, the A box, which is required for the Cdh1-dependent destruction of the kinase Aurora-A during mitotic exit. *Genes & Development* **16**: 2274–2285.

Lloret A, Badía MC, Mora NJ, Ortega A, Pallardó FV, Alonso MD, Atamna H, Viña J (2008) Gender and age-dependent differences in the mitochondrial apoptogenic pathway in Alzheimer's disease. *Free Radical Biology and Medicine* **44**: 2019-25.

Lloret A, Fuchsberger T, Giraldo E, Viña J (2015) Molecular mechanisms linking amyloid β toxicity and Tau hyperphosphorylation in Alzheimer's disease. *Free Radical Biology and Medicine* **83**: 186-91.

Lopes JP & Agostinho P (2011) Cdk5: Multitasking between physiological and pathological conditions. *Progress in Neurobiology* **94**: 49-63.

Lukas C, Storgaard Sørensen C, Kramer E, Santoni-Rugiu E, Lindeneg C, Peters JM, Bartek J, Lukas J (1999) Accumulation of cyclin B1 requires E2F and cyclin-A-dependent rearrangement of the anaphase-promoting complex. *Nature* **401**: 815-818.

Maestre C, Delgado-Esteban M, Gomez-Sanchez JC, Bolaños JP, Almeida A (2008) Cdk5 phosphorylates Cdh1 and modulates cyclin B1 stability in excitotoxicity. *EMBO* **20**, 2736-45.

McShea A, Harris PL, Webster KR, Wahl AF, Smith MA (1997) Abnormal expression of the cell cycle regulators P16 and CDK4 in Alzheimer's disease. *American Journal of Pathology* **150**: 1933–1939.

Mu Y & Gage FH (2011) Adult hippocampal neurogenesis and its role in Alzheimer's disease. *Molecular Neurodegeneration* **6**: 85.

Nagy Z, Esiri MM, Smith AD (1997) Expression of cell division markers in the hippocampus in Alzheimer's disease and other neurodegenerative conditions. *Acta Neuropathologica* **93**: 294–300.

Nayeem N, Kerr F, Naumann H, Linehan J, Lovestone S, Brandner S (2007) Hyperphosphorylation of tau and neurofilaments and activation of CDK5 and ERK1/2 in PTEN-deficient cerebella. *Molecular and Cellular Neuroscience* **34**: 400-408.

Norenberg MD, Rama Rao KV, Jayakumar AR (2004) Ammonia neurotoxicity and the mitochondrial permeability transition. *Journal of Bioenergetics and Biomembranes* **36**: 303-307.

Norris CM, Blalock EM, Thibault O, Brewer LD, Clodfelter GV, Porter NM, Landfield PW (2006) Electrophysiological Mechanisms of Delayed Excitotoxicity: Positive Feedback Loop Between

NMDA Receptor Current and Depolarization-Mediated Glutamate Release. *Journal of Neurophysiology* **96**: 2488-2500.

Patrick GN, Zukerberg L, Nikolic M, Monte S, Dikkesk P, Tsai LH (2000) Conversion of p35 to p25 deregulates Cdk5 activity and promotes neurodegeneration. *Nature* **402**: 615-622.

Pearson-Leary J & McNay EC (2012) Intrahippocampal Administration of Amyloid-1-42 Oligomers Acutely Impairs Spatial Working Memory, Insulin Signaling, and Hippocampal Metabolism. *Journal of Alzheimer's Disease* **30**: 413-422.

Penas C, Govek EE, Fang Y, Ramachandran V, Daniel M, Wang W, Maloof ME, Rahaim RJ, Bibian M, Kawauchi D, Finkelstein D, Han JL, Long J, Li B, Robbins DJ, Malumbres M, Roussel MF, Roush WR, Hatten ME, Ayad NG (2015) Casein Kinase 1d Is an APC/CCdh1 Substrate that Regulates Cerebellar Granule Cell Neurogenesis. *Cell Reports* **11**: 1–12.

Perrin RJ, Fagan AM, Holtzman DM (2009) Multimodal techniques for diagnosis and prognosis of Alzheimer's disease. *Nature* **461**: 916-22.

Pfleger CM, Kirschner MW (2000) The KEN box: an APC recognition signal distinct from the D box targeted by Cdh1. *Genes & Development* **14**: 655-65.

Pick JE, Malumbres M, Klann E (2013) The E3 ligase APC/C–Cdh1 is required for associative fear memory and long-term potentiation in the amygdala of adult mice. *Learning & Memory* **20**: 11–20.

Pick JE, Wang L, Mayfield JE, & Klann E (2013) Neuronal Expression of the Ubiquitin E3 ligase APC/C-Cdh1 During Development is Required for Long-term Potentiation, Behavioral Flexibility, and Extinction. *Neurobiology of Learning & Memory* **100**: 25–31.

Pickart CM, Eddins MJ. Ubiquitin: structures, functions, mechanisms. (2004) *Biochimica et Biophysica Acta* **1695**: 55-72.

Pines J. (2011) Cubism and the cell cycle: the many faces of the APC/C. *Nature Reviews Molecular Cell Biology* **12**: 427–438.

Ping Z, Lim R, Bashir T, Pagano M, and Guardavaccaro D (2012) APC/CCdh1 controls the proteasome-mediated degradation of E2F3 during cell cycle exit. *Cell Cycle* **11**: 1999–2005.

Pomara N, Singh R, Deptula D, Chou JC, Schwartz MB, LeWitt PA (1992) Glutamate and other CSF amino acids in Alzheimer's disease. *American Journal of Psychiatry* **149**: 251-254.

Price DL, Tanzi RE, Borchelt DR, Sisodia SS (1998) Alzheimer's disease: genetic studies and transgenic models. *Annual Review Genetics* **32**: 461-93.

Puram SV, Kim AH, and Bonni A (2010) An Old Dog Learns New Tricks: A Novel Function for Cdc20-APC in Dendrite Morphogenesis in Neurons. *Cell Cycle* **9**: 482–485.

Qiao X, Zhang L, Gamper AM, Fujita T, Wan Y (2010) APC/C-Cdh1: From cell cycle to cellular differentiation and genomic integrity. *Cell Cycle* **9**: 3904–3912.

Reis A, Levasseur M, Chang HY, Elliott DJ, Jones KT (2006) The CRY box: a second APC cdh1-dependent degron in mammalian cdc20. *EMBO Reports* **7**, 1040–1045.

Rodriguez-Rodriguez P, Fernandez E, Almeida A, Bolanos JP (2012) Excitotoxic stimulus stabilizes PFKFB3 causing pentose-phosphate pathway to glycolysis switch and neurodegeneration. *Cell Death and Differentiation* **10**: 1582-9.

Rodriguez-Rodriguez P, Almeida A, Bolaños JP (2013) Brain energy metabolism in glutamate-receptor activation and excitotoxicity: role for APC/C-Cdh1 in the balance glycolysis/pentose phosphate pathway. *Neurochemistry International* **62**: 750-756.

Sailer N (2002) Ammonia and Alzheimer's disease. *Neurochemistry International* **41**: 189-207.

Sajman J, Zenvirth D, Nitzan M, Margalit H, Simpson-Lavy KJ, Reiss Y, Cohen I, Ravid T, Brandeis M (2015) Degradation of Ndd1 by APC/CCdh1 generates a feed forward loop that times mitotic protein accumulation. *Nature Communications* **8075**.

Sato Y Heuckeroth RO (2008) Retinoic acid regulates murine enteric nervous system precursor proliferation, enhances neuronal precursor differentiation, and reduces neurite growth in vitro. *Developmental Biology* **320**: 185-198.

Scimemi A, Meabon JS, Woltjer RL, Sullivan JM, Diamond JS, Cook DG (2013) Amyloid-β Slows Clearance of Synaptically Released Glutamate by Mislocalizing Astrocytic GLT-1. *The Journal of Neuroscience* **33**: 5312-5318.

Simón AM, de Maturana RL, Ricobaraza A, Escribano L, Schiapparelli L, Cuadrado-Tejedor M, Pérez-Mediavilla A, Avila J, Del Río J, Frechilla D (2009) Early changes in hippocampal Eph receptors precede the onset of memory decline in mouse models of Alzheimer's disease. *Journal of Alzheimers Disease* **17**: 773-86.

Smith TW, Lippa CF (1995) Ki-67 immunoreactivity in Alzheimer's disease and other neurodegenerative disorders. *Journal of Neuropathology and Experimental Neurology*. **54**: 297–303.

Song MS, Carracedo A, Salmena L, Song SJ, Egia A, Malumbres M, Pandolfi PP (2011) Nuclear PTEN regulates the APC-CDH1 tumor suppressive complex in a phosphatase-independent manner. *Cell* **144**: 187–199.

Starborg M, Brundell E, Gell K, Hoog C (1994) A novel murine gene encoding a 216-kDa protein is related to a mitotic checkpoint regulator previously identified in Aspergillus nidulans. *Journal of Biological Chem*istry **269**: 24133–24137.

Stegmüller J, Konishi Y, Huynh MA, Yuan Z, Dibacco S, Bonni A (2006) Cell-intrinsic regulation of axonal morphogenesis by the Cdh1-APC target SnoN. *Neuron* **50**: 389-400.

Stroschein SL, Bonni S, Wrana JL, Luo K (2001) Smad3 recruits the anaphase-promoting complex for ubiquitination and degradation of SnoN. *Genes & Developtment* **15**: 2822-36.

Teplow, DB (2006) Preparation of Amyloid *β*-Protein for Structural and Functional Studies. *Methods In Enzymology* **413**: 20-33.

Tu S, Okamoto S, Lipton SA, Xu H (2014) Oligomeric Aβ-induced synaptic dysfunction in Alzheimer's disease. *Molecular Neurodegeneration* **9**: 48-60.

van Roessel P, Elliott DA, Robinson IM, Prokop A, Brand AH (2004) Independent regulation of synaptic size and activity by the anaphase-promoting complex. *Cell* **119**: 707-18.

Viña J, Lloret A, Giraldo E, Badia MC, Alonso MD (2011) Antioxidant pathways in Alzheimer's disease: possibilities of intervention. *Current Pharmaceutical Design* **35**: 3861-4.

Vincent I, Jicha G, Rosado M, Dickson DW (1997) Aberrant expression of mitotic cdc2/cyclin B1 kinase in degenerating neurons of Alzheimer's disease brain. *Journal of Neuroscience* **17**: 3588-98.

Visintin R, Prinz S, Amon A. (1997) CDC20 and CDH1: a family of substrate-specific activators of APC-dependent proteolysis. *Science* **278**: 460-3.

Wang X, Di K, Zhang X, Han HY, Wong YC, Leung SC, Ling MT (2008) Id-1 promotes chromosomal instability through modification of APC/C activity during mitosis in response to microtubule disruption. *Oncogene* **27**: 4456-4466.

Wasch R, Robbins JA, Cross FR (2010). The emerging role of APC/CCdh1 in controlling differentiation, genomic stability and tumor suppression. *Oncogene* **29**: 1–10.

Yang Y, Kim AH, Yamada T, Wu B, Bilimoria PM, Ikeuchi Y, de la Iglesia N, Shen J, Bonni A (2009) A Cdc20-APC ubiquitin signaling pathway regulates presynaptic differentiation. *Science* **326**: 575-578.

Yu Y, He J, Zhang Y, Luo H, Zhu S, Yang Y, Zhao T, Wu J, Huang Y, Kong J, Tan Q, Li XM (2009) Increased hippocampal neurogenesis in the progressive stage of Alzheimer's disease phenotype in an APP/PS1 double transgenic mouse model. *Hippocampus* **12**: 1247-53.

Zachariae W, Schwab M, Nasmyth K, Seufert W (1998) Control of Cyclin Ubiquitination by CDK-Regulated Binding of Hct1 to the Anaphase Promoting Complex. *Science* **282**: 1721-1724.

Zádori D, Veres G, Szalárdy L, Klivényi P, Toldi J, Vécsei L (2014) Glutamatergic dysfunctioning in Alzheimer's disease and related therapeutic targets. *Journal of Alzheimers Disease* **42**, 177-87.

Zhang J, Cicero SA, Wang L, Romito-DiGiacomo RR, Yang Y, Herrup K (2008) Nuclear localization of Cdk5 is a key determinant in the postmitotic state of neurons. *PNAS* **105**: 8772-8777.

Zhang Y, Yao W, Qiu J, Qian W, Zhu C, Zhang C (2011) The involvement of down-regulation of Cdh1-APC in hippocampal neuronal apoptosis after global cerebral ischemia in rat. *Neuroscience Letters* **505**: 71-75.

Zhao N, Lai F, Fernald AA, Eisenbart JD, Espinosa R, Wang PW, Le Beau MM (1998). Human CDC23: cDNA cloning, mapping to 5q31, genomic structure, and evaluation as a candidate tumor suppressor gene in myeloid leukemias. *Genomics* **53**: 184–190.

Zhou Y, Ching YP, Chun ACS, Jin DY (2003) Nuclear Localization of the Cell Cycle Regulator CDH1 and Its Regulation by Phosphorylation. *Journal of Biological Chemistry* **278**: 12530-12536.

Books

Brady ST, Siegel GJ, Albers RW, Price DL. Basic Neurochemistry: Molecular, Cellular and Medical Aspects, 8th edition, Academic Press Eslevier (2011).

Kandel ER, Schwartz JH, Jessell TM, Siegelbaum SA, Hudspeth AJ. Principles of Neural Science, Fifth Edition, The McGraw Hill Companies (2013).

Santello M, Calì C, Bezzi P. Chapter Synaptic Plasticity: Gliotransmission and the tripartite synapse. In: Volume 970 of the series Advances in Experimental Medicine and Biology pp 307-331, Springer (2012).

Paxinos G & Watson C. The rat brain in stereotaxic coordinates: hard cover edition. Access Online via Elsevier, (2006).

Purves D, Augustine GJ, Fitzpatrick D, Hall WC, LaMantia AS, McNamara JO, Williams SM, Neuroscience, 3rd edition, Sinauer Associates Sunderland MA (2004).